UNIVERSIDADE FEDERAL DE MINAS GERAIS
FACULDADE DE FARMÁCIA
PROGRAMA DE PÓS-GRADUAÇÃO EM CIÊNCIAS FARMACÊUTICAS

EDUARDO BURGARELLI LAGES

CARREADORES LIPÍDICOS NANOESTRUTURADOS CONTENDO DOXORRUBICINA, ÁCIDO DOCOSAHEXAENÓICO E SUCCINATO DE α-TOCOFEROL: FORMULAÇÃO, CARACTERIZAÇÃO E AVALIAÇÃO DO POTENCIAL TERAPÊUTICO CONTRA O CÂNCER

BELO HORIZONTE - MG
2021

UNIVERSIDADE FEDERAL DE MINAS GERAIS
FACULDADE DE FARMÁCIA
PROGRAMA DE PÓS-GRADUAÇÃO EM CIÊNCIAS FARMACÊUTICAS

EDUARDO BURGARELLI LAGES

CARREADORES LIPÍDICOS NANOESTRUTURADOS CONTENDO DOXORRUBICINA, ÁCIDO DOCOSAHEXAENÓICO E SUCCINATO DE α-TOCOFEROL: FORMULAÇÃO, CARACTERIZAÇÃO E AVALIAÇÃO DO POTENCIAL TERAPÊUTICO CONTRA O CÂNCER

Tese apresentada ao Programa de Pós-Graduação em Ciências Farmacêuticas da Faculdade de Farmácia da Universidade Federal de Minas Gerais, como requisito parcial à obtenção do grau de Doutor em Ciências Farmacêuticas.

Orientador: Prof. Dr. Lucas Antônio Miranda Ferreira
Coorientador: Prof. Dr. André Luís Branco de Barros

BELO HORIZONTE - MG
2021

Lages, Eduardo Burgarelli.
L174c Carreadores lipídicos nanoestruturados contendo doxorrubicina, ácido docosahexaenóico e succinato de α-tocoferol: formulação, caracterização e avaliação do potencial terapêutico contra o câncer / Eduardo Burgarelli Lages. – 2021.
130 f. : il.

Orientador: Lucas Antônio Miranda Ferreira.
Coorientador: André Luís Branco de Barros.

Tese (doutorado) – Universidade Federal de Minas Gerais, Faculdade de Farmácia, Programa de Pós-Graduação em Ciências Farmacêuticas.

1. Doxorrubicina – Teses. 2. Sinergismo – Teses. 3. Farmacocinética – Teses. 4. Atividade antitumoral – Teses. 5. Cardiotoxicidade – Teses. 6. Câncer – Tratamento – Teses. I. Ferreira, Lucas Antônio Miranda. II. Barros, André Luís Branco de. III. Universidade Federal de Minas Gerais. Faculdade de Farmácia. IV. Título.

CDD:616.994

Elaborado por Aline Guimarães Amorim – CRB-6/2292

UNIVERSIDADE FEDERAL DE MINAS GERAIS
FACULDADE DE FARMÁCIA
PROGRAMA DE PÓS-GRADUAÇÃO EM CIÊNCIAS FARMACÊUTICAS

FOLHA DE APROVAÇÃO

CARREADORES LIPÍDICOS NANOESTRUTURADOS CONTENDO DOXORRUBICINA, ÁCIDO DOCOSAHEXAENÓICO E SUCCINATO DE α-TOCOFEROL: FORMULAÇÃO, CARACTERIZAÇÃO E AVALIAÇÃO DO POTENCIAL TERAPÊUTICO CONTRA O CÂNCER

EDUARDO BURGARELLI LAGES

Tese submetida à Banca Examinadora designada pelo Colegiado do Programa de Pós-Graduação em CIÊNCIAS FARMACÊUTICAS, como requisito para obtenção do grau de Doutor em CIÊNCIAS FARMACÊUTICAS, área de concentração CIÊNCIAS FARMACÊUTICAS.

Dr. Samuel Vidal Mussi
ACHÉ Laboratórios Farmacêuticos

Profa. Dra. Carolina de Aguiar Ferreira
University of Wisconsin - Madison

Prof. Dr. Pedro Pires Goulart Guimarães
Universidade Federal de Minas Gerais - UFMG

Profa. Dra. Marta Marques Gontijo de Aguiar
Universidade Federal de Minas Gerais - UFMG

Prof. Dr. Lucas Antônio Miranda Ferreira - Orientador
Universidade Federal de Minas Gerais - UFMG

Prof. Dr. André Luís Branco de Barros - Coorientador
Universidade Federal de Minas Gerais - UFMG

Belo Horizonte, 09 de setembro de 2021.

Documento assinado eletronicamente por **Carolina de Aguiar Ferreira**, **Usuário Externo**, em 09/09/2021, às 11:38, conforme horário oficial de Brasília, com fundamento no art. 5º do Decreto nº 10.543, de 13 de novembro de 2020.

Documento assinado eletronicamente por **Andre Luis Branco de Barros**, **Professor do Magistério Superior**, em 09/09/2021, às 18:37, conforme horário oficial de Brasília, com fundamento no art. 5º do Decreto nº 10.543, de 13 de novembro de 2020.

Documento assinado eletronicamente por **Samuel Vidal Mussi**, **Usuário Externo**, em 09/09/2021, às 18:39, conforme horário oficial de Brasília, com fundamento no art. 5º do Decreto nº 10.543, de 13 de novembro de 2020.

Documento assinado eletronicamente por **Pedro Pires Goulart Guimaraes**, **Professor do Magistério Superior**, em 09/09/2021, às 18:39, conforme horário oficial de Brasília, com fundamento no art. 5º do Decreto nº 10.543, de 13 de novembro de 2020.

Documento assinado eletronicamente por **Marta Marques Gontijo de Aguiar**, **Professora do Magistério Superior**, em 09/09/2021, às 18:41, conforme horário oficial de Brasília, com fundamento no art. 5º do Decreto nº 10.543, de 13 de novembro de 2020.

Documento assinado eletronicamente por **Lucas Antonio Miranda Ferreira**, **Professor do Magistério Superior**, em 09/09/2021, às 19:00, conforme horário oficial de Brasília, com fundamento no art. 5º do Decreto nº 10.543, de 13 de novembro de 2020.

A autenticidade deste documento pode ser conferida no site https://sei.ufmg.br/sei/controlador_externo.php?acao=documento_conferir&id_orgao_acesso_externo=0, informando o código verificador **0949814** e o código CRC **3A145A82**.

Dedico este trabalho ao meu pai (*in memoriam*),
que nunca mediu esforços pela
minha educação.
Te amo eternamente!
E também a todos aqueles que sofrem com o câncer.
Que possamos um dia vencer o combate contra essa doença terrível...

AGRADECIMENTOS

A Deus, por ser presença contínua em minha vida e sempre me dar forças para superar as dificuldades.

Aos meus pais, Elizabeth e Hugo, pelo amor incondicional, apoio e por não medirem esforços para que eu chegasse até aqui. Às minhas irmãs, Melina e Marina, pelo carinho e incentivo.

Ao Lucas, pelo exemplo profissional, ensinamentos, paciência e atenção ao longo desses anos.

Ao André, pela disponibilidade, pelas contribuições sempre relevantes e pelo apoio na condução do trabalho.

Aos colaboradores, sem os quais nada disso teria sido possível: Renata, Ju, Marina, Christian, Renata Barbosa, Ângelo, Geovanni, Kim, Pierre e Sylvain. Muito obrigado!

Aos funcionários da Faculdade de Farmácia e PhyMedExp, em especial Adelaide, Batista, Ângela, Raquel, Nazaré, Marton e Azzouz, pela gentileza e auxílio sempre que necessário.

Aos membros da banca examinadora pela disponibilidade em participar e pelas valiosas considerações para o enriquecimento do trabalho.

Aos professores e amigos do Laboratório de Tecnologia Farmacêutica, em especial Isabela, Jaque, Eliza, Dani, Thais e Gabriel, pela convivência harmoniosa e incentivo.

Ao Sylvain e Pierre, por terem me recebido tão bem em Montpellier e terem contribuído enormemente para minha formação.

Ao Gabriel e Dayan, por terem dividido comigo momentos inesquecíveis em Montpellier!

À FAPEMIG, CAPES e CNPq, pelo auxílio financeiro e bolsas de estudo concedidas.

A todos meus amigos e familiares pelo incentivo e por participarem dessa trajetória junto comigo.

A todos que de alguma forma contribuíram para a realização deste trabalho e para minha formação pessoal e profissional ao longo desses anos. Muito obrigado!

COLABORADORES

Dra. Renata Salgado Fernandes (Faculdade de Farmácia - UFMG)

Dra. Juliana de Oliveira Silva (Faculdade de Farmácia - UFMG)

Ma. Marina Mol Sena Andrade (Faculdade de Farmácia - UFMG)

Prof. Dr. Christian Fernandes (Faculdade de Farmácia - UFMG)

Profa. Dra. Renata Barbosa de Oliveira (Faculdade de Farmácia - UFMG)

Prof. Dr. Ângelo Malachias de Souza (Instituto de Ciências Exatas - UFMG)

Prof. Dr. Geovanni Dantas Cassali (Instituto de Ciências Biológicas - UFMG)

Me. Nitchawat Paiyabhroma (PhyMedExp - Université de Montpellier)

Dr. Pierre Sicard (PhyMedExp - Université de Montpellier)

Dr. Sylvain Richard (PhyMedExp - Université de Montpellier)

RESUMO

A encapsulação da doxorrubicina (DOX) em nanocarreadores tem sido proposta a fim de superar suas limitações. Neste trabalho, foi desenvolvida uma formulação de carreadores lipídicos nanoestruturados (NLC) contendo DOX e os adjuvantes anticâncer ácido docosahexaenóico (DHA) e succinato de α-tocoferol (TS). O NLC foi preparado pelo processo de emulsificação-ultrassom e a DOX foi incorporada posteriormente, o que evitou sua degradação durante a fabricação. Alta eficiência de encapsulação da DOX foi obtida devido à formação de um par iônico com o TS, o que diminuiu sua solubilidade aquosa e reduziu sua cristalinidade. Estudos *in vitro* indicaram que a combinação de DOX, DHA e TS possui efeitos sinérgicos frente células tumorais 4T1. A formulação mostrou alta eficácia antitumoral ao reduzir o crescimento do tumor 4T1 em camundongos, além de diminuir a toxicidade sistêmica induzida pela DOX. Apesar dos resultados promissores, a avaliação da farmacocinética após administração intravenosa em camundongos revelou um perfil farmacocinético semelhante entre o nanocarreador e a DOX livre (solução), sugerindo rápida desestabilização do par iônico e liberação da DOX. A partir desses dados, a síntese de conjugados covalentes DOX-TS foi proposta para aumentar a retenção da DOX no NLC. A DOX foi conjugada com sucesso ao TS por meio de uma ligação amida ou hidrazona. Estudos *in vitro* indicaram alta citotoxicidade do derivado hidrazona frente células 4T1, ao contrário do conjugado amida. A encapsulação do derivado hidrazona no sistema NLC, juntamente com DHA, resultou em partículas de tamanho reduzido (90 nm), alta eficiência de encapsulação e liberação de DOX sensível ao pH. Essa formulação mostrou melhor perfil farmacocinético em comparação à DOX livre e à formulação anteriormente preparada (par iônico). Estudos *in vivo* revelaram grande potencial terapêutico para o nanocarreador, que foi capaz de prevenir o desenvolvimento de cardiotoxicidade aguda em camundongos, inibir consideravelmente o crescimento do tumor 4T1 e reduzir os efeitos tóxicos sistêmicos provocados pela DOX. Esses resultados indicam que o sistema NLC contendo DHA e o conjugado hidrazona DOX-TS pode ser uma formulação promissora para o tratamento do câncer.

Palavras-chave: doxorrubicina; nanomedicina; sinergismo; par iônico hidrofóbico; farmacocinética; atividade antitumoral; cardiotoxicidade.

ABSTRACT

Encapsulation of doxorubicin (DOX) in nanocarriers has been proposed to overcome its limitations. In this work, a nanostructured lipid carriers (NLC) formulation containing DOX and the anticancer adjuvants docosahexaenoic acid (DHA) and α-tocopherol succinate (TS) was developed. NLC was prepared by the emulsification-ultrasound method and DOX was later incorporated, which prevented its degradation during manufacturing. High DOX encapsulation efficiency was obtained due to the formation of an ion pair with TS, which decreased its aqueous solubility and reduced its crystallinity. *In vitro* studies indicated that the combination of DOX, DHA and TS has synergistic effects against 4T1 tumor cells. The formulation showed high antitumor efficacy by reducing 4T1 tumor growth in mice, in addition to decreasing DOX-induced systemic toxicity. Despite these promising results, the evaluation of pharmacokinetics after intravenous administration in mice revealed a similar pharmacokinetic profile between the nanocarrier and free DOX (solution), suggesting rapid destabilization of the ion pair and release of DOX. From these data, the synthesis of DOX-TS covalent conjugates was proposed to increase the retention of DOX in NLC. DOX was successfully conjugated to TS via an amide or hydrazone bond. *In vitro* studies indicated high cytotoxicity of the hydrazone derivative against 4T1 cells, unlike the amide conjugate. The encapsulation of the hydrazone derivative in the NLC system, plus DHA, resulted in reduced particle size (90 nm), high encapsulation efficiency, and pH-sensitive DOX release. This formulation showed a better pharmacokinetic profile compared to free DOX and the previously prepared formulation (ion pair). *In vivo* studies revealed great therapeutic potential for this nanocarrier, which was able to prevent the development of acute cardiotoxicity in mice, considerably inhibit the 4T1 tumor growth and reduce the systemic toxic effects caused by DOX. These results indicate that the NLC system containing DHA and the hydrazone DOX-TS conjugate may be a promising formulation for cancer treatment.

Keywords: doxorubicin; nanomedicine; synergism; hydrophobic ion-pairing; pharmacokinetics; antitumor activity; cardiotoxicity.

SUMÁRIO

1 INTRODUÇÃO..... 11
2 REVISÃO DA LITERATURA..... 13
2.1 Câncer..... 13
2.2 Doxorrubicina..... 15
2.3 Ácido docosahexaenóico..... 19
2.4 Succinato de α-tocoferol..... 21
2.5 Sistemas nanocarreadores de fármacos..... 22
2.5.1 Carreadores lipídicos nanoestruturados..... 24
2.5.2 Nanocarreadores lipídicos contendo doxorrubicina..... 26
3 OBJETIVOS..... 32
3.1 Objetivo geral..... 32
3.2 Objetivos específicos..... 32
CAPÍTULO 1..... 33
1 Introduction..... 35
2 Materials and methods..... 37
3 Results and discussion..... 44
4 Conclusion..... 66
CAPÍTULO 2..... 68
1 Introduction..... 70
2 Materials and methods..... 72
3 Results..... 82
4 Discussion..... 102
5 Conclusion..... 107
4 DISCUSSÃO GERAL..... 108
5 CONCLUSÕES GERAIS..... 112
6 PERSPECTIVAS..... 113
REFERÊNCIAS..... 114
APÊNDICE A..... 127

1 INTRODUÇÃO

A doxorrubicina (DOX) é uma antraciclina citotóxica utilizada no tratamento de diversas condições neoplásicas, incluindo leucemias linfoblásticas e mieloblásticas agudas, sarcomas de tecidos moles e ossos, cânceres de mama, ovário e bexiga. Entretanto, sua eficácia é limitada pela baixa penetração em tumores sólidos, desenvolvimento de resistência pelas células tumorais e baixa seletividade, que resulta em efeitos adversos graves, como a cardiotoxicidade (Carvalho *et al.*, 2009; Tacar, Sriamornsak e Dass, 2013).

Sistemas nanocarreadores contendo DOX têm sido desenvolvidos com o intuito de aumentar sua eficácia e reduzir sua toxicidade. Os nanocarreadores podem melhorar a farmacocinética e o perfil de biodistribuição dos fármacos encapsulados, levando a um menor acúmulo em órgãos não-alvo e melhorando a entrega na região do tumor devido ao efeito de permeabilidade vascular aumentada e retenção das nanoestruturas no microambiente tumoral (Cagel *et al.*, 2017; Kanwal *et al.*, 2018).

Lipossomas encapsulando DOX foram os primeiros nanossistemas aprovados para terapia do câncer e demonstraram uma redução significativa no desenvolvimento da cardiotoxicidade em comparação à terapia convencional (fármaco em solução) (Barenholz, 2012; Boix-Montesinos *et al.*, 2021; Liu *et al.*, 2020). Entretanto, o alto custo dessas preparações e as limitações relacionadas ao processo de fabricação dos lipossomas, como a necessidade de uso de solventes orgânicos e dificuldades na etapa de esterilização, ainda permanecem um desafio (Toh e Chiu, 2013; Wu, Wang e Li, 2020).

Nesse sentido, os carreadores lipídicos nanoestruturados (NLC) têm se mostrado um sistema promissor e vantajoso para a entrega de fármacos quimioterápicos. Esses sistemas são compostos por uma matriz lipídica sólida desorganizada, na qual estão inseridos compartimentos de lipídios líquidos. Os NLC podem ser fabricados em escala industrial sem o uso de solventes orgânicos, permitem alta carga de fármaco e a natureza sólida da matriz lipídica aumenta a estabilidade e retenção do ativo em comparação com vesículas lipossomais e nanoemulsões

(Gordillo-Galeano e Mora-Huertas, 2018; Haider *et al.*, 2020; Weber, Zimmer e Pardeike, 2014).

Em sua forma comercial, a DOX é disponibilizada como um sal cloridrato a fim de aumentar sua solubilidade aquosa. Assim, o encapsulamento da DOX comercial (hidrofílica) em sistemas NLC é geralmente baixo e a formação de um par iônico hidrofóbico com um contra íon lipofílico tem sido proposta como uma alternativa para aumento da encapsulação (Gamboa *et al.*, 2020; Oliveira *et al.*, 2017; Ristroph e Prud'homme, 2019). Particularmente, o uso de um ânion lipofílico que também possui atividade anticâncer constitui uma alternativa interessante para aumento da encapsulação e, simultaneamente, da atividade antitumoral. Usando essa estratégia, nosso grupo de pesquisa já desenvolveu nanocarreadores encapsulando DOX por meio da formação de pares iônicos com o ácido docosahexaenóico (DHA) na forma de ácido graxo livre e com o succinato de α-tocoferol (TS) (Mussi *et al.*, 2013; Oliveira *et al.*, 2016a). O DHA é um ácido graxo poli-insaturado ômega-3 e o TS é um derivado lipofílico da vitamina E. Estudos anteriores já demonstraram que esses compostos podem aumentar a atividade citotóxica de vários fármacos anticâncer, incluindo a DOX (Neuzil, 2003; Siddiqui *et al.*, 2011).

Também visando aumento da atividade antitumoral, nosso grupo desenvolveu uma formulação NLC co-encapsulando DOX e DHA na forma de triglicerídeos. Nesse caso, o DHA foi utilizado como constituinte da matriz lipídica (lipídeo líquido) já que ele se apresenta como um óleo à temperatura ambiente. O par iônico DOX-ácido oleico foi utilizado para melhorar a eficiência de encapsulação da DOX no sistema (Mussi *et al.*, 2014).

Nesse contexto, o desenvolvimento de um sistema NLC contendo a combinação da DOX, DHA e TS poderia representar uma alternativa inovadora na terapia do câncer. Tanto o DHA quanto o TS podem ser utilizados como excipientes funcionais na composição da formulação: o DHA pode constituir a matriz lipídica enquanto o TS pode formar um par iônico hidrofóbico com a DOX. Essa associação poderia promover efeitos sinérgicos na ação antitumoral, além de combinar as vantagens proporcionadas pelo nanocarreador lipídico.

2 REVISÃO DA LITERATURA

2.1 Câncer

O câncer representa um conjunto diverso de doenças em que as células apresentam crescimento descontrolado e o potencial de se tornarem malignas por meio da aquisição de características aberrantes durante seu desenvolvimento. A carcinogênese é um processo crônico e complexo que envolve mutação e seleção de células com capacidade progressivamente crescente de proliferação, sobrevivência, invasão e metástase. Conceitualmente, esse processo pode ser dividido em quatro etapas: iniciação do tumor, promoção do tumor, conversão maligna e progressão do tumor (Abel e DiGiovanni, 2011; Bertram, 2000).

O processo pelo qual as células normais se transformam progressivamente em malignas exige a aquisição sequencial de mutações que surgem como consequência de danos ao genoma. Esses danos podem ser resultado de processos endógenos, como erros na replicação do DNA, instabilidade química intrínseca de certas bases do DNA ou o ataque de radicais livres gerados durante o metabolismo. Também podem ser resultado de interações com agentes exógenos, como a radiação ionizante, radiação UV e agentes químicos (Bertram, 2000).

O câncer é um dos principais problemas de saúde pública no mundo e já está entre as quatro principais causas de morte prematura (antes dos 70 anos de idade) na maioria dos países (Fane e Weeraratna, 2020). A crescente incidência e mortalidade por câncer reflete o envelhecimento e o crescimento populacional, bem como as mudanças na distribuição e prevalência dos fatores de risco para a doença, especialmente os associados ao desenvolvimento socioeconômico (Shirai e Iso, 2014). Dados da Organização Mundial da Saúde (OMS) apontam que, em todo o mundo, cerca de 19,3 milhões de novos casos e quase 10 milhões de mortes por câncer ocorreram em 2020. Como mostrado na Tabela 1, o câncer de mama feminino ultrapassou o câncer de pulmão como o mais comumente diagnosticado, com estimativa de 2,3 milhões de novos casos (11,7%), seguido pelo câncer de pulmão (11,4%), próstata (7,3%), cólon (6,0%) e estômago (5,6%). Por sua vez, o câncer de pulmão permaneceu como a principal causa de morte por câncer, com

uma estimativa de 1,8 milhões de mortes (18%), seguido pelo câncer de fígado (8,3%), estômago (7,7%), câncer de mama feminino (6,9%) e cólon (5,8%) (Sung *et al.*, 2021).

Tabela 1. Número de novos casos e mortes para os 10 tipos de câncer mais incidentes em todo o mundo em 2020.

Local do câncer	Nº de novos casos (% em relação ao total)		Nº de novas mortes (% em relação ao total)	
Mama feminino	2.261.419	(11,7)	684.996	(6,9)
Pulmão	2.206.771	(11,4)	1.796.144	(18,0)
Próstata	1.414.259	(7,3)	375.304	(3,8)
Cólon	1.148.515	(6,0)	576.858	(5,8)
Estômago	1.089.103	(5,6)	768.793	(7,7)
Fígado	905.677	(4,7)	830.180	(8,3)
Reto	732.210	(3,8)	339.022	(3,4)
Colo do útero	604.127	(3,1)	341.831	(5,5)
Esófago	604.100	(3,1)	544.076	(0,4)
Tireoide	586.202	(3,0)	43.646	(2,1)

Fonte: Adaptado de Sung *et al*., 2021.

O câncer é uma condição agressiva e difícil de ser tratada devido a vários motivos. Dentre eles, tem-se a heterogeneidade inter- e intra-tumoral e as mutações em centenas de genes diferentes que contribuem para a manutenção e progressão da doença. Além disso, o câncer pode afetar diferentes órgãos do corpo e uma ampla gama de células com características distintas, como as epiteliais, estromais e sanguíneas (Bidram *et al.*, 2019; Zugazagoitia *et al.*, 2016). Nos últimos anos, grandes avanços no tratamento do câncer foram alcançados graças a uma melhor compreensão do desenvolvimento da doença. A radioterapia, a remoção cirúrgica e a quimioterapia convencional permanecem como as modalidades tradicionais de tratamento do câncer. Por sua vez, novas estratégias terapêuticas incluem a imunoterapia, terapia fotodinâmica, terapia foto-térmica e a nanomedicina (Bidram *et al.*, 2019; Falzone, Salomone e Libra, 2018; Schirrmacher, 2019).

2.2 Doxorrubicina

A doxorrubicina (DOX, Figura 1) é um antibiótico citotóxico que foi extraído pela primeira vez da bactéria *Streptomyces peucetius var. césio* e desde a década de 1960 vem sendo amplamente utilizada como agente quimioterápico. Ela pertence à família das antraciclinas, que inclui também a daunorrubicina, idarrubicina, epirrubicina, entre outros. Até hoje a DOX permanece entre os agentes antineoplásicos mais prescritos e eficazes para o tratamento de uma variedade de cânceres adultos e pediátricos, incluindo leucemias linfoblásticas e mieloblásticas agudas, sarcomas de tecidos moles e ossos, cânceres de mama, ovário e bexiga, linfoma de Hodgkin e não Hodgkin, entre outros (Carvalho *et al.*, 2009; Tacar, Sriamornsak e Dass, 2013; Thorn *et al.*, 2011).

Figura 1. Estrutura química da DOX.

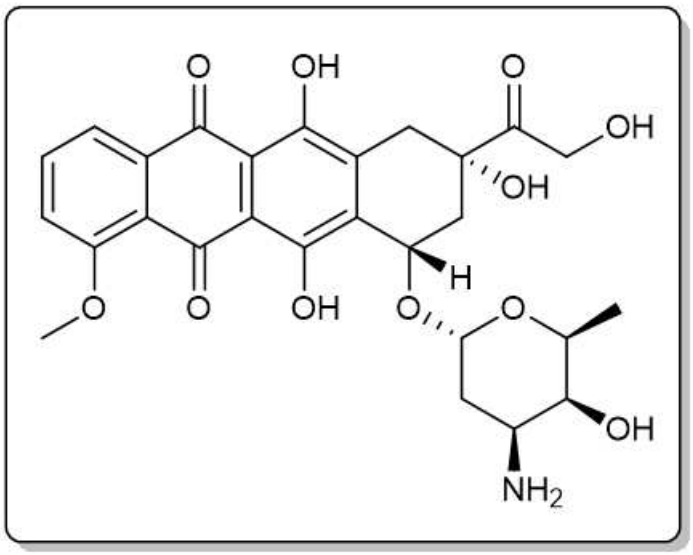

Vários mecanismos têm sido propostos para explicar a ação citotóxica da DOX e ainda não foram completamente elucidados. Os principais deles estão ilustrados na Figura 2 e são:

(i) alterações no DNA: o principal mecanismo da DOX baseia-se em sua capacidade de se ligar à enzima topoisomerase II formando um complexo estável, o que bloqueia a replicação do DNA e resulta na morte celular por apoptose. Além disso, a

DOX também pode se intercalar entre as fitas de DNA, levando a mudanças na estrutura da cromatina e desencadeando apoptose;

(ii) formação de radicais livres e espécies reativas de oxigênio (ROS): o estresse oxidativo é originado a partir da superprodução de ROS e redução nos níveis de antioxidantes, o que provoca danos ao material nuclear, proteínas e lipídios, podendo levar à morte celular;

(iii) alterações na membrana celular: a DOX pode diminuir a fluidez e organização lipídica das membranas biológicas. Isso ocorre devido à sua alta afinidade pelas membranas carregadas negativamente, o que permite que ela se ligue à membrana mitocondrial interna dando origem à peroxidação lipídica;

(iv) superprodução de ceramidas: a DOX é capaz de aumentar nas células tumorais os níveis de ceramidas, que constituem uma classe de lipídios endógenos envolvidos na apoptose, parada do crescimento e senescência das células (Kawase *et al.*, 2002; Nitiss, 2009; Yang *et al.*, 2014).

Todos esses mecanismos podem induzir uma série de eventos celulares que levam à interrupção do crescimento ou morte celular. Os principais eventos celulares desencadeados pela DOX consistem na apoptose, autofagia, senescência e necrose (Di *et al.*, 2009; Tacar, Sriamornsak e Dass, 2013). Recentemente, tem-se demonstrado que outras formas de morte celular regulada também são iniciadas pela DOX, como a necroptose, piroptose e ferroptose (Ma *et al.*, 2020).

Figura 2. Representação dos principais mecanismos responsáveis pela ação citotóxica da DOX.

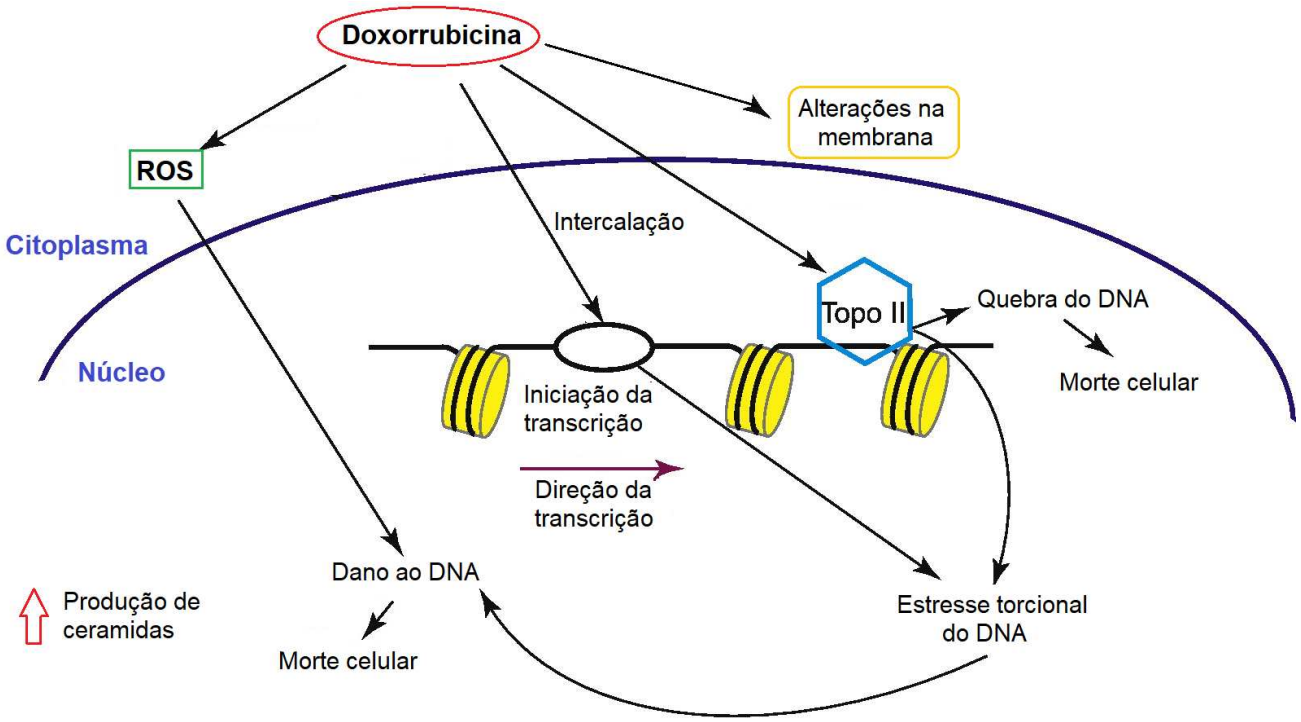

Fonte: Adaptado de Yang *et al.*, 2014

Embora seja um fármaco altamente potente e eficaz para o tratamento de diversos tumores, a utilização da DOX é limitada por seus efeitos adversos sistêmicos, como a supressão hematopoiética, náuseas, vômitos, alopecia, mucosite e cardiotoxicidade (Carvalho *et al.*, 2009; Santos e Goldenberg, 2018). A toxicidade cardíaca é o efeito mais relevante, sendo dose-dependente e muitas vezes irreversível. Os mecanismos moleculares responsáveis pelo dano cardíaco induzido pela DOX envolvem um conjunto de fatores complexos e que ainda não foram totalmente elucidados, incluindo a produção de radicais livres, dano ao DNA, acúmulo de ferro mitocondrial, diminuição da função mitocondrial, desregulação da homeostase de cálcio, alterações na estrutura sarcomérica, modulação da expressão gênica e apoptose (Kalyanaraman, 2020; Peres Diaz *et al.*, 2020).

Clinicamente, a cardiotoxicidade induzida pela DOX pode se manifestar de várias formas, que vão desde a alterações assintomáticas no eletrocardiograma até a cardiomiopatia descompensada, caracterizada por diminuição da fração de ejeção do ventrículo esquerdo (Cardinale, Iacopo e Cipolla, 2020; Santos e Goldenberg,

2018). Esses eventos cardiotóxicos podem ser classificados em três tipos, como demostrado na Tabela 2.

Tabela 2. Classificação da cardiotoxicidade induzida por antraciclinas.

Características	Cardiotoxicidade Aguda	Cardiotoxicidade crônica de início precoce	Cardiotoxicidade crônica de início tardio
Início	Durante ou dentro de 2 semanas após o tratamento com DOX	Dentro de 1 ano após a conclusão do tratamento com DOX	> 1 ano após a conclusão do tratamento com DOX
Dose-dependente	Desconhecido	Sim	Sim
Sinais clínicos	Redução da contratilidade miocárdica	Cardiomiopatia dilatada/ hipocinética	Cardiomiopatia dilatada/ hipocinética
Curso	Normalmente reversível	Normalmente irreversível; Refratário à terapia tradicional para insuficiência cardíaca; Prognóstico ruim	Normalmente irreversível; Refratário à terapia tradicional para insuficiência cardíaca; Prognóstico ruim

Fonte: Adaptado de Cardinale, Iacopo e Cipolla, 2020.

A fim de diminuir a incidência e principalmente a severidade dos efeitos tóxicos provocados pela DOX, sua encapsulação em sistemas nanocarreadores de fármacos tem sido amplamente proposta nas últimas décadas. Esses sistemas permitem aumentar a seletividade e eficácia do fármaco ao proporcionar o acúmulo preferencial nos tecidos-alvo, diminuindo assim os danos aos tecidos sadios. Dentre os sistemas mais promissores para encapsulação da DOX tem-se os lipossomas, os

carreadores poliméricos e as nanopartículas lipídicas, como será abordado adiante (Bobo *et al.*, 2016; Cagel *et al.*, 2017; Kanwal *et al.*, 2018).

2.3 Ácido docosahexaenóico

Vários estudos epidemiológicos já estabeleceram uma relação entre o consumo de peixes gordurosos com uma redução na incidência de certos tipos de câncer, como o câncer de mama, próstata e colorretal. Um dos principais componentes bioativos presente nos peixes gordurosos é o ácido docosahexaenóico (DHA, Figura 3), um ácido graxo poliinsaturado ômega-3 (Fabian, Kimler e Hursting, 2015; Ma *et al.*, 2015; Nabavi *et al.*, 2015). Quimicamente, o DHA é mais frequentemente encontrado ligado a uma estrutura lipídica complexa, como triglicerídeos, fosfolipídios ou éster de colesterol (Calder, 2016).

Figura 3. Estrutura química do DHA.

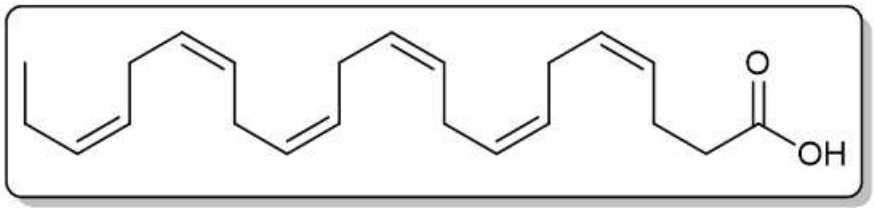

Embora o DHA possa ser sintetizado endogenamente a partir de lipídios precursores contendo ácido α-linolênico, este mecanismo não é muito eficiente, fazendo com que ele deva ser obtido principalmente pela dieta. Juntamente com os ácidos eicosapentaenóico e docosapentaenóico, o DHA é encontrado em quantidades bastante elevadas em frutos do mar e produtos derivados, como óleo de algas, fígado de peixe e óleo de krill (Calder, 2016; Riediger *et al.*, 2009).

Diversos estudos têm mostrado que o DHA pode modular as respostas celulares que levam à redução da viabilidade de células cancerígenas e diminuição da proliferação *in vitro* e *in vivo*. Os mecanismos responsáveis por sua ação antineoplásica ainda não foram completamente elucidados, mas os principais deles envolvem: (i) aumento do estresse oxidativo e produção de ROS, levando as células tumorais a apoptose; (ii) incorporação nas membranas celulares, causando

mudanças na fluidez, permeabilidade e composição lipídica; (iii) alteração na função de receptores de superfície celular, como o receptor do fator de crescimento epidérmico, levando à sinalização apoptótica e inibição do crescimento; (iv) regulação da expressão de genes pró-inflamatórios e produção de mediadores lipídicos pró-resolução, como as resolvinas, protectinas e maresinas (Berquin, Edwards e Chen, 2008; D'Eliseo e Velotti, 2016; Merendino *et al.*, 2013; Song e Kim, 2016).

Curiosamente, as células tumorais e sadias apresentam diferenças significativas não só na captação e distribuição do DHA, mas também em suas capacidades em gerar espécies reativas e estresse oxidativo. As células sadias podem utilizar o DHA para se proteger da apoptose induzida pelo estresse oxidativo, usando mecanismos que incluem a ativação da via de sobrevivência celular (PI3K/Akt) e o aumento na produção de mediadores citoprotetores, como as resolvinas e protectinas. Por outro lado, as células tumorais possuem níveis mais elevados de radicais de oxigênio em comparação com as células sadias e, na presença de DHA, aumentam a produção de hidroperóxidos lipídicos e outros peróxidos citotóxicos, levando a apoptose (D'Eliseo e Velotti, 2016; Song e Kim, 2016).

Também tem sido demonstrado que o DHA pode aumentar a sensibilidade de células tumorais, potencializando a eficácia de vários antineoplásicos, como a DOX, docetaxel, paclitaxel e bortezomibe (Chen, Garssen e Redegeld, 2021; Siddiqui *et al.*, 2011). Em geral, a indução da morte celular por estresse oxidativo e a supressão das vias de sobrevivência celular são os mecanismos mais relevantes para explicar seus efeitos sensibilizadores, principalmente se os fármacos usados em combinação com o DHA também induzem o estresse oxidativo (Serini *et al.*, 2017; Song e Kim, 2016).

A capacidade do DHA em reduzir a toxicidade de quimioterápicos, melhorando a tolerância aos fármacos e o prognóstico da doença, também tem sido amplamente reportada. Tem-se demonstrado que a suplementação com DHA pode prevenir ou aliviar efeitos adversos graves induzidos pelos antineoplásicos, incluindo a disfunção cognitiva, a neuropatia periférica e a cardiotoxicidade induzida por antraciclinas (Newell *et al.*, 2021; Serini *et al.*, 2016, 2017).

2.4 Succinato de α-tocoferol

O succinato de α-tocoferol (TS, Figura 4) é um derivado succínico do α-tocoferol e um dos compostos com atividade anticâncer mais proeminente na família da vitamina E (Neuzil, 2003; Prasad *et al.*, 2003). Os efeitos antineoplásicos do TS têm sido demonstrados frente a linhagens celulares originárias de diversos tecidos, incluindo câncer de mama, próstata, pulmão, ovário, estômago e cólon (Angulo-Molina *et al.*, 2014; Liang e Qiu, 2021; Neuzil, 2003). Curiosamente, a citotoxicidade do TS está amplamente restrita às células tumorais, com baixa ou nenhuma toxicidade para as células sadias, o que está relacionado com as maiores taxas de proliferação e maior susceptibilidade a apoptose nas células cancerígenas (Neuzil, 2003).

Figura 4. Estrutura química do TS.

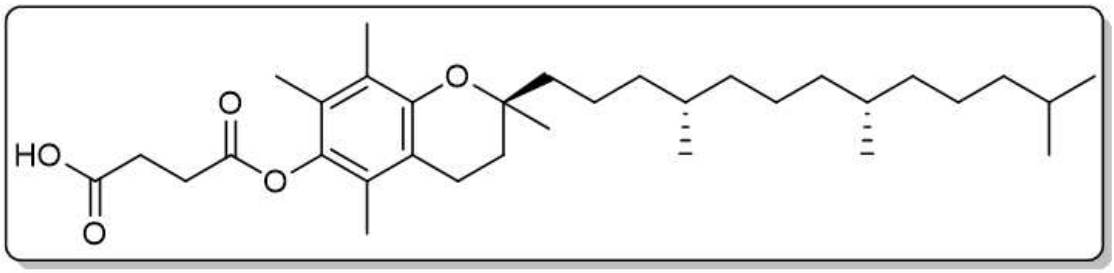

Os mecanismos pelos quais o TS exerce atividade antineoplásica ainda não foram completamente elucidados, mas os principais deles envolvem: (i) desestabilização mitocondrial e desregulação das vias de sinalização na mitocôndria, levando as células tumorais a apoptose; (ii) inibição da proliferação celular, principalmente prejudicando a síntese de DNA, bloqueando o ciclo celular e regulando fatores associados a diferenciação; (iii) inibição da angiogênese por meio da regulação da expressão de fatores de crescimento, como o fator de crescimento endotelial vascular e o fator de crescimento fibroblástico (Liang e Qiu, 2021; Neuzil, 2003; Neuzil *et al.*, 2007).

Assim como o DHA, o TS tem-se mostrado um promissor adjuvante na terapia anticâncer, uma vez que é capaz de potencializar a eficácia antitumoral de diversos

quimioterápicos, incluindo DOX, paclitaxel, metotrexato e cisplatina (Liang e Qiu, 2021; Wei *et al.*, 2019). Além disso, devido sua capacidade em produzir dano mitocondrial, o TS tem mostrado potencial para aumentar a sensibilidade ou reverter a resistência de células tumorais aos quimioterápicos convencionais, principalmente desencadeando a apoptose celular intrínseca e interrompendo o fornecimento de energia para os transportadores de efluxo, como a glicoproteína P (Liang, Peng e Qiu, 2021; Zhang *et al.*, 2011; Zheng *et al.*, 2021).

2.5 Sistemas nanocarreadores de fármacos

Os sistemas carreadores em nanoescala surgiram como uma estratégia para alterar a farmacocinética e a biodistribuição dos quimioterápicos encapsulados, aumentando o acúmulo na região do tumor e diminuindo a entrega aos órgãos não-alvo (Boix-Montesinos *et al.*, 2021; Peer *et al.*, 2007; Shi *et al.*, 2017). Mecanismos de direcionamento passivo e ativo, os quais estão relacionados às propriedades únicas dos nanossistemas e a características intrínsecas do tumor, permitem que os nanocarreadores atinjam a região tumoral de forma mais eficiente. O mecanismo passivo é baseado no efeito da Permeabilidade e Retenção Aumentada (EPR), que possibilita o acúmulo das nanoestruturas no tumor devido a vasculatura com fenestrações características e a ausência de drenagem linfática no microambiente tumoral (Figura 5A). Por sua vez, o direcionamento ativo envolve a fixação na superfície dos nanocarreadores de ligantes com alta afinidade para as células tumorais. O princípio dessa estratégia consiste em utilizar ligantes para os quais as células cancerígenas expressam uma grande quantidade de receptores específicos, enquanto as células normais expressam muito pouco. Uma grande variedade de ligantes tem sido utilizada para esse fim, incluindo o ácido fólico, ácido hialurônico e a transferrina (Figura 5B) (Borges *et al.*, 2021; Shi *et al.*, 2017; Wicki *et al.*, 2015).

Figura 5. Representação dos mecanismos de direcionamento passivo e ativo dos nanocarreadores.

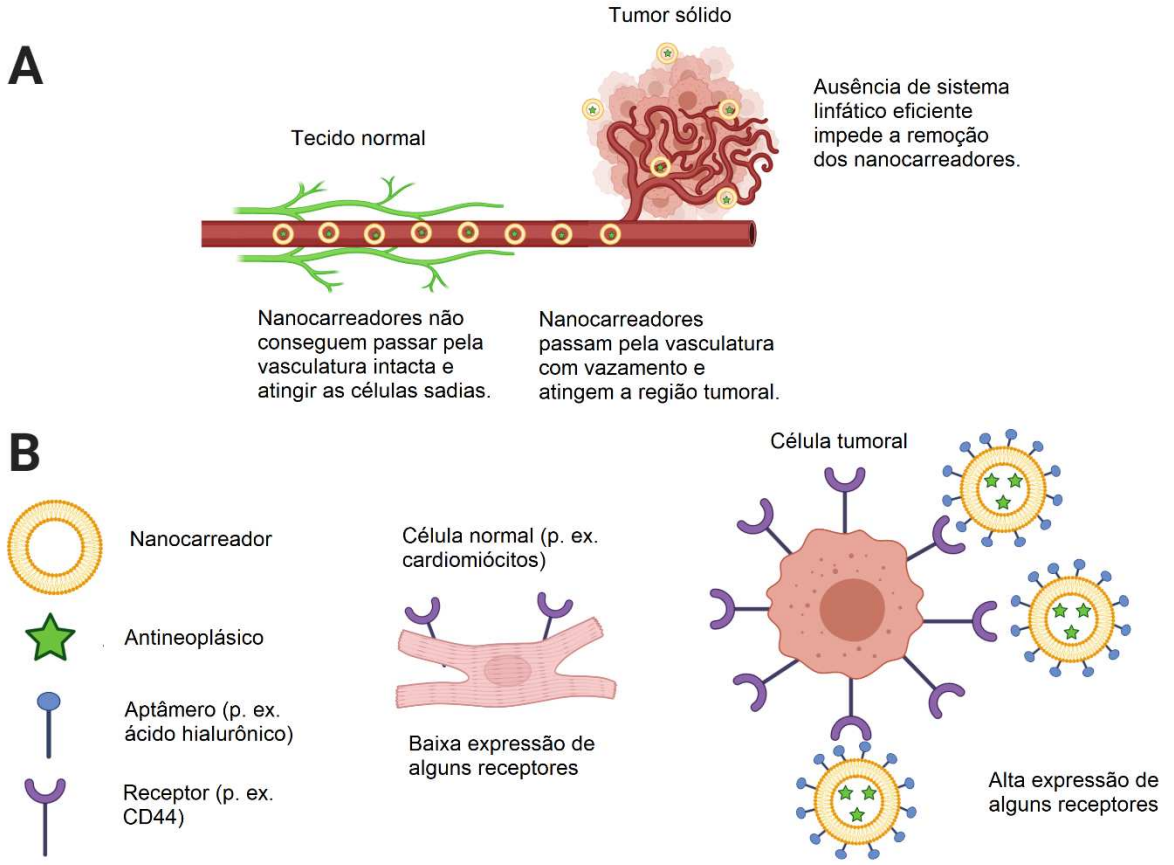

Fonte: Adaptado de Borges *et al.*, 2021.

O Doxil® foi o primeiro nanomedicamento anticâncer aprovado pelo FDA em 1995 e consiste em uma formulação lipossomal encapsulando DOX em seu núcleo aquoso. Ele representa uma terapia efetiva para o sarcoma de Kaposi e um tratamento de segunda linha para o câncer de mama metastático, câncer de ovário e mieloma múltiplo. Diversos ensaios clínicos demostraram que o Doxil® apresenta eficácia similar à DOX convencional (solução injetável), enquanto reduz significativamente o risco de desenvolvimento de cardiotoxicidade clínica associada ao tratamento (Barenholz, 2012; Boix-Montesinos *et al.*, 2021; Liu *et al.*, 2020). Apesar dos benefícios clínicos evidentes, novos efeitos adversos também surgiram com o uso do Doxil®, como a toxicidade cutânea (eritrodisestesia palmo-plantar), que ocorre devido ao tempo de circulação prolongado dos lipossomas e à alta tendência de acúmulo na pele, e também a pseudoalergia relacionada à ativação do complemento (Cagel *et al.*, 2017; Kanwal *et al.*, 2018; Liu *et al.*, 2020).

Atualmente, outros nanocarreadores já foram aprovados pelo FDA para o tratamento do câncer, incluindo fármacos como o paclitaxel, irinotecano e docetaxel. Embora os materiais aprovados pelo FDA sejam compostos principalmente pelos lipossomas, nanopartículas poliméricas e nanocristais, uma variedade enorme de novos nanocarreadores vem sendo estudada e testada em ensaios clínicos (Bobo *et al.*, 2016; Boix-Montesinos *et al.*, 2021). Dentre esses novos sistemas, os carreadores lipídicos nanoestruturados (NLC) podem ser considerados como uma das plataformas mais promissoras para a encapsulação e entrega de fármacos no combate ao câncer (Beloqui *et al.*, 2016; Haider *et al.*, 2020; Rizwanullah *et al.*, 2021; Salvi e Pawar, 2019; Selvamuthukumar e Velmurugan, 2012).

2.5.1 Carreadores lipídicos nanoestruturados

Os primeiros relatos de incorporação de fármacos lipofílicos em gotículas oleosas remetem à década de 1960, com o desenvolvimento de emulsões lipídicas parenterais que são hoje amplamente utilizadas para a aplicação de fármacos pouco solúveis em água, como o propofol e o diazepam (Weber, Zimmer e Pardeike, 2014). Posteriormente, no começo da década de 1990, o componente oleoso dessas emulsões foi substituído por um lipídeo sólido ou uma mistura de lipídeos sólidos, fazendo com que a matriz lipídica do sistema fosse sólida nas temperaturas ambiente e corporal. Esse sistema foi então nomeado de nanopartículas lipídicas sólidas (SLN). As SLN são compostas por uma fase lipídica dispersa em uma solução aquosa de tensoativos e apresentam diâmetro médio variável dentro da escala nanométrica (normalmente 40 a 1000 nm) (Gordillo-Galeano e Mora-Huertas, 2018; Weber, Zimmer e Pardeike, 2014).

As principais características das SLN consistem em boa estabilidade física, capacidade de proteção do fármaco incorporado contra a degradação, potencial de liberação controlada do fármaco e baixa toxicidade graças ao uso de lipídeos biocompatíveis e biodegradáveis. Além disso, as etapas de produção das SLN não requerem o uso de solventes orgânicos e podem ser facilmente escalonadas para a escala industrial. Por outro lado, entre as desvantagens mais relevantes desse sistema tem-se a baixa capacidade de carga de fármacos e o alto risco de expulsão

do fármaco encapsulado durante o armazenamento, que ocorre devido à reorganização da matriz lipídica para uma estrutura cristalina mais organizada e, portanto, com menos espaço para a acomodação do fármaco (Haider *et al.*, 2020; Müller, Radtke e Wissing, 2002; Weber, Zimmer e Pardeike, 2014).

A fim de superar as limitações apresentadas pelas SLN, uma nova geração de partículas lipídicas foi desenvolvida ainda no final da década de 1990 e denominada de carreadores lipídicos nanoestruturados (NLC). Os NLC são constituídos por uma mistura de lipídeos sólidos e líquidos em diferentes proporções, preferencialmente de 70: 30 até 99,9: 0,1, respectivamente. Dessa forma, a matriz lipídica do sistema ainda permanece sólida nas temperaturas ambiente e corporal, porém é menos ordenada e com mais espaços disponíveis (imperfeições na matriz lipídica) para acomodação do fármaco (Figura 6). Os NLC também oferecem maior estabilidade, uma vez que não permitem a recristalização dos lipídios sólidos e, assim, o tamanho da partícula e a encapsulação do fármaco são pouco alterados durante o armazenamento (Gordillo-Galeano e Mora-Huertas, 2018; Haider *et al.*, 2020; Müller, Radtke e Wissing, 2002; Subramaniam, Siddik e Nagoor, 2020).

Figura 6. Representação esquemática das diferenças na estrutura e carga de fármaco das SLN e NLC.

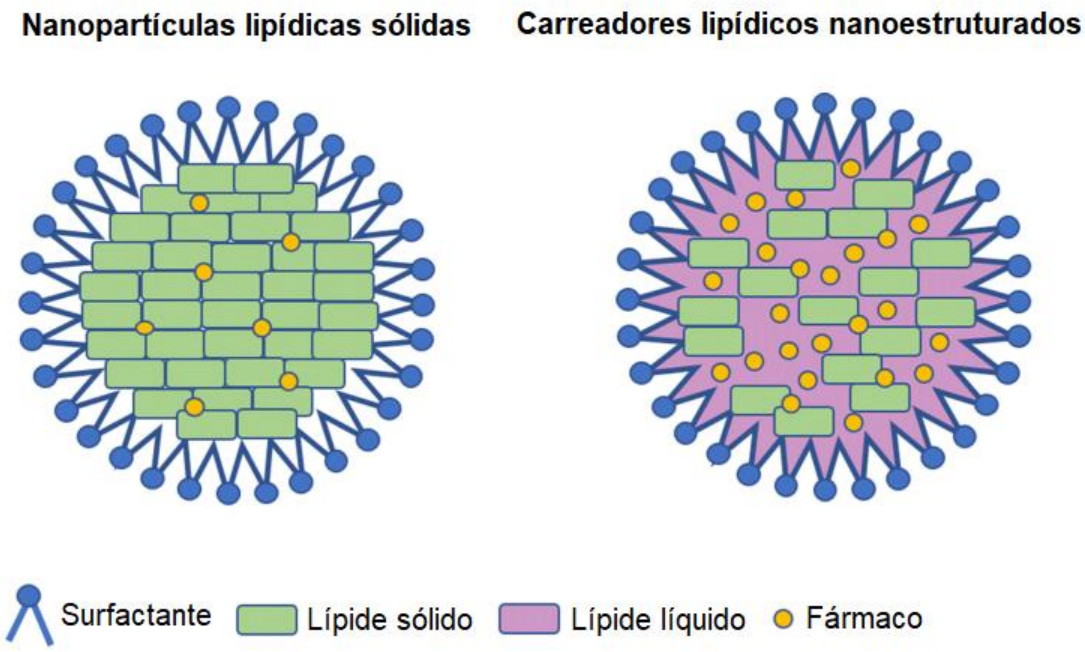

Fonte: Adaptado de Subramaniam, Siddik e Nagoor, 2020.

Até hoje, a maioria dos lipídios usados para a preparação dos NLC são excipientes inertes, sem nenhum papel ativo na prevenção ou tratamento de doenças. Entretanto, alguns estudos vêm descrevendo o uso de lipídios funcionais na composição desses sistemas, uma estratégia interessante já que eles poderiam tanto formar a matriz lipídica quanto desempenhar um papel terapêutico. Alguns exemplos dessa abordagem incluem o óleo de peixe (ácidos graxos ômega-3), óleo de sucupira e o óleo de semente de romã, todos eles com propriedades biológicas já estabelecidas (Lanna *et al.*, 2021; Mussi *et al.*, 2014; Talkar, Kharkar e Patravale, 2020; Vieira *et al.*, 2020).

2.5.2 Nanocarreadores lipídicos contendo doxorrubicina

A encapsulação da DOX em diferentes carreadores lipídicos, incluindo os lipossomas, SLN e NLC, tem sido proposta para melhorar a eficácia terapêutica e reduzir seus efeitos adversos. Essas formulações utilizam tanto estratégias de direcionamento passivo quanto ativo e visam a entrega de DOX isoladamente ou em combinação com mais fármacos para as células tumorais (Cagel *et al.*, 2017; Kanwal *et al.*, 2018; Shafei *et al.*, 2017). Dentre os nanocarreadores lipídicos, os NLC têm se mostrado uma alternativa interessante frente aos demais, principalmente pela facilidade de escalonamento, baixo custo de preparo e por dispensarem o uso de solventes orgânicos durante seu processo de fabricação (Beloqui *et al.*, 2016; Gordillo-Galeano e Mora-Huertas, 2018; Haider *et al.*, 2020).

Em sua forma comercial, o grupo amino da DOX é protonado pela formação do cloridrato de DOX com o intuito de aumentar sua solubilidade aquosa. Assim, o uso da DOX comercial (hidrofílica) normalmente resulta em baixa eficiência de encapsulação do fármaco em sistemas de matriz lipídica, como as SLN e NLC. Isso faz com que a conversão da DOX para a forma de base livre, a qual é mais lipofílica do que a forma de cloridrato, seja uma etapa usual na preparação desses sistemas (Mohan e Rapoport, 2010).

Uma abordagem alternativa e que será empregada nesse trabalho é baseada no pareamento iônico hidrofóbico, que surgiu como um método para modular a

solubilidade de moléculas hidrofílicas ionizáveis (Gamboa *et al.*, 2020; Oliveira *et al.*, 2017; Ristroph e Prud'homme, 2019). Essas moléculas podem se emparelhar por meio de interações iônicas com compostos hidrofóbicos de carga oposta, resultando em um complexo pouco solúvel em água e com alta afinidade pela matriz lipídica dos nanocarreadores. No caso da DOX, seu grupo amino catiônico (pKa = 9,53) é capaz de interagir eletrostaticamente com um composto hidrofóbico aniônico, como o ácido oleico, formando um par iônico que é encapsulado com maior eficiência em um nanossistema lipídico (Figura 7). Uma das principais vantagens dessa estratégia é a possibilidade de pH sensibilidade conferida pelo pareamento iônico, que pode resultar em desestabilização e liberação mais seletiva do fármaco no microambiente ácido do tumor (Oliveira *et al.*, 2016a; Zhao *et al.*, 2016).

Figura 7. Representação esquemática do par iônico DOX-ácido oleico encapsulado na matriz lipídica do nanocarreador.

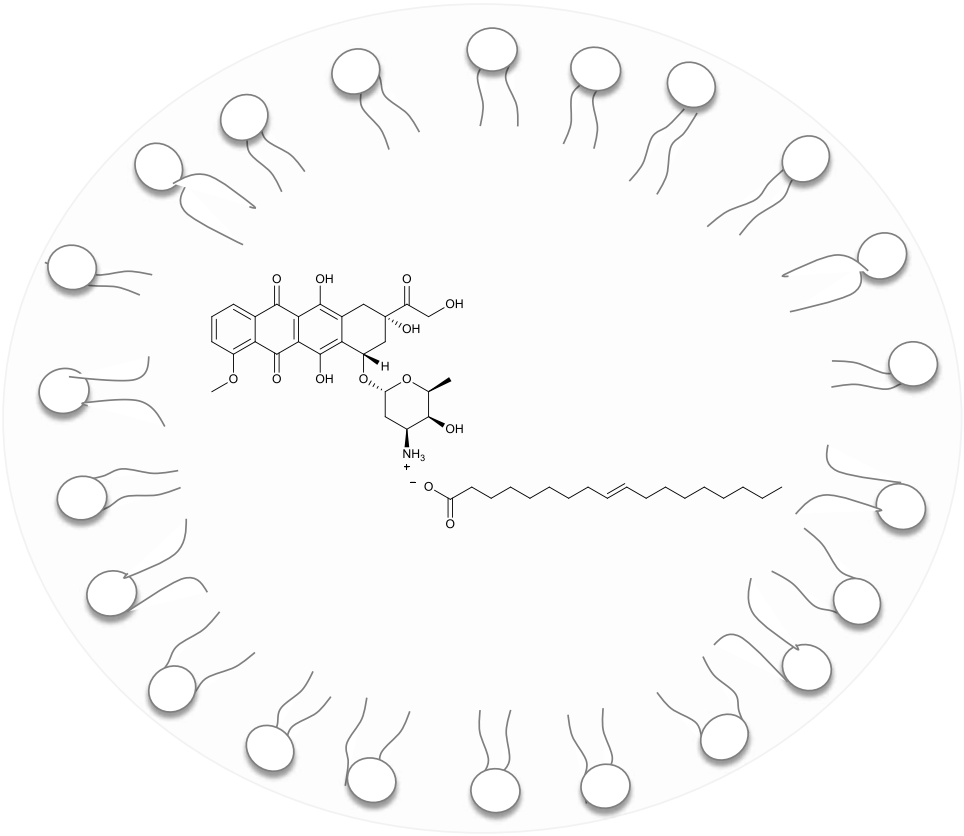

Utilizando essa estratégia, Zara *et al*. (1999) desenvolveram uma formulação SLN contendo DOX por meio da formação de um par iônico com o hexadecilfosfato. Após

administração endovenosa em camundongos, a formulação apresentou melhor farmacocinética e perfil de biodistribuição mais favorável em comparação à DOX livre (solução aquosa), resultando em maiores concentrações plasmáticas e menor acúmulo no fígado, coração e rins. Posteriormente, Serpe *et al*. (2004) reportaram que essa formulação SLN teve maior citotoxicidade *in vitro* e maior captação intracelular em células de câncer colorretal HT-29 do que o fármaco livre.

Zhang *et al*. (2011) sintetizaram o par iônico DOX-ácido oleico e o encapsularam em uma nanoemulsão lipídica, que apresentou maior citotoxicidade que a DOX livre contra células tumorais HepG2 e T2780. O nanossistema também mostrou um comportamento *in vivo* mais favorável do que a DOX livre, refletido em melhor farmacocinética e menor acúmulo nos rins e coração após administração endovenosa em camundongos. O par iônico DOX-ácido oleico também foi sintetizado por Zhao *et al*. (2016) e encapsulado em um sistema NLC. A formulação mostrou liberação controlada de DOX *in vitro*, com liberação aumentada em meio ácido, e maior captação intracelular em células de câncer de cólon humano HCT 116.

Battaglia *et al*. (2014) desenvolveram uma formulação SLN para potencial entrega de DOX às células de glioblastoma. Inicialmente, pares iônicos hidrofóbicos foram sintetizados utilizando-se diferentes contra íons aniônicos: dioctil sulfosuccinato de sódio, taurodeoxicolato de sódio e decanossulfonato de sódio. A encapsulação do par iônico DOX-dioctil sulfosuccinato de sódio no sistema SLN permitiu a maior eficiência de encapsulação de DOX, além de aumentar a citotoxicidade em comparação à DOX livre em três linhagens de glioma humano (CV17, 01010627 e U87).

Ma *et al*. (2009) também investigaram o potencial de diferentes contra íons para formar pares iônicos com a DOX: dextrano sulfato de sódio, taurodeoxicolato de sódio e tetradecil sulfato de sódio. O par iônico formado entre a DOX e o tetradecil fosfato de sódio apresentou a maior lipofilicidade e foi encapsulado em um sistema SLN. A formulação mostrou maior citotoxicidade *in vitro* contra células leucêmicas P388/ADR em comparação à DOX livre. A formulação também foi eficaz em um

modelo murino de leucemia (P388/ADR), além de aumentar o tempo de sobrevivência dos animais.

Na última década, nosso grupo de pesquisa vem utilizando a formação de pares iônicos hidrofóbicos para encapsular a DOX em sistemas lipídicos SLN e NLC. Duas estratégias particularmente interessantes são utilizadas: (i) a primeira consiste na formação de pares iônicos *in situ*, durante o preparo da formulação; (ii) a segunda estratégia consiste na co-encapsulação da DOX com adjuvantes quimioterápicos, o que pode aumentar sua eficácia e reduzir sua toxicidade.

Nesse sentido, Mussi *et al*. (2013) desenvolveram uma formulação SLN que apresentou alta eficiência de encapsulação da DOX devido à formação de um par iônico com o DHA (Figura 8). O par iônico foi formado pela adição de trietanolamina à composição da formulação. O sistema SLN contendo DOX-DHA mostrou liberação controlada da DOX *in vitro*, com liberação aumentada em pH ácido, e maior citotoxicidade do que a combinação dos fármacos livre contra células de câncer de pulmão A549.

Posteriormente, Mussi *et al*. (2014) também encapsularam a associação DOX e DHA em um sistema NLC. Nesse caso, o DHA foi utilizado na forma de triglicerídeos para compor a matriz lipídica do sistema (lipídeo líquido). Já o par iônico DOX-ácido oleico foi obtido *in situ* e permitiu alta eficiência de encapsulação da DOX. Estudos celulares *in vitro* demonstraram maior captação intracelular e maior citotoxicidade do nanossistema em células MCF-7/ADR do que a DOX livre, sugerindo uma supressão do efluxo relacionando à atividade da glicoproteína-P. A administração repetida dessa formulação em camundongos portadores de tumor de mama 4T1 resultou em baixo crescimento tumoral e baixa toxicidade em comparação com a DOX livre (Fernandes *et al.*, 2018a).

Figura 8. Representação esquemática da formação e encapsulação do par iônico DOX-DHA na matriz lipídica da SLN.

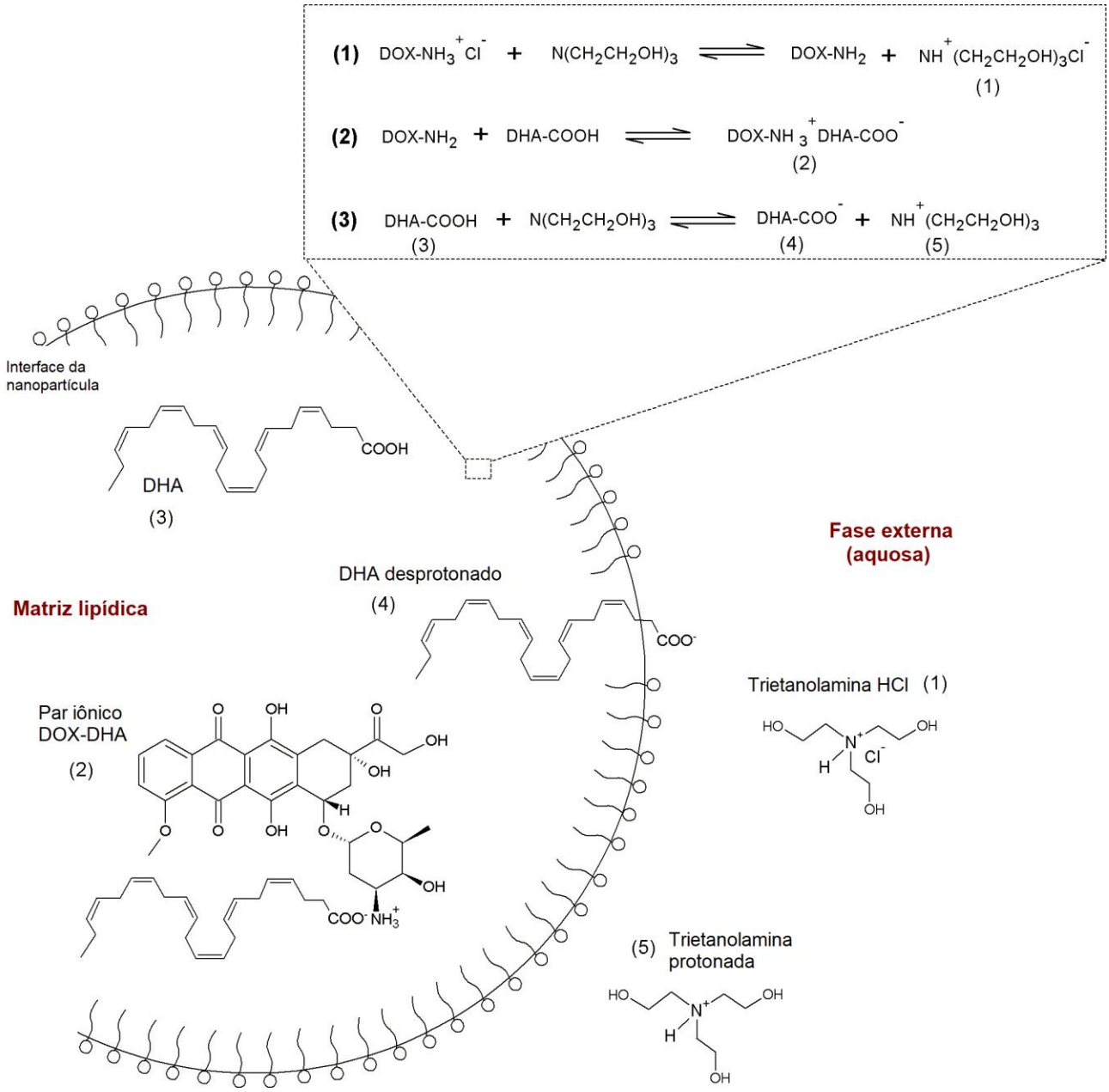

Fonte: Adaptado de Mussi *et al*., 2013.

Oliveira *et al*. (2016a) desenvolveram um sistema SLN para co-entrega de DOX e do adjuvante TS. Os autores reportaram o uso do TS como um contra íon aniônico capaz de formar um par iônico hidrofóbico com a DOX. Um aumento na eficiência de encapsulação da DOX de 30% para 96% foi alcançado pela adição de 0,4% de TS na composição da formulação. O sistema mostrou liberação controlada da DOX *in*

vitro e maior citotoxicidade do que a DOX livre em linhagens celulares de câncer de mama 4T1 e MDA-MB-231. Dados posteriores também revelaram efeitos citotóxicos maiores para o nanocarreador em comparação ao fármaco livre em células tumorais resistentes MCF-7/ADR e NCI/Adr, sugerindo uma reversão da bomba de efluxo relacionado à glicoproteína-P (Oliveira *et al.*, 2016b). Fernandes *et al*. (2018b) confirmaram o efeito sinérgico da combinação entre os compostos em um modelo murino de tumor de mama 4T1, já que a administração de um sistema NLC encapsulando o par iônico DOX-TS resultou em alta eficácia antitumoral e menor toxicidade em comparação com o nanossistema contendo apenas DOX ou a DOX livre.

Diante do exposto, o desenvolvimento e avaliação do potencial terapêutico de um sistema NLC contendo a combinação da DOX com os adjuvantes DHA e TS mostrou-se uma abordagem interessante. Essa associação poderia promover efeitos sinérgicos na ação antitumoral, além de combinar as vantagens proporcionadas pelo nanocarreador. O DHA na forma de triglicerídeos apresenta-se líquido à temperatura ambiente, podendo ser utilizado para compor a matriz lipídica do NLC. O TS, por sua vez, pode formar um par iônico hidrofóbico com a DOX, aumentando a eficiência de encapsulação no nanossistema.

Embora a estratégia de pareamento iônico hidrofóbico venha consistentemente apresentando resultados satisfatórios *in vitro*, poucos estudos *in vivo* têm sido realizados até o momento. A investigação da farmacocinética tem se mostrado uma etapa crítica e permanece como a principal perspectiva para os próximos anos (Oliveira *et al.*, 2017). Assim, adicionalmente ao preparo da formulação baseada na formação do par iônico DOX-TS, esse trabalho propõe a síntese de conjugados covalentes DOX-TS como uma estratégia para melhoria do perfil farmacocinético do sistema.

3 OBJETIVOS

3.1 Objetivo geral

Desenvolver, caracterizar e avaliar o potencial terapêutico no tratamento do câncer de um sistema NLC contendo DOX, DHA e TS.

3.2 Objetivos específicos

- Preparar uma formulação NLC encapsulando a combinação de DOX, DHA e TS;
- Realizar estudos de caracterização da formulação quanto ao tamanho de partícula, índice de polidispersão, potencial zeta, eficiência de encapsulação e morfologia;
- Avaliar o perfil de liberação *in vitro* da DOX a partir do sistema NLC;
- Sintetizar e caracterizar o par iônico DOX-TS quanto sua solubilidade aquosa e cristalinidade;
- Sintetizar e caracterizar conjugados covalentes DOX-TS por meio de ligações amida e hidrazona;
- Avaliar a citotoxicidade e captação da formulação em células de câncer de mama 4T1;
- Avaliar a farmacocinética da formulação após administração endovenosa em camundongos;
- Investigar a eficácia antitumoral da formulação em camundongos portadores de tumor de mama 4T1;
- Investigar a toxicidade sistêmica da formulação em camundongos portadores de tumor de mama 4T1.

CAPÍTULO 1

Co-delivery of doxorubicin, docosahexaenoic acid, and α-tocopherol succinate by nanostructured lipid carriers has a synergistic effect to enhance antitumor activity and reduce toxicity

Eduardo Burgarelli Lages, Renata Salgado Fernandes, Juliana de Oliveira Silva, Ângelo Malachias de Souza, Geovanni Dantas Cassali, André Luís Branco de Barros, Lucas Antônio Miranda Ferreira

Artigo publicado em Biomedicine & Pharmacotherapy, v. 132, 110876, 2020.

Abstract

Doxorubicin (DOX) is widely used in cancer treatment, however, its use is often limited due to its side effects. To avoid these shortcomings, the encapsulation of DOX into nanocarriers has been suggested. Herein, we proposed a novel nanostructured lipid carrier (NLC) formulation loading DOX, docosahexaenoic acid (DHA), and α-tocopherol succinate (TS) for cancer treatment. DHA is an omega-3 fatty acid and TS is a vitamin E derivative. It has been proposed that these compounds can enhance the antitumor activity of chemotherapeutics. Thus, we hypothesized that the combination of DOX, DHA, and TS in NLC (NLC-DHA-DOX-TS) could increase antitumor efficacy and also reduce toxicity. NLC-DHA-DOX-TS was prepared using emulsification-ultrasound. DOX was incorporated after preparing the NLC, which prevented its degradation during manufacture. High DOX encapsulation efficiency was obtained due to the ion-pairing with TS. This ion-pairing increases lipophilicity of DOX and reduces its crystallinity, contributing to its encapsulation in the lipid matrix. Controlled DOX release from the NLC was observed *in vitro*, with increased drug release at the acidic environment. *In vitro* cell studies indicated that DOX, DHA, and TS have synergistic effects against 4T1 tumor cells. The *in vivo* study showed that NLC-DHA-DOX-TS exhibited the greatest antitumor efficacy by reducing tumor growth in 4T1 tumor-bearing mice. In addition, this formulation reduced mice mortality, prevented lung metastasis, and decreased DOX-induced toxicity to the heart and liver, which was demonstrated by hematologic, biochemical, and histologic analyses. These results indicate that NLC-DHA-DOX-TS may be a promising carrier for breast cancer treatment.

Keywords: doxorubicin, combination therapy, ion-pairing, synergism, antitumor activity, cardiotoxicity.

1 Introduction

Doxorubicin (DOX) is a cytotoxic anthracycline widely used to treat solid tumors and hematologic malignancies, such as acute lymphoblastic leukemia, metastatic breast cancer, and metastatic bone sarcomas (Carvalho *et al.*, 2009; Tacar, Sriamornsak e Dass, 2013). Despite the high antitumor activity, DOX causes cumulative and dose-dependent cardiotoxicity, ranging from occult changes in myocardial structure and function to severe cardiomyopathy and congestive heart failure, which restricts its use in clinical practice (McGowan *et al.*, 2017). In addition, drug resistance is another obstacle that limits the clinical use of DOX, because it often results in therapy failure (Tacar, Sriamornsak e Dass, 2013).

DOX-based nanocarriers have been designed to reduce adverse effects and overcome drug resistance since they offer several advantages due to their design, selectivity, and stability in the cancer microenvironment. The entrapment of DOX in nanocarriers can prevent its degradation in circulation, enhance pharmacokinetic profile, and alter biodistribution ultimately reducing its accumulation and toxicity in the heart (Cagel *et al.*, 2017; Kanwal *et al.*, 2018). In addition, nanoparticles can pass through the leaky blood vessels of the tumor and passively accumulate within the target site via enhanced permeability and retention (EPR) effect, which can result in superior therapeutic activity (Park *et al.*, 2019).

Doxil®, a DOX-loaded liposomal formulation, was the first FDA-approved nanocarrier for clinical application as an anticancer agent. At present, several commercial formulations of DOX-loaded liposomes are available (Kanwal *et al.*, 2018). The decreased risk for the cardiotoxicity of liposomes combined with its comparable efficacy to free DOX has made it an alternative therapy in cancer treatment. However, new toxicity issues have also arisen with these formulations, such as palmar-plantar erythrodysesthesia and the complement activation-related pseudo-allergy. Besides, it has been demonstrated that the cellular uptake of the liposomes is limited in the tumor microenvironment and the release rate of DOX from the nanocarrier is slow (Cagel *et al.*, 2017).

Nanostructured lipid carriers (NLC) are promising drug delivery systems that have attracted expanding attention in recent years. They were proposed as the second generation of lipid nanocarriers to surpass the limitations of solid lipid nanoparticles (SLN). The lipid matrix in NLC is composed of a blend of solid and liquid lipids that results in a partially crystallized lipid system and imparts many advantages over SLN, including enhanced drug loading capacity, minimized drug expulsion, more controlled drug release, and improved stability (Beloqui *et al.*, 2016; Gordillo-Galeano e Mora-Huertas, 2018).

Our research group has successfully incorporated DOX into NLC, obtaining systems with excellent physicochemical properties, such as high encapsulation efficiency, particle size less than 100 nm, and controlled DOX release. An interesting strategy used by us is the co-encapsulation of DOX with an adjuvant, which can enhance DOX activity, leading to increased antitumor efficacy and reduced toxicity (Borges *et al.*, 2019; Fernandes *et al.*, 2018a,b). Continuing our efforts, we proposed a novel nanocarrier combining DOX, docosahexaenoic acid (DHA), and α-tocopherol succinate (TS) for cancer therapy.

DHA, an omega-3 polyunsaturated fatty acid, has been shown to enhance the cytotoxic activity of several anticancer drugs, especially by increasing the sensitivity of cancer cells and producing oxidative damage species (Fabian, Kimler e Hursting, 2015; Mahéo *et al.*, 2005; Siddiqui *et al.*, 2011). In addition, cardioprotective effects have been attributed to DHA, which can be extremely useful when used in combination therapy with DOX (Adkins e Kelley, 2010; Serini *et al.*, 2017). The ability of TS, a vitamin E derivative, to enhance the efficacy of other anticancer drugs and to protect normal cells from chemotherapy-induced toxicity has also been described (Lee *et al.*, 2015; Neuzil, 2003; Zhang *et al.*, 2011). Hence, we suggested that the combination of DOX, DHA, and TS in NLC could be an effective strategy to fight cancer because of the passive tumor targeting, the ability to sensitize cancer cells, and the protective role against adverse effects.

In our previous reports, we evaluated the antitumor activity *in vivo* of DOX-DHA- and DOX-TS-loaded NLC (Fernandes *et al.*, 2018a,b). Both formulations showed increased efficacy and reduced toxicity compared to free DOX. Therefore, we

proposed that both DHA and TS could be used as adjuvants in a DOX-loaded formulation. Both DHA and TS have interesting properties that justify their use in the formulation composition: DHA is a liquid lipid that can form the lipid matrix of NLC and TS is an anionic counterion that can form a hydrophobic ion-pair with DOX. Moreover, these compounds are inexpensive, have no adverse effects, and have been found to enhance DOX activity.

Herein, we report the assembly of NLC loading DOX, DHA, and TS (NLC-DHA-DOX-TS) and its physicochemical characterization. *In vitro* studies in 4T1 breast cancer cells were performed to investigate the synergistic effects of this combination, cytotoxicity, and drug uptake. Then, the *in vivo* antitumor activity and preliminary toxicity of this nanocarrier were evaluated in a breast tumor model.

2 Materials and methods

2.1 Materials

Doxorubicin hydrochloride (DOX) was obtained from ACIC Chemicals (Ontario, Canada). α-Tocopherol succinate (TS) and ethylenediaminetetraacetic acid sodium (EDTA) were purchased from Sigma-Aldrich (St. Louis, USA). Triethanolamine (TEA) was obtained from Merck (Darmstadt, Germany). Compritol® 888 ATO (a mixture of mono-, di-, and triglycerides of behenic acid) was kindly provided by Gattefossé (Saint-Priest, France). Super refined Polysorbate 80™ (Tween 80) and docosahexaenoic acid (DHA) as triglyceride (OmeRx™ DHA 500TG) were kindly provided by Croda Inc. (Edison, USA). RPMI 1640 medium, fetal bovine serum, and trypsin-EDTA (0.25%) were purchased from Gibco-Invitrogen (Grand Island, USA). All other chemicals and reagents used in this study were of analytical grade.

2.2 Preparation of NLC

NLC loading DOX, DHA, and TS, alone or combined, were prepared. DHA was used in a triglyceride form (OmeRx™ DHA 500TG) to compose the lipid matrix of the nanocarrier. An ion pair between DOX and TS was formed *in situ* to increase DOX encapsulation efficiency. We proposed two strategies for DOX incorporation: the first

using the conventional emulsification-ultrasound method, in which DOX was added to the oily phase; and the second, incubating DOX with a previously prepared NLC. Briefly, the oily phase (Compritol 110 mg; DHA 40 mg; Tween 80 100 mg; TS 40 mg; TEA 6 mg; with or without DOX 10 mg) and the aqueous phase (EDTA 4 mg; ultrapure water 8 mL) were heated, separately, to 80 ºC. With the temperature maintained at 80 ºC, the aqueous phase was gently dropped onto the oily phase under constant agitation, at 8000 rpm, with an Ultra Turrax T-25 homogenizer (Ika Labortechnik, Germany). The formed emulsion was immediately submitted to a high-intensity probe sonication for 10 min (CPX 500 model, Cole-Palmer Instruments, USA). After this period, the formulations were cooled down to room temperature with manual agitation and the volume was adjusted to 10 mL with ultrapure water. To incorporate DOX using the incubation method, the drug (10 mg) was incubated with the blank NLC under magnetic agitation at room temperature for 10 min. All formulations were stored at 4 °C, protected from light in a nitrogen atmosphere.

2.3 Characterization of NLC

2.3.1 Size distribution and shape

The mean particle size and zeta potential (ZP) were measured by dynamic light scattering (DLS) and DLS coupled with electrophoretic mobility, respectively, using Zetasizer Nano-ZS90 (Malvern Instruments, UK) with a fixed angle (90º) laser beam at 25 ºC. The formulations were diluted in ultrapure water 100-times before the analyses. All experiments were performed in triplicate. The data were reported as average size, polydispersity index (PDI), and ZP. Particle size distribution was also assessed by nanoparticle tracking analysis (NTA), carried out with a NanoSight NS300 (Malvern Instruments, UK). Data collection and analysis were performed using NTA 3.1 software. NLC was diluted 1×10^5 times in ultrapure water and introduced into the sample chamber with a disposable syringe. The analyses were executed at room temperature for 60 s with automatic detection. All measurements were performed in triplicate. The morphology of nanocarriers was examined by transmission electron microscopy (TEM) using a negative staining method. Before analysis, the sample was diluted 50-times in ultrapure water and placed on a Formvar-copper grid. After washing with water, the grid was stained with 2% (w/v) aqueous uranyl acetate, dried at room temperature overnight and then observed

using a transmission electron microscope (Tecnai G2-12, 120 kV, FEI, Hillsboro, USA). Particle sizes were estimated using the Image J software (US National Institutes of Health, Bethesda MD), and the Gaussian distribution of particle sizes was constructed.

2.3.2 Drug content and encapsulation efficiency (EE)

The DOX content and %EE in NLC were determined as previously described by our research group, without modifications (Borges *et al.*, 2019). TS concentration in the nanocarrier was determined by HPLC. Briefly, the separation was carried out on a Zorbax Eclipse XDB-C18 column (250 x 4.6 mm, 5 µm), using a mixture of acetonitrile: water (95:5) containing 0.1% phosphoric acid as the mobile phase with a flow rate of 1.2 mL/min. The injection volume was 20 µL and UV detection was performed at 205 nm. To evaluate the total TS concentration, an aliquot of NLC was dissolved first in THF and then, in the mobile phase before injection in HPLC. To evaluate the non-encapsulated TS, an aliquot of NLC was submitted to filtration (polyvinylidene fluoride membrane, 0.45 µm pore size, Millipore, USA). In this way, precipitated TS, which was not properly incorporated into the NLC, was removed by filtration. Afterward, the filtered formulation was dissolved first in THF, then in the mobile phase and injected in HPLC. The TS concentration in the aqueous phase of the NLC was evaluated using centrifugal devices (Amicon® Ultra-4 100 kDa, Millipore, USA). As expected, the values were negligible since TS is a highly hydrophobic drug. Therefore, TS %EE was calculated using the following equation: $\%EE = C_{AF}/C_T \times 100$. Where: C_T = total TS concentration in NLC and C_{AF} = TS concentration after filtration of the NLC in 0.45 µm pore size membrane.

2.3.3 *In vitro* DOX release

In vitro DOX release study was performed using the dialysis method. Dialysis tubes with a cutoff size of 14 kDa and diameter of 21 mm (cellulose ester membrane; Sigma–Aldrich, St Louis, USA) were filled with 2 mL of formulation, sealed, and incubated with 50 mL of phosphate-buffered saline (PBS; pH 7.4 and 6.8) for 24 h at 37 °C, under magnetic stirring at 250 rpm. An aqueous solution of DOX (1.0 mg/mL) was used as a control (free DOX). At various time points, aliquots were withdrawn

and DOX concentration was determined by HPLC, as previously described (Borges *et al.*, 2019). The values were plotted as a cumulative percentage of DOX released, calculated according to the following equation: Released DOX (%) = $C_R/C_T \times 100$. Where: C_R = released fraction of DOX to the external medium and C_T = total initial concentration of DOX inside the dialysis bag at the beginning.

2.3.4 Differential scanning calorimetry (DSC)

NLC formulations were lyophilized prior to analysis using a freeze-dryer (E-C Apparatus, USA; Pump Edwards E2M18, UK). Dipping the vial containing the NLC preparation into liquid nitrogen performed rapid freezing of the sample. The samples were lyophilized for 24 h at a temperature of -45 °C. DSC analyses were performed using a DSC 2910 differential scanning calorimeter (TA Instruments, USA). For DSC measurements, a scan rate of 10 °C/min was used at a temperature range of 0-300 °C, under a nitrogen purge (50 mL/min). Lyophilized NLC and raw materials (Compritol and DOX) were placed directly in aluminum pans for DSC analyses.

2.3.5 Small-angle X-ray scattering (SAXS)

SAXS measurements were carried out at the SAXS1 beamline of the National Synchrotron Light Laboratory (LNLS, Brazil), at a fixed X-ray wavelength (λ = 0.1488 nm, E = 8.332 keV). The scattered X-ray photons were detected using a Pilatus 300K detector, covering a momentum transfer reciprocal space range of $0.5 < q < 4.5$ nm^{-1}; where $q = (4\pi/\lambda) \sin(2\theta/2)$, and 2θ is the scattering angle. Lyophilized NLC were deposited on metal rings, which were sealed by a polyimide film (Kapton). The lattice spacing (d) was calculated using the formula $d = 2\pi/q$, which was determined for the first-order peaks of all structure types analyzed in this study.

2.4 Preparation and characterization of the ion pair

The formation of an ion pair *in situ*, during NLC preparation, was described by our group to increase DOX encapsulation (Oliveira *et al.*, 2016a). Herein, we prepared the ion pair between DOX and TS to demonstrate that it has different properties compared to the raw materials. In brief, DOX was dissolved in distilled water, and

then a small volume of $NaHCO_3$ solution was added (1:3, M_{DOX}:M_{NaHCO3}). After vigorous stirring for 5 min, DOX free base was extracted three times with dichloromethane, followed by solvent evaporation under reduced pressure at 35 °C to collect the product. DOX free base and TS, at a molar ratio of 1:1, were dissolved in dichloromethane. DOX-TS ion pair was obtained by stirring at room temperature for 24 h, followed by removal of the solvent under reduced pressure. The ion pair was dried under high vacuum for 3 h at room temperature and stored at 4 ºC. SAXS analyses of DOX, TS, and DOX-TS were performed using a PAN analytical X-ray generator PW 17110 (PANalytical, Netherlands), equipped with a copper anode (Cu Kα radiation, λ = 0.15418 nm). DSC curves were obtained as described above. To compare the lipophilicity of DOX and DOX-TS, their aqueous solubility was also evaluated. An excess amount of DOX-TS was dispersed in distilled water, and then the supersaturated solution was shaken at 150 rpm at 25 °C. Since DOX has a high aqueous solubility, a 5 mg/mL solution was prepared instead of a supersaturated solution. At 24 h later, all samples were centrifuged at 10,000 g for 15 min. The supernatant was diluted in methanol and the concentration of soluble DOX was determined by HPLC, as previously described (Borges *et al.*, 2019).

2.5 Cell culture

4T1 cells, a murine breast cancer cell line, were purchased from ATCC® (ATCC® CRL-2539, American Type Culture Collection, USA). Cells were grown and maintained in RPMI medium supplemented with FBS (10% v/v), penicillin (100 IU/mL), and streptomycin (100 µg/mL) in a 5% CO_2 atmosphere at 37 ºC.

2.6 Cytotoxicity assay and synergism analysis

Cell viability was assessed using the sulforhodamine B (SRB) assay as published elsewhere (Fernandes *et al.*, 2018b). The effects of DOX, DHA, and TS encapsulated alone or combined in NLC were evaluated. Briefly, 4T1 cells were seeded in 96-well plates (5×10^3 cells/well) at 24 h before treatment. Then, cells were exposed to a range of concentrations of NLC-DHA, NLC-DOX, NLC-TS, NLC-DHA-DOX-TS, and blank-NLC. After 48 h of incubation, 10% trichloroacetic acid (TCA) was added to each well to fix cells for one hour. Then, plates were washed with water

to remove TCA and stained with SRB for 30 min. Afterward, the plate was washed with 1% acetic acid to remove the unbound SRB. Then, 10 mM Tris-Base solution (pH 10.5) was added to solubilize the protein-bound dye, and the optical density was read at 510 nm using a microplate spectrophotometer Spectra Max Plus 384 (Molecular Devices, Sunnyvale, CA, USA). All experiments were performed in triplicate and IC_{50} values were calculated with GraphPad Prism® 6 software. Synergism or antagonism between DOX, DHA, and TS encapsulated in NLC was calculated with the CompuSyn® software (Biosoft, Cambridge, UK) through the analysis of the combination index (CI). Assuming 1.0 as the cutoff, CI < 1.0, CI = 1.0, or CI > 1.0 indicates synergistic, additive, or antagonistic effects, respectively (Chou, 2006).

2.7 *In vitro* cellular uptake

4T1 cells were seeded in 12-well plates (1×10^6 cells/well) at 24 h before treatment. The cells were then exposed to free DOX and NLC-DHA-DOX-TS, both with the same concentration of DOX (3.2 µg/mL), for 1 h, 2 h, 4 h, 8 h, and 24 h incubation. Afterward, all medium was removed carefully, cells were washed twice with PBS, and detached by trypsinization. The suspension was centrifuged at 800 g for 5 min at room temperature. The pellet was washed with PBS and resuspended in 1.0 mL of isopropanol. The samples were kept in an ultrasound bath for 15 min to promote cell disruption. Finally, the cell lysate was centrifuged at 5,000 g for 15 min at room temperature, and the DOX concentration in the supernatant was analyzed by HPLC, as previously described (Borges *et al.*, 2019). The percentage of DOX uptake was calculated by using the following equation: DOX Uptake (%) = $C_I/C_T \times 100$. Where: C_I = intracellular concentration of DOX in different times and C_T = total concentration of DOX added to the cells.

2.8 Evaluation of antitumor activity

In vivo studies were conducted under the approval of the local Ethics Committee on Animal Use (CEUA) (Protocol 310/2018) following the National Institutes of Health guide for the care and use of Laboratory Animals. BALB/c mice (female, 8-weeks old,

18-22 g) were kept in an environment with controlled light cycle and ventilation and allowed free access to food and water.

Cultured 4T1 cells (2.5×10^6 cells in 100 µL PBS) were collected and injected subcutaneously into the right thigh of BALB/c mice to establish the tumor-bearing mouse model. When tumor volume reached approximately 150 mm^3, they were randomly divided into 4 groups (n = 6 mice per group): NLC-DHA-DOX-TS, NLC-DOX (loading only DOX), free DOX (DOX solution), and blank-NLC (without DOX, DHA, and TS). For all treatments, the DOX dose was 5 mg/kg/day, in a total of 5 administrations, every 2 days, injected by the tail vein. Hence, the total dose of DOX in the treatment groups was 25 mg/kg.

Antitumor efficacy was determined by measuring the tumor volume (TV) with a fine caliper (Mitutoyo, MIP/E-103) every two days, from the first day of treatment (D0) until two days after the last administration (D10). It was calculated according to the following equation: $TV = 0.5 \times d1 \times (d2)^2$, where d1 and d2 being the largest and the smallest perpendicular diameters, respectively. The relative tumor volume (RTV) and the inhibition ratio (IR) were calculated on day 10 according to the equations: RTV = TV on D10 / TV on D0 and IR = 1 - (RTV from each treated group / RTV of blank-NLC group) × 100.

2.9 Toxicity evaluation

Throughout the study, mice were observed and behavioral/clinical modifications, body weight, and mortality were evaluated. The body weight was monitored every two days, and the weight variation was calculated according to the initial weight of each animal. On the last day of the study (D11), mice were anesthetized with a mixture of ketamine (80 mg/kg) and xylazine (15 mg/kg) and blood was collected by puncture of the brachial plexus in tubes containing an anticoagulant (0.1% w/v EDTA). Hematologic and biochemical analyses were performed as described elsewhere (Boratto *et al.*, 2020). After blood collection, the animals were euthanized and the heart, spleen, lungs, kidneys, and tumor were removed for histopathological examination. Samples were fixed in 10% buffered formalin for 48 h, dehydrated in alcohol, and included in paraffin blocks. Five-micrometer sections were obtained and

stained with hematoxylin and eosin. The slides were evaluated by trained pathologists and images were captured by a camera connected to an optical microscope (Olympus BX-40; Olympus, Tokyo, Japan).

2.10 Statistical analysis

Statistical analyses were performed using GraphPad Prism software (version 6.00, La Jolla, California, USA). The difference between the experimental groups was tested by Student's t-test or one-way ANOVA followed by Tukey's test. For all analyses, it was adopted the confidence range of 95%, and differences were considered significant when the p-value was less than 0.05 ($p < 0.05$).

3 Results and discussion

3.1 Selection of the DOX incorporation method

NLC was prepared by the hot melting homogenization method using emulsification-ultrasound. We proposed two procedures to incorporate DOX into the nanocarrier: the first using the conventional method of emulsification-ultrasound, in which DOX was added to the oily phase at the beginning of the procedure; and the second, incubating DOX with a previously prepared NLC. The use of the first procedure resulted in DOX degradation during the manufacturing process. Thus, the total content of DOX was around 82% after NLC preparation (Table 1). Indeed, the HPLC assay of this formulation revealed an evident peak of a degradation product, eluting around 6.5 min, in the chromatogram from the ultrafiltration (Fig. 1A). On the other hand, the incubation of DOX with a previously prepared NLC was able to prevent drug degradation, possibly by avoiding DOX exposure to heat and high-intensity sonication. Furthermore, the incubation method reduces some of the safety concerns that arise when manufacturing cytotoxic formulations, limiting these concerns to the DOX incorporation step. This is a great advantage compared to the first method, in which all stages of NLC production must be executed under safe conditions. Based on this, Wehbe *et al*. proposed a simple passive equilibration method for loading the anticancer drug carboplatin into preformed liposomes (Wehbe *et al.*, 2017). DOX encapsulation in gold nanoparticles has also been described using this strategy,

through the preparation of resveratrol gold nanoparticles and the subsequent addition of DOX to the preformed system (Mohanty, Thennarasu e Mandal, 2014).

Table 1. Influence of the DOX incorporation method (emulsification-ultrasound or incubation) on the mean size, PDI, zeta potential, total content, and EE of NLC-DHA-DOX-TS.

Parameters	NLC-DHA-DOX-TS	
	Emulsification-ultrasound	Incubation
Mean size (nm)	85 ± 3	78 ± 2
PDI	0.22 ± 0.01	0.19 ± 0.01
Zeta potential (mV)	- 41 ± 1	- 42 ± 2
Total content $_{DOX}$ (%)	82 ± 2	101 ± 2[a]
EE $_{DOX}$ (%)	81 ± 2	100 ± 1[a]
Total content $_{TS}$ (%)	100 ± 1	100 ± 2
EE $_{TS}$ (%)	98 ± 2	98 ± 1

Notes: Results expressed as the mean ± standard deviation (n = 3). [a] Represents a significant difference between groups. These analyses were performed by Student's t-test ($p < 0.05$).

Abbreviations: PDI: polydispersity index; EE: encapsulation efficiency; DOX: doxorubicin; TS: α-tocopherol succinate; NLC-DHA-DOX-TS: nanostructured lipid carriers loading doxorubicin, docosahexaenoic acid, and α-tocopherol succinate.

The influence of the DOX incorporation method on the drug release profile was evaluated and the results are shown in Fig. 1B. Both at pH 7.4 and 6.8, the two formulations showed the same DOX release profile, indicating no differences between them and suggesting that DOX was equally inserted in the lipid matrix.

Fig. 1. NLC characterization. (A) Chromatograms of DOX ultrafiltration analyses in NLC. DOX was incorporated into the NLC by the methods of emulsification-ultrasound or incubation. (B) *In vitro* release studies of free and encapsulated DOX, in PBS medium (pH 7.4 and 6.8), at 37 °C, by dialysis (data represented as mean ± SD, n = 3). (C) Transmission electron microscopy image of NLC. (D)

Gaussian distribution of particle sizes estimated following transmission electron microscopy.

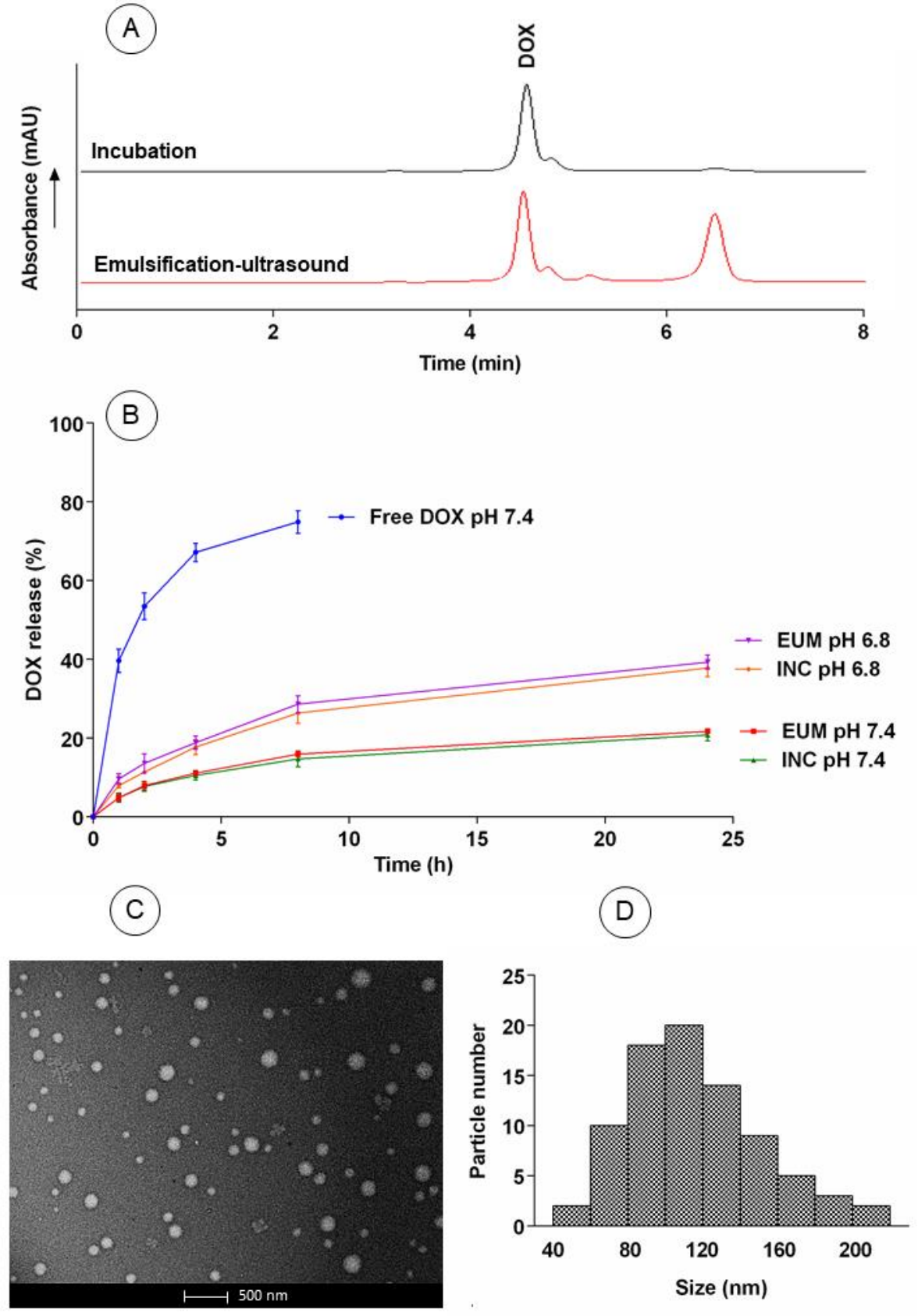

Abbreviations: NLC: nanostructured lipid carriers; DOX: doxorubicin; Free DOX: doxorubicin solution; PBS: phosphate buffer saline; EUM: emulsification-ultrasound method; INC: incubation method; SD: standard deviation.

To further confirm this hypothesis, SAXS analysis were carried out in order to verify possible structural differences between the two formulations. SAXS diffractograms of NLC prepared by both methods were similar (see Fig. S1). NLC submitted to the methods of emulsification-ultrasound and incubation presented a scattering peak at q close to 1.0 nm^{-1}, with a lattice spacing of 6.70 ± 0.05 nm and 6.64 ± 0.05 nm, respectively. Again, the data suggest that there is no difference in the structural organization of the lipid matrix and probably in the location of DOX in the NLC. Considering these results and the mentioned advantages, the incubation method to incorporate DOX into the NLC was selected for further studies.

Fig. S1. SAXS diffractograms of NLC. DOX was incorporated into the NLC by the methods of emulsification-ultrasound or incubation.

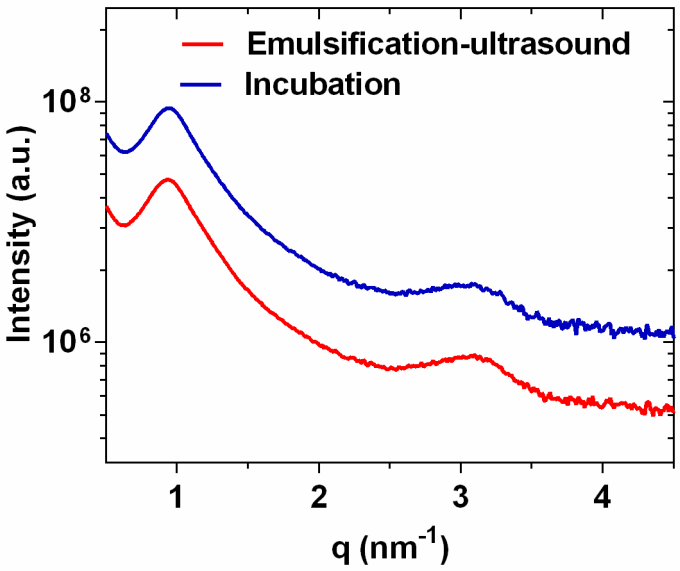

Abbreviations: SAXS: small-angle X-ray scattering; DOX: doxorubicin; NLC: nanostructured lipid carriers.

3.2 NLC characterization

The particle size, PDI, and zeta potential data are presented in Table 1. The average size was close to 80 nm with narrow size distribution (PDI < 0.30), suggesting a monodisperse system. The zeta potential was highly negative, likely due to the excess of ionized TS on the surface of NLC. Nanoparticle size distribution was also evaluated by NTA. The average diameter measured by NTA (81 ± 4 nm) was similar to that determined by DLS. In addition, the size distribution profile of NLC (90% < 168 nm, 50% < 100 nm, 10% < 78 nm) confirmed the narrow distribution as previously observed. Morphological analysis of the NLC was performed by TEM. In general, the particles showed spherical morphology, with dense content and visible boundary (Fig. 1C). The estimated particle sizes ranged from 50 to 220 nm, with a mean size close to 100 nm, and presented a normal distribution, indicated by the Kolmogorov-Smirnov test (Fig. 1D). These results confirmed a single population of particles as demonstrated by DLS and NTA.

DOX %EE was determined by the ultrafiltration method using centrifugal devices. A high DOX encapsulation, close to 100%, was observed (Table 1). This might be attributed to the ion-pairing between DOX and TS, as previously described by our group (Oliveira *et al.*, 2016a). Oliveira *et al*. showed an increase in DOX %EE into SLN from 30% to 96% after the addition of 0.4% TS in the formulation composition. DOX presents an amino group in its glycosidic moiety that can form an ion pair with the acid group of TS, as shown in Fig. 2A. This ion-pairing enhances the hydrophobicity of the conjugate, improving DOX encapsulation. In fact, the aqueous solubility of the DOX-TS ion pair was significantly lower than that observed to DOX (Fig. 2B). Regarding the total content of TS and TS %EE, the values were found to be close to 100% (Table 1). In fact, TS is a hydrophobic molecule and was expected to be properly incorporated into the lipid matrix of the NLC.

NLC was assessed for *in vitro* DOX release at pH 7.4 and 6.8, as previously described and shown in Fig. 1B. The drug release from aqueous solution (free DOX) was around 75% after 8 h. The high release ratio of the DOX solution was already expected since the drug can pass freely through the dialysis membrane (cutoff size: 14 kDa). At physiological pH, a low release of DOX from NLC was observed, reaching 21% up to 24 h. In contrast, at pH 6.8, a release of 9% of DOX occurs within 1 h and approximately 39% was released up to 24 h. The faster release of

DOX at pH 6.8, when compared to pH 7.4, might be explained by the increased protonation of the carboxyl group from TS (pKa 5.64) with pH reduction, which decreases the ion-pairing interaction and, consequently, reduces the DOX retention in the lipid matrix. Moreover, lowering pH decreases the distribution coefficient (log D) of DOX, favoring its partition into the aqueous phase and, thus, increasing its release rate. Several authors have shown that the ion-pairing strategy can retain the drug encapsulated in the nanocarrier after intravenous administration, resulting in improved pharmacokinetics (Zara *et al.*, 1999; Zhang *et al.*, 2013; Zhao *et al.*, 2013). Then, the drug release would be accelerated by the relatively low pH surrounding the tumor tissue or by the acidic environment inside the endosomes and lysosomes of tumor cells, favoring the target release of DOX from the NLC (Oliveira *et al.*, 2016a; Zhao *et al.*, 2016).

Fig. 2. Ion pairing effects. (A) Chemical structure representing the ion-pairing between DOX and TS. (B) Aqueous solubility and macroscopic appearance of DOX and DOX-TS ion-pair (data represented as mean ± SD, n = 3). (C) Influence of ion pairing on DSC curves of NLC. (D) DSC curves and (E) SAXS diffractograms of raw (dry) DOX and TS, as well as the dispersed DOX-TS ion pair. (F) Influence of ion pairing on SAXS diffractograms of NLC formulations.

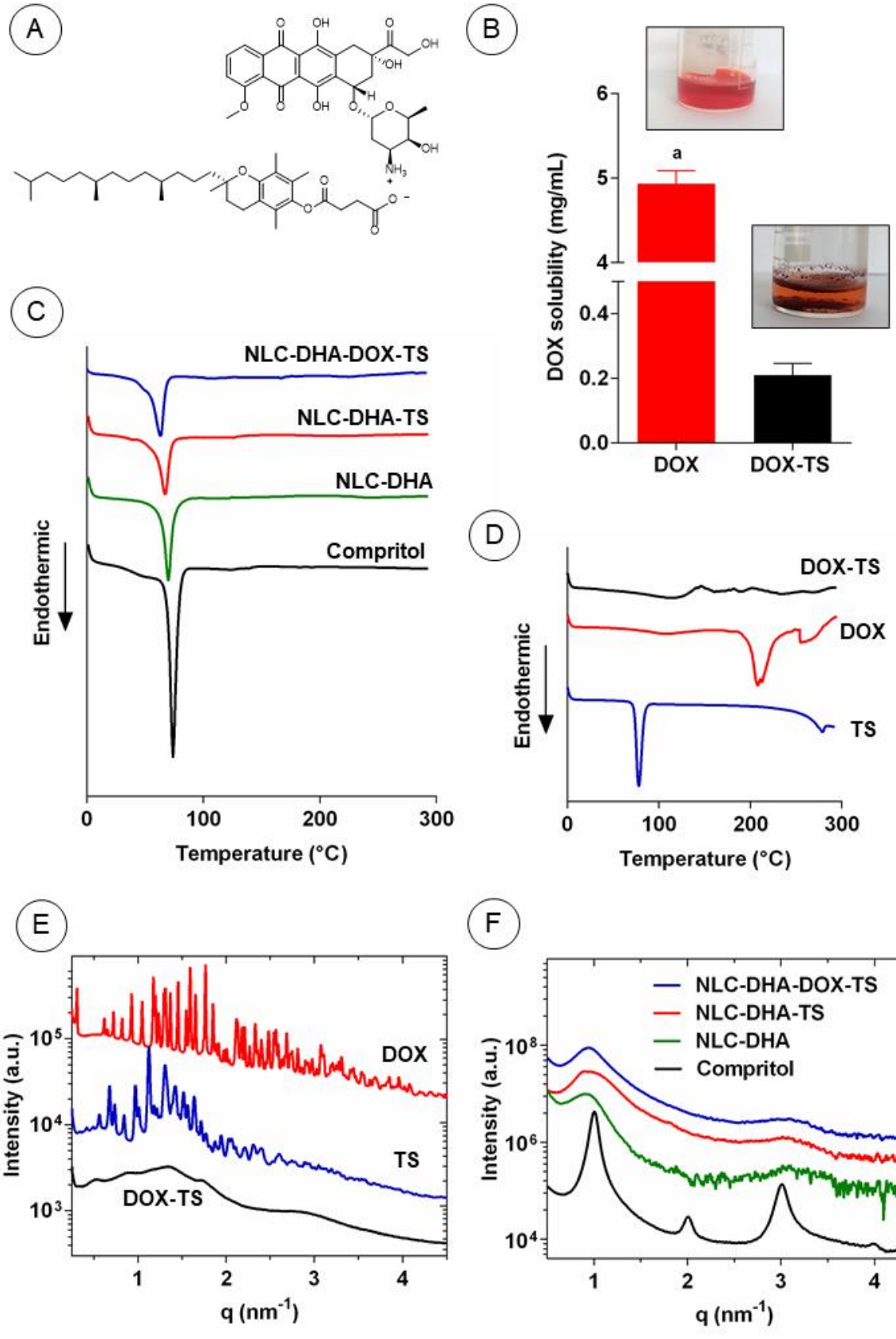
A
B
DOX solubility (mg/mL)
a
DOX
DOX-TS
C
NLC-DHA-DOX-TS
NLC-DHA-TS
NLC-DHA
Compritol
Endothermic
Temperature (°C)
D
DOX-TS
DOX
TS
Endothermic
Temperature (°C)
E
Intensity (a.u.)
DOX
TS
DOX-TS
q (nm-1)
F
NLC-DHA-DOX-TS
NLC-DHA-TS
NLC-DHA
Compritol
Intensity (a.u.)
q (nm-1)

Abbreviations: DOX: doxorubicin; TS: α-tocopherol succinate; DSC: differential scanning calorimetry; NLC: nanostructured lipid carriers; SAXS: small-angle X-ray scattering; NLC-DHA: nanostructured lipid carriers loading docosahexaenoic acid; NLC-DHA-TS: nanostructured lipid carriers loading docosahexaenoic acid and α-tocopherol succinate; NLC-DHA-DOX-TS: nanostructured lipid carriers loading doxorubicin, docosahexaenoic acid, and α-tocopherol succinate; SD: standard deviation.

In order to understand the influence of ion pairing on the structure of the NLC lipid matrix, DSC and SAXS measurements were performed. NLC loading DOX, DHA, and TS, alone or combined, were prepared. As shown in Fig. 2C, all the NLC exhibited lower melting temperature values than Compritol raw material as well as a gradual broadening of this peak (74 °C for pure lipid, 70 °C for NLC-DHA, 67 °C for NLC-DHA-TS, and 65 °C for NLC-DHA-DOX-TS). This indicates that the crystallinity of Compritol is higher in its bulk form than in NLC. Moreover, these results show that the addition of TS to the formulation (NLC-DHA-TS) induces modifications in the lipid matrix that can be further increased when DOX is also added (NLC-DHA-DOX-TS). Similar findings were described by Zhao *et al*. for NLC loading DOX and oleic acid (Zhao *et al.*, 2016). The authors suggested that the ion-pairing between DOX and oleic acid forms more liquid nano compartments of oil in the solid matrix of NLC and this shift would promote drug solubility and further increase the total drug loading capacity. DSC analyses also provided strong evidence of the ion pair formation since the endothermal peaks of DOX and TS disappeared in the DSC curve of DOX-TS (Fig. 2D). DOX endothermal peak was also absent in the DSC curve of NLC, in which only the melting point of Compritol could be observed (see Fig. S2). These findings indicate that DOX and TS exist as a molecular dispersion into the NLC and not in their crystalline forms. In fact, we used SAXS to demonstrate a significant reduction in the crystallinity of DOX and TS when the ion pair between them was formed in comparison to the raw materials (Fig. 2E). Raw (dry) DOX and TS exhibit several narrow peaks which are related to their own (bulk) crystalline structure, while dispersed DOX-TS only exhibit shallow and smooth intensity humps along the probed q-range, indicating poor local order and/or amorphization of the compounds.

Fig. S2. DSC curves of Compritol, DOX, and NLC-DHA-DOX-TS.

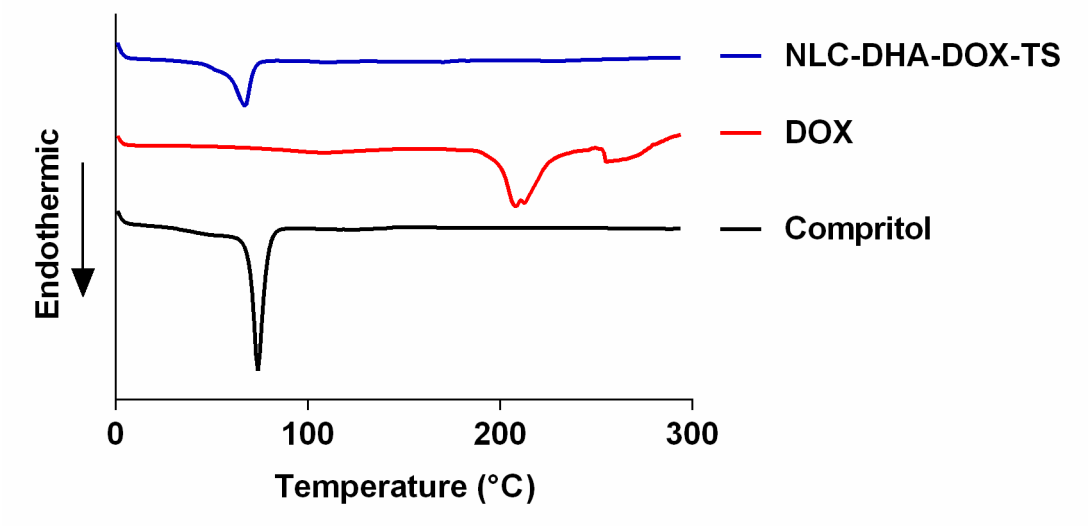

Abbreviations: DSC: differential scanning calorimetry; DOX: doxorubicin; NLC-DHA-DOX-TS: nanostructured lipid carriers loading doxorubicin, docosahexaenoic acid, and α-tocopherol succinate.

The lower crystallinity of NLC was also evidenced by SAXS analyses, in which NLC showed broad peaks of supramolecular structure, with decreased intensity compared to the lamellar organization of Compritol observed in SAXS diffractograms (Fig. 2F). Compritol exhibited a periodicity of Bragg reflections with ratios close to 1, 2, 3, and 4, while the NLC showed only two scattering peaks with ratios close to 1 and 3, indicating systems with lower degree of lamellar organization (Fernandes *et al.*, 2018b). Lattice spacings of Compritol powder and NLC were calculated and the following values were found: 6.86(5) nm for Compritol, 6.88(5) nm for NLC-DHA, 7.01(5) nm for NLC-DHA-TS, and 6.64(5) nm for NLC-DHA-DOX-TS. These values were in good agreement with literature data for the raw material and Compritol-based systems (Borges *et al.*, 2019; Castro *et al.*, 2009). Compared to NLC-DHA, an enlargement in lattice spacing was observed when TS was added, increasing the value from 6.88(5) nm to 7.01(5) nm. This shift suggests that TS interacted with the lipid matrix and increased the repulsion between lamellae, possibly induced by its negative charge. On the other hand, the insertion of DOX into the system was able to neutralize part of the TS charges, due to the ion pairing, promoting the approximation between lamellae and shading light onto the smallest lattice spacing for NLC-DHA-DOX-TS. These findings are consistent with previous studies, which reported the ion-pairing triggered structural changes in the lipid matrix of nanocarriers (Castro *et al.*,

2009; Zhao *et al.*, 2016). These results are also in agreement with the DSC curves and the high DOX %EE values, supporting the hydrophobic ion pairing as a strategy to increase the encapsulation of hydrophilic drugs.

3.3 Cell viability and synergism analysis

The cytotoxicity of DOX, DHA, and TS, encapsulated in NLC, was investigated using 4T1 breast cancer cells. Blank-NLC had no effects on the cell viability and showed a similar result to the non-treated cells, indicating negligible toxicity of the formulation excipients (data not shown). As demonstrated in Fig. 3A, while DHA and TS alone did not inhibit cell proliferation, when both were combined with DOX (at the same concentrations above), a slight reduction in cell viability was observed compared to DOX alone.

Fig. 3. *In vitro* studies in 4T1 tumor breast cancer cells. (A) Cytotoxicity of NLC formulations loading DOX, DHA, and TS, alone or combined. (B) Fa-CI plot for the NLC-DOX-DHA, NLC-DOX-TS, and NLC-DHA-DOX-TS formulations. (C) DOX uptake percentage after exposure to free DOX and NLC at different times. All data represented as mean ± SD (n = 3). Different letters indicate statistically significant differences between the groups. These analyses were performed by Student's t-test ($p < 0.05$).

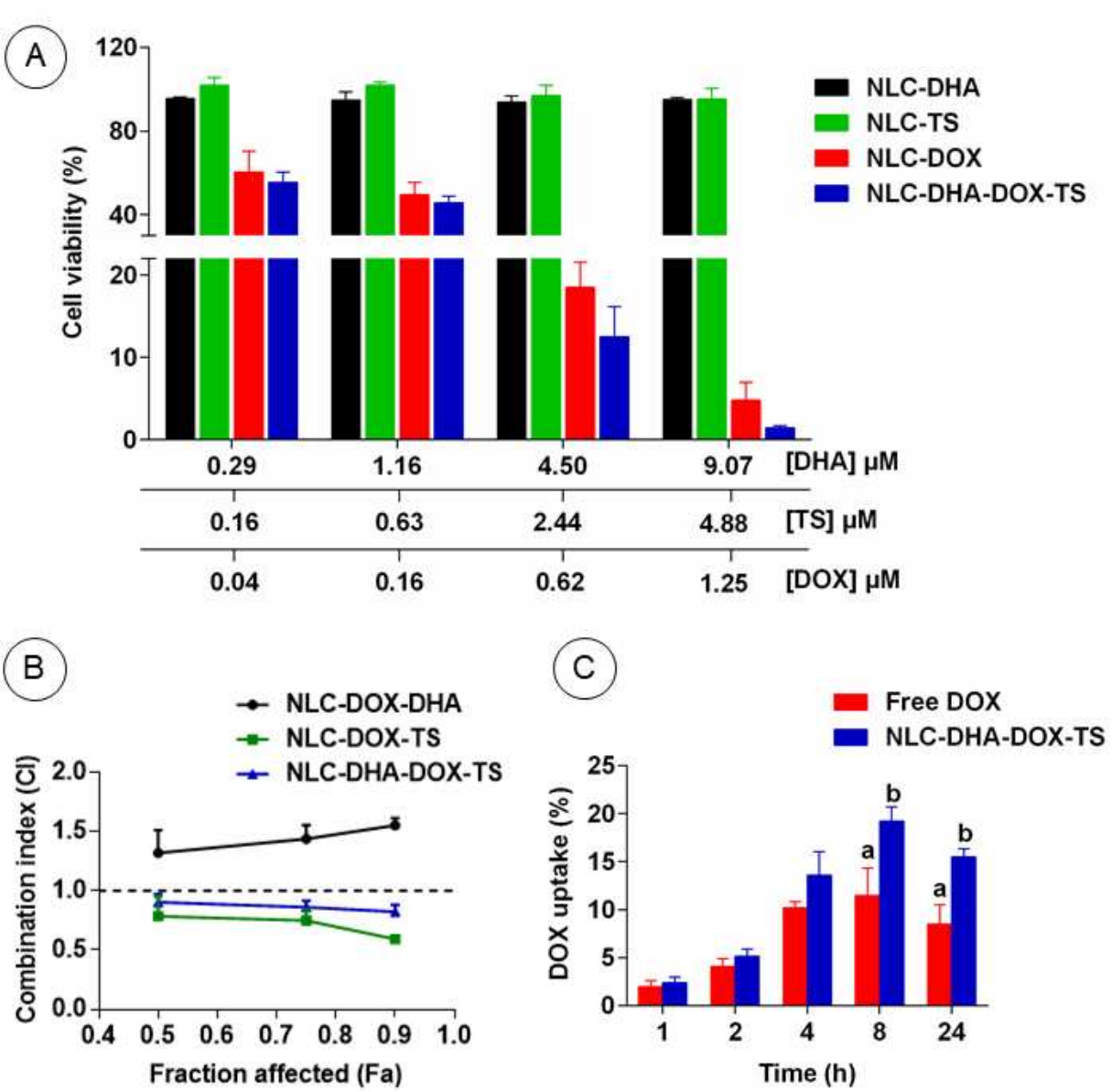

Abbreviations: DOX: doxorubicin; DHA: docosahexaenoic acid; TS: α-tocopherol succinate; NLC: nanostructured lipid carriers; NLC-DHA: nanostructured lipid carriers loading docosahexaenoic acid; NLC-TS: nanostructured lipid carriers loading α-

tocopherol succinate; NLC-DOX: nanostructured lipid carriers loading doxorubicin; NLC-DOX-DHA: nanostructured lipid carriers loading doxorubicin and docosahexaenoic acid; NLC-DOX-TS: nanostructured lipid carriers loading doxorubicin and α-tocopherol succinate; NLC-DHA-DOX-TS: nanostructured lipid carriers loading doxorubicin, docosahexaenoic acid, and α-tocopherol succinate; CI: combination index; Fa: fraction affected; Free DOX: doxorubicin solution.

The effect of a combination of two or more drugs is not necessarily more effective than that of a single drug. Proving whether the interaction produced by drug combination is synergistic is difficult according to only the perspective of curative effect. Therefore, several scientific evaluation methods have been used to evaluate the combined effect of drugs (Chou, 2006; Huang *et al.*, 2019). To comprehensively analyze the possible synergy between DOX, DHA, and TS, cell viability data were analyzed with CompuSyn software. Interestingly, the results showed that there was an antagonistic effect between DOX and DHA, with CI values ranging from 1.32 to 1.55 for fractions affected (Fa) from 0.5 to 0.9 (Fig. 3B). Previous studies have shown that DHA can selectively increase the cytotoxicity of certain cancer therapies, while antagonizing or having little or no effect on the cytotoxicity of other anticancer drugs, including DOX. However, a better understanding of the mechanisms of action of DHA is still needed, especially when it is used with other anticancer compounds, emphasizing that differences in the *in vitro-in vivo* correlation may occur (Jiao *et al.*, 2018; Zhelev *et al.*, 2016). Regarding NLC-DOX-TS, CI values ranging from 0.59 to 0.78 were found, revealing a moderate synergistic effect for the combination between DOX and TS. In our previous report, NLC-DOX-TS showed enhanced antitumor efficacy *in vivo* compared to DOX alone, corroborating the synergy of this combination against 4T1 cells (Fernandes *et al.*, 2018b). Similarly, the synergy analysis revealed that the combination of DOX, DHA, and TS also had synergistic effects, indicating that the addition of DHA did not impair the synergistic effect of the formulation. It is important to underscore that several reports have shown the beneficial role of DHA to reduce chemotherapy side effects, especially preventing anthracycline-induced cardiotoxicity and improving cancer prognosis (Adkins e Kelley, 2010; Siddiqui *et al.*, 2011). Hence, NLC-DHA-DOX-TS could result not only in increased antitumor activity due to the synergistic effect between the drugs, but

also in reduced toxicity due to the protective role of DHA and TS against the adverse effects of DOX.

3.4 Cellular uptake

The *in vitro* drug uptake was studied using HPLC to quantify intracellular concentrations of DOX in 4T1 cells treated with the free drug and NLC. As shown in Fig. 3C, an increase of DOX concentration could be observed inside the cells over time (until 8 h) for both free DOX and NLC. At 8 h and 24 h, NLC showed significantly higher drug uptake than free DOX. A similar finding was reported by Zhao *et al*., who observed increased cell uptake for NLC loading DOX, compared to the free drug (Zhao *et al.*, 2016). This can be explained by the different mechanisms of cell uptake. Free DOX is transported into cells via a passive diffusion mechanism, diffusing through the cell membrane, whereas nanoparticles enter the cells through endocytic mechanisms and release DOX intracellularly (Kanwal *et al.*, 2018). Interestingly, at 24 h, a reduction in DOX concentration was observed for both free drug and NLC compared to 8 h. This decrease in intracellular drug concentration could be a result of its metabolism and the increased detoxification capacity of cells due to the activation of efflux pumps (Ho-Lun *et al.*, 2006; Kanwal *et al.*, 2018). Nevertheless, the values remained higher in the NLC-incubated group, which could make cells more susceptible to the DOX action, resulting in increased cytotoxic effects.

3.5 *In vivo* antitumor efficacy

The *in vivo* therapeutic performances of free DOX and NLC formulations were studied in 4T1 tumor-bearing BALB/c mice at 5 mg/kg DOX for a total of five doses. The results of tumor volume (Fig. 4A) showed that the tumors of mice in the blank-NLC group grew rapidly, given the aggressiveness and high rate of cell proliferation of the 4T1 cell line. On the other hand, slower tumor growth was observed in all other groups treated with DOX. The tumors of mice treated with free DOX and NLC-DOX showed a similar growth profile, indicating that DOX encapsulation in NLC was not able to increase antitumor efficacy. Similar findings have been reported by other authors using different nanoparticles (Boratto *et al.*, 2020; Borges *et al.*, 2019; Fernandes *et al.*, 2018b). Nanocarriers loading anticancer drugs were designed to

prolong systemic circulation and improve target-specific therapeutic delivery, due to their passive accumulation in tumor tissue promoted by the EPR effect. However, the therapeutic efficacy of passively targeted nanosystems is not always satisfactory because it is largely influenced by the intensity of the EPR effect exhibited within a tumor, which varies with the type of tumor, heterogeneity, stage, and even individual variations (Park *et al.*, 2019). In addition, several studies have shown that the size, shape, and elasticity of nanoparticles affect extravasation from the vessel and retention in tumor tissue, resulting in varied therapeutic efficacy (Cagel *et al.*, 2017; Park *et al.*, 2019).

The group treated with NLC-DHA-DOX-TS exhibited the lowest tumor growth rate, evincing that DHA and TS acted synergistically with DOX to increase antitumor efficacy (Fig. 4A). DHA is known to promote apoptosis and cell cycle arrest by inducing reactive oxygen species (ROS) in many types of cancers. Moreover, when combined with another drug, DHA can modulate responses to anticancer treatment through its ability to be incorporated into cell membranes, inhibit cell enzyme activities, and interact with cell signaling mediators (Fabian, Kimler e Hursting, 2015; Mahéo *et al.*, 2005; Siddiqui *et al.*, 2011). TS also has anticancer properties due to the induction of apoptosis, inhibition of cell proliferation, and disruption of DNA synthesis. Besides, it can increase the antitumor efficacy of chemotherapeutic agents, mainly by inducing apoptosis, and promoting the intracellular influx and suppressing the efflux of the drug (Lee *et al.*, 2015; Neuzil, 2003; Zhang *et al.*, 2011).

The treatment with NLC-DHA-DOX-TS also led to a higher tumor inhibition ratio (76.6%) compared to the groups treated with NLC-DOX (66.5%) and free DOX (64.6%). These data demonstrate the effect of DHA and TS in potentializing the antitumor activity of DOX against 4T1 cells, in accordance with synergism analysis performed *in vitro*. To our knowledge, this was the first study evaluating the effect of DOX, DHA, and TS combined to fight cancer cells, and further studies can be performed to investigate the mechanisms involved in this process.

Fig. 4. *In vivo* antitumor activity. (A) Effect of different treatments on tumor growth of 4T1 tumor-bearing BALB/c mice. Each treatment was intravenously administered five times, every 2 days, at a dose of 5 mg/kg of DOX. (B) Percentage of body weight variation, on day 10, after the different treatments. All data represented as mean ± SEM, n = 6. Different letters indicate statistically significant differences between the groups at the end of treatments. These analyses were performed by one-way ANOVA followed by Tukey's test ($p < 0.05$).

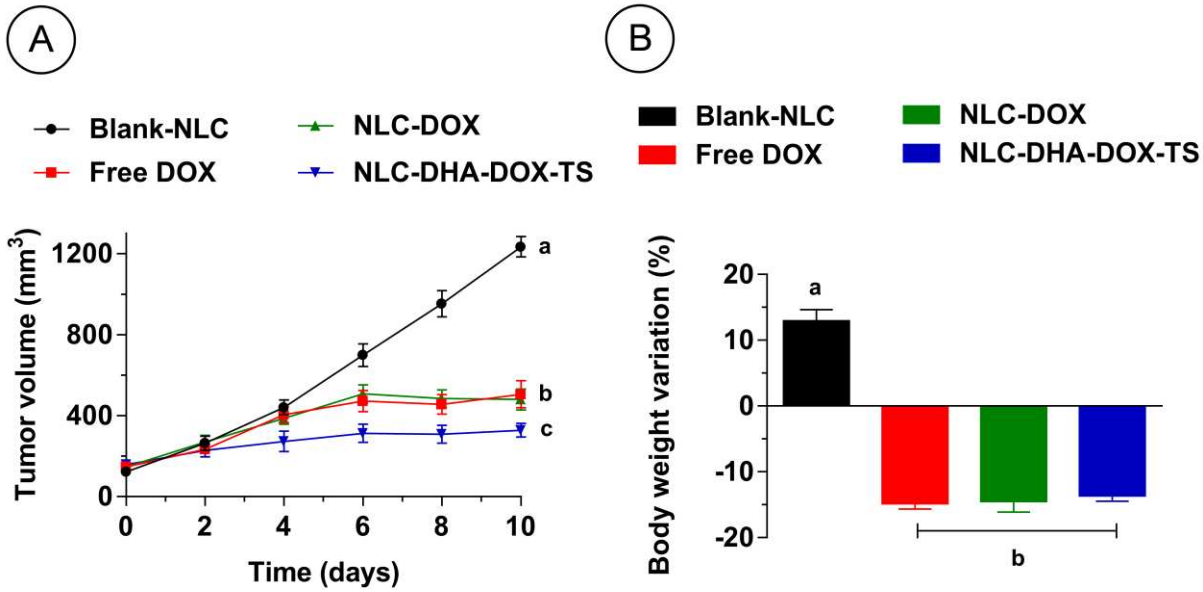

Abbreviations: DOX: doxorubicin; Blank-NLC: nanostructured lipid carriers without doxorubicin, docosahexaenoic acid, and α-tocopherol succinate; Free DOX: doxorubicin solution; NLC-DOX: nanostructured lipid carrier loading doxorubicin; NLC-DHA-DOX-TS: nanostructured lipid carrier loading doxorubicin, docosahexaenoic acid, and α-tocopherol succinate; SEM: standard error of the mean; ANOVA: analysis of variance.

Histological sections of tumor tissue were evaluated after treatments and the images are presented in Fig. S3. Mice treated with blank-NLC showed tumors with ulceration and necrosis in the central region, as well as extensive areas of viable cells. Compared to this group, all the others showed more extensive areas of necrosis and fewer viable cells, due to DOX-induced cell death.

Fig. S3. Photomicrographs of the tumor tissue of 4T1 tumor-bearing BALB/c mice treated with Blank-NLC (A), free DOX (B), NLC-DOX (C), and NLC-DHA-DOX-TS (D). Hematoxylin-eosin staining, original magnification x 2.

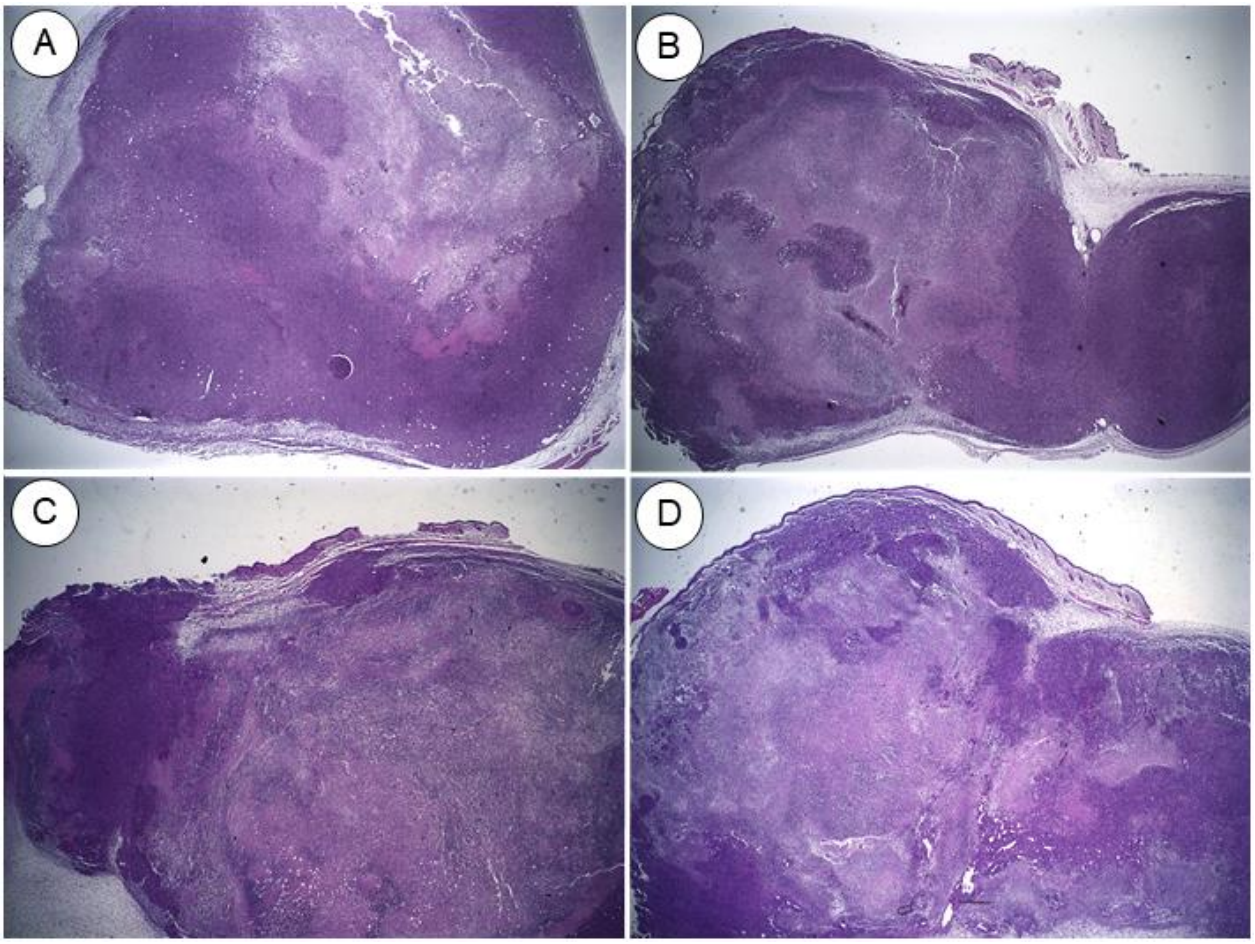

Abbreviations: Blank-NLC: nanostructured lipid carriers without doxorubicin, docosahexaenoic acid, and α-tocopherol succinate; Free DOX: doxorubicin solution; NLC-DOX: nanostructured lipid carriers loading doxorubicin; NLC-DHA-DOX-TS: nanostructured lipid carriers loading doxorubicin, docosahexaenoic acid, and α-tocopherol succinate.

3.6 Preliminary toxicity evaluation

Mice body weight was monitored every two days throughout the study and the results are shown in Fig. 4B. It was observed weight gain only in mice treated with blank-NLC, which may be a result of the tumor growth, but also evidence of the safety of blank-formulation. In contrast, all mice treated with DOX-formulations lost weight, with no difference between them. In groups treated with free DOX and NLC-DOX, the

death of mice was observed from the eighth day after the beginning of the study (Table 2). In fact, pronounced clinical toxicity signs (prostration and intense piloerection) were observed in mice treated with these formulations. On the other hand, no deaths and no clinical alterations were observed in mice treated with blank-NLC and NLC-DHA-DOX-TS. These data suggest that DHA and TS may not only increase antitumor activity but also reduce DOX toxicity. Previous studies have shown that DHA can mitigate weight loss induced by chemotherapy in mice and reduce the toxicity of paclitaxel in breast cancer patients, strongly indicating that DHA protects against toxicity in normal tissues (Bradley *et al.*, 2001; Payne *et al.*, 2006). In addition, a phase II clinical trial is been conducted to investigate the benefit of DHA supplementation in combination with neoadjuvant chemotherapy in patients with early breast cancer (Newell *et al.*, 2019). Regarding TS, its cytoprotective properties have also been reported. A recent study described reduced toxicity when DOX and TS were encapsulated in pH-sensitive liposomes, avoiding damage to the heart and liver, the main target organs of DOX toxicity (Boratto *et al.*, 2020).

Table 2. Mortality of 4T1 tumor-bearing BALB/c mice after different treatments. Each treatment was intravenously administered five times, every 2 days, at a dose of 5 mg/kg of DOX.

Group (n = 6)	Number of deaths	Mortality (%)
Blank-NLC	0	0
Free DOX	3	50.0
NLC-DOX	2	33.3
NLC-DHA-DOX-TS	0	0

Abbreviations: DOX: doxorubicin; Blank-NLC: nanostructured lipid carriers without doxorubicin, docosahexaenoic acid, and α-tocopherol succinate; Free DOX: doxorubicin solution; NLC-DOX: nanostructured lipid carriers loading doxorubicin; NLC-DHA-DOX-TS: nanostructured lipid carriers loading doxorubicin, docosahexaenoic acid, and α-tocopherol succinate.

The hematologic analysis was performed at the end of the study and results are summarized in Table 3. The 4T1 murine breast cancer is known to induce a severe leukemoid reaction and an anemic phenotype in mice, with low red blood cells count,

platelet, hematocrit, and hemoglobin levels (Boratto *et al.*, 2020; duPre' e Hunter, 2007), which is in agreement with our findings. In fact, a significant increase in the number of white blood cells was observed in the animals treated with blank-NLC due to the rapid tumor growth, while it was not observed in all other groups treated with DOX. Concerning the platelet counts, there was a significant reduction in all DOX-treated groups compared to the treatment with blank-NLC, indicating a certain bone marrow toxicity induced by the drug. DOX is known as a myelosuppressive drug and, in addition, it can directly induce platelet cytotoxicity through the ROS generation, reducing glutathione levels, and depleting thiol proteins (Kim *et al.*, 2009). Red blood cells count, hemoglobin, hematocrit, and RDW were similar in all treatment groups.

Table 3. Hematologic parameters of 4T1 tumor-bearing BALB/c mice after different treatments. Each treatment was intravenously administered five times, every 2 days, at a dose of 5 mg/kg of DOX.

Parameters	Reference values (Everds, 2007)	Treatments			
		Blank-NLC	Free DOX	NLC-DOX	NLC-DHA-DOX-TS
White blood cells (10^9/L)	2 – 10	78.6 ± 10.9	2.4 ± 0.5[a]	2.8 ± 0.4[a]	2.3 ± 0.3[a]
Red blood cells (10^{12}/L)	7 – 11	5.7 ± 0.1	5.3 ± 0.1	4.5 ± 0.2	4.6 ± 0.1
Hemoglobin (g/L)	13 – 18	11.5 ± 0.4	9.6 ± 0.2	7.7 ± 0.4	8.2 ± 0.2
Hematocrit (%)	40 – 50	28.5 ± 0.6	26.1 ± 0.5	21.7 ± 0.8	22.8 ± 0.4
RDW (%)	11 – 15	14.3 ± 0.3	14.4 ± 0.3	14.0 ± 0.2	13.8 ± 0.2
Platelets (10^9/L)	1000 – 2000	349 ± 41	118 ± 19[a]	108 ± 17[a]	128 ± 13[a]

Note: Results expressed as mean ± SEM (n = 6). [a] Represents a significant difference compared to the group treated with blank-NLC. [b] Represents a significant difference compared to the group treated with free DOX. [c] Represents a significant

difference compared to the group treated with NLC-DOX. These analyses were performed by one-way ANOVA followed by Tukey's test ($p < 0.05$).

Abbreviations: Blank-NLC: nanostructured lipid carriers without doxorubicin, docosahexaenoic acid, and α-tocopherol succinate; Free DOX: doxorubicin solution; NLC-DOX: nanostructured lipid carriers loading doxorubicin; NLC-DHA-DOX-TS: nanostructured lipid carriers loading doxorubicin, docosahexaenoic acid, and α-tocopherol succinate; RDW: red cell distribution width; SEM: standard error of the mean; ANOVA: analysis of variance.

Biochemical analysis was also performed in order to investigate renal and hepatic toxicity. Mice treated with free DOX presented a significant increase in AST and ALT levels compared to those treated with blank-NLC (Table 4). This may indicate hepatic toxicity induced by DOX since the liver is a common site for DOX-induced cell death and tissue damage (Cagel *et al.*, 2017; Carvalho *et al.*, 2009). The metabolism of high DOX concentrations results in the production of a large number of ROS. Consequently, ROS causes an excessive amount of damage, ranging from damage to DNA, production of lipid peroxidation, and decreased levels of vitamin E (Tacar, Sriamornsak e Dass, 2013). On the other hand, mice that received NLC-DHA-DOX-TS showed similar AST levels to the control group and significantly lower than those treated with free DOX. These results suggest an important role for the combination of DHA and TS in preventing liver damage. It is known that DHA can control inflammatory reactions and balance lipid peroxidation, which could relieve oxidative damage in the liver. In turn, TS is a vitamin E derivative that can recover its antioxidant activity when hydrolyzed, avoiding liver toxicity.

Table 4. Biochemical parameters of 4T1 tumor-bearing BALB/c mice after different treatments. Each treatment was intravenously administered five times, every 2 days, at a dose of 5 mg/kg of DOX.

Parameters	Treatments			
	Blank-NLC	Free Dox	NLC-DOX	NLC-DHA-DOX-TS
Creatinine (mg/dL)	0.22 ± 0.02	0.19 ± 0.02	0.20 ± 0.01	0.22 ± 0.02
Urea (mg/dL)	35.4 ± 2.4	37.5 ± 3.8	43.3 ± 1.6	42.3 ± 2.1
AST (U/L)	92.5 ± 3.7	134.6 ± 11.6[a]	102.1 ± 1.8	102.1 ± 5.1[b]
ALT (U/L)	15.1 ± 1.8	58.7 ± 17.5[a]	22.9 ± 3.6	25.1 ± 2.4

Note: Results expressed as mean ± SEM (n = 6). [a] Represents a significant difference compared to the group treated with blank-NLC. [b] Represents a significant difference compared to the group treated with free DOX. [c] Represents a significant difference compared to the group treated with NLC-DOX. These analyses were performed by one-way ANOVA followed by Tukey's test ($p < 0.05$).

Abbreviations: Blank-NLC: nanostructured lipid carriers without doxorubicin, docosahexaenoic acid, and α-tocopherol succinate; Free DOX: doxorubicin solution; NLC-DOX: nanostructured lipid carriers loading doxorubicin; NLC-DHA-DOX-TS: nanostructured lipid carriers loading doxorubicin, docosahexaenoic acid, and α-tocopherol succinate; AST: aspartate aminotransferase; ALT: alanine aminotransferase; SEM: standard error of the mean; ANOVA: analysis of variance.

Histopathologic analysis was carried out in the heart, lungs, spleen, and kidneys for all experimental groups. The 4T1 breast cancer is known to be highly tumorigenic, invasive, and able to spontaneously metastasize from the primary tumor to multiple distant sites, closely resembling metastatic breast cancer in human patients (duPre' e Hunter, 2007). In fact, histologic analysis of the lungs showed extensive and multiples metastasis foci in mice receiving blank-NLC, as shown in Fig. 5. On the other hand, all treatments with DOX were able to prevent lung metastasis (data shown only for the NLC-DHA-DOX-TS group). An enlarged spleen was also observed in animals that received blank-NLC, which is consistent with the splenomegaly caused by the 4T1 tumor. In all other groups, normal-sized spleens were found, indicating that the treatments were able to overcome splenomegaly.

Concerning renal histopathology, all groups showed preserved tissues with their typical architecture, in accordance with the biochemical results.

Fig. 5. Photomicrographs of the lung tissue of 4T1 tumor-bearing BALB/c mice treated with Blank-NLC (A and B) and NLC-DHA-DOX-TS (C and D). Hematoxylin-eosin staining, original magnification x 4 (A and C), and x 20 (B and D). Red arrows indicate metastasis in the lung.

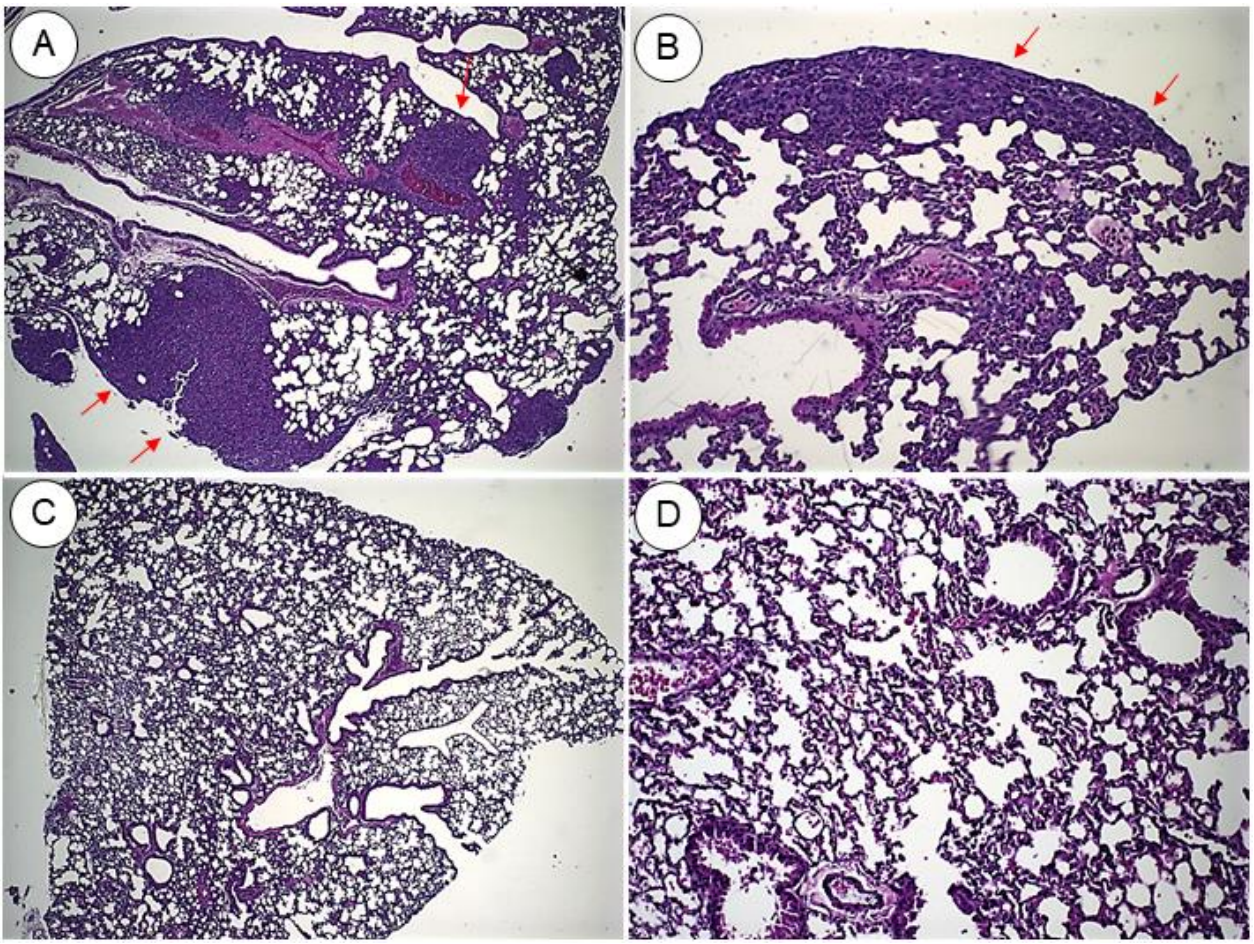

Abbreviations: Blank-NLC: nanostructured lipid carriers without doxorubicin, docosahexaenoic acid, and α-tocopherol succinate; NLC-DHA-DOX-TS: nanostructured lipid carriers loading doxorubicin, docosahexaenoic acid, and α-tocopherol succinate.

Cardiac muscle images are illustrated in Fig. 6. The animals treated with blank-NLC revealed cardiac tissue with normal architecture and cardiac fibers of usual thickness. In the groups treated with free DOX and NLC-DOX, large areas of cardiomyocytes vacuolization, hyaline degeneration, and loss of striation were

detected, indicating injury due to DOX cardiotoxicity. In contrast, in the group treated with NLC-DHA-DOX-TS, discrete loss of striation was observed, and vacuoles and hyaline degeneration were rare, indicating greater protection against the cardiotoxic effects of DOX when DHA and TS were also co-encapsulated in the NLC. Recently, several mechanisms have been sought to explain the protective effects of omega-3 fatty acids, some of them involve their anti-inflammatory activities, as well as their ability to negatively modulate some molecular pathways (Adkins e Kelley, 2010; Serini *et al.*, 2017). Interestingly, some of these mechanisms are involved in the DOX-induced cardiotoxicity. For example, it has been shown that DHA can inhibit the decrease in the expression of mitochondrial uncoupling protein 2, the increase in ROS production, and the subsequent mitochondrial membrane potential change that contribute to the cardiotoxicity of DOX (Hsu, Chen e Chen, 2014). Previous studies regarding the cardioprotective effects of vitamin E have also been described, mainly through an antioxidant mechanism (Berthiaume *et al.*, 2005; Das, Nesaretnam e Das, 2007). As mentioned above, TS can recover its antioxidant activity when hydrolyzed to vitamin E, contributing to reduce DOX-induce cardiotoxicity.

Fig. 6. Photomicrographs of the cardiac tissue of 4T1 tumor-bearing BALB/c mice treated with Blank-NLC (A), free DOX (B), NLC-DOX (C), and NLC-DHA-DOX-TS (D). Hematoxylin-eosin staining, original magnification x 40. Red arrows indicate vacuolization.

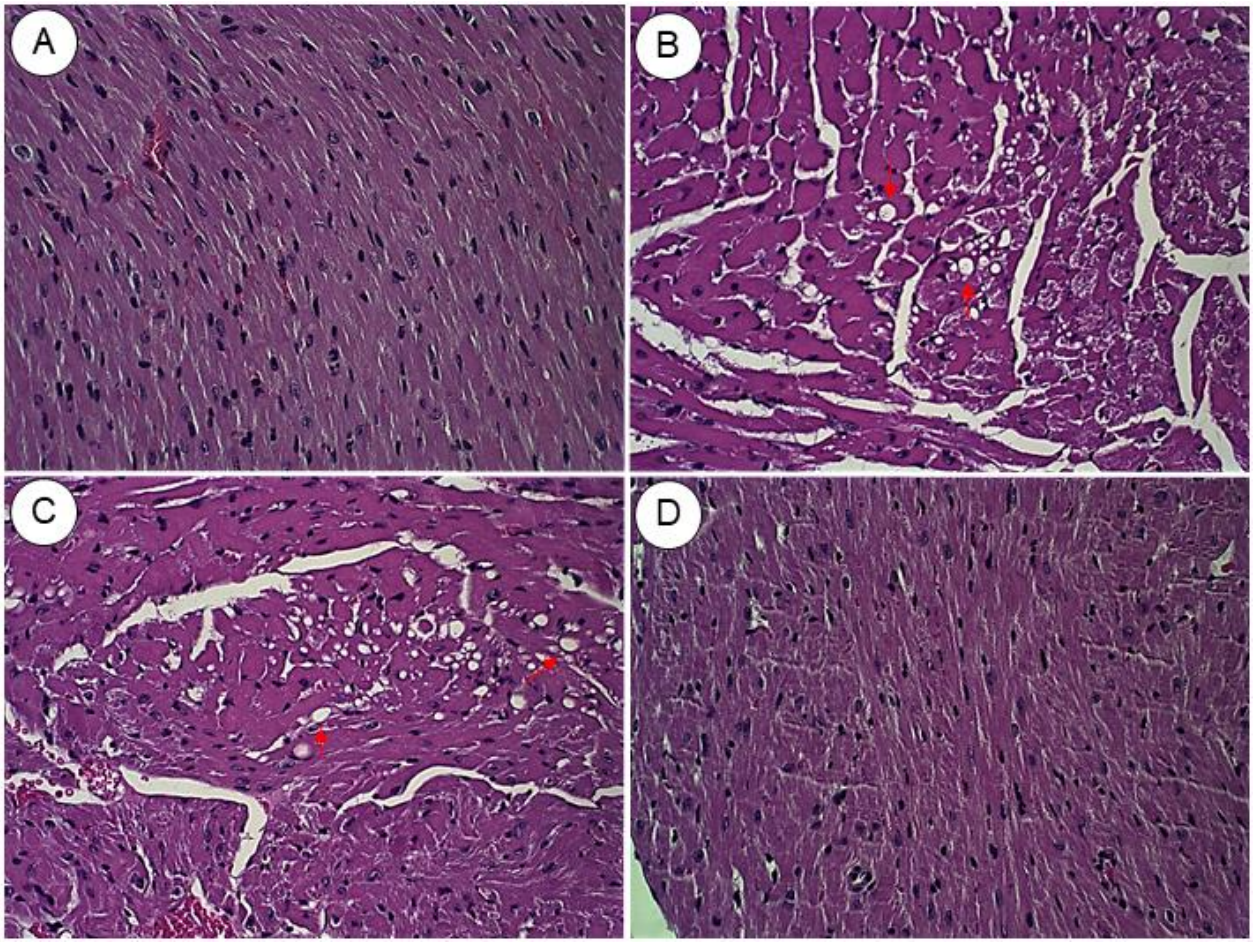

Abbreviations: Blank-NLC: nanostructured lipid carriers without doxorubicin, docosahexaenoic acid, and α-tocopherol succinate; Free DOX: doxorubicin solution; NLC-DOX: nanostructured lipid carriers loading doxorubicin; NLC-DHA-DOX-TS: nanostructured lipid carriers loading doxorubicin, docosahexaenoic acid, and α-tocopherol succinate.

4 Conclusion

NLC loading DOX, DHA, and TS was successfully prepared showing reduced particle size and homogeneous size distribution. DOX encapsulation into the nanoparticles was performed after NLC preparation, using the incubation method, which could prevent DOX degradation during the NLC manufacturing. High DOX encapsulation

efficiency, close to 100%, was achieved due to the ion-pairing with TS. We demonstrated that the DOX-TS ion pair has increased lipophilicity and reduced crystallinity compared to DOX, which contributes to its encapsulation in the lipid matrix. *In vitro* release studies showed a controlled DOX release from the NLC, with increased drug release at the acidic environment. *In vitro* cell analysis indicated that DOX, DHA, and TS combined in NLC have synergistic effects against 4T1 tumor cells. Moreover, DOX encapsulation in this NLC increased its cellular uptake compared to the free drug. In fact, the *in vivo* study demonstrated that this formulation not only significantly inhibited the tumor growth of 4T1 breast cancer, but also reduced mice mortality, prevented lung metastasis, and decreased DOX-induced toxicity to the heart and liver. In conclusion, these results endorse the proposal that NLC loading DOX, DHA, and TS can be considered as a promising formulation to be used for breast cancer treatment.

CAPÍTULO 2

pH-sensitive doxorubicin-tocopherol succinate prodrug encapsulated in docosahexaenoic acid-based nanostructured lipid carriers: an effective strategy to improve pharmacokinetics and reduce toxic effects

Eduardo Burgarelli Lages, Renata Salgado Fernandes, Marina Mol Sena Andrade, Nitchawat Paiyabhroma, Renata Barbosa de Oliveira, Christian Fernandes, Geovanni Dantas Cassali, Pierre Sicard, Sylvain Richard, André Luís Branco de Barros, Lucas Antônio Miranda Ferreira

Artigo publicado em Biomedicine & Pharmacotherapy, v. 144, 112373, 2021.

Abstract

Side effects often limit the use of doxorubicin (DOX) in cancer treatment. We have recently developed a nanostructured lipid carrier (NLC) formulation for synergistic chemotherapy, encapsulating DOX and the anticancer adjuvants docosahexaenoic acid (DHA) and α-tocopherol succinate (TS). Hydrophobic ion-pairing with TS allowed a high DOX entrapment in the nanocarrier. In this work, we investigated the pharmacokinetics of this formulation after intravenous administration in mice. The first data obtained led us to propose synthesizing covalent DOX-TS conjugates to increase DOX retention in the NLC. We successfully conjugated DOX to TS via an amide or hydrazone bond. In vitro studies in 4T1 tumor cells indicated low cytotoxicity of the amide derivative, while the hydrazone conjugate was effective in killing cancer cells. We encapsulated the hydrazone derivative in a DHA-based nanocarrier (DOX-hyd-TS/NLC), which had reduced particle size and high drug encapsulation efficiency. The pH-sensitive hydrazone bond allowed controlled DOX release from the NLC, with increased drug release at acidic conditions. In vivo studies revealed that DOX-hyd-TS/NLC had a better pharmacokinetic profile than free DOX and attenuated the short-term cardiotoxic effects caused by DOX, such as QT prolongation and impaired left ventricular systolic function. Moreover, this formulation showed excellent therapeutic performance by reducing tumor growth in 4T1 tumor-bearing mice and decreasing DOX-induced toxicity to the heart and liver, demonstrated by hematologic, biochemical, and histologic analyses. These results indicate that DOX-hyd-TS/NLC may be a promising nanocarrier for breast cancer treatment.

Keywords: doxorubicin, nanomedicine, ion-pairing, amide, hydrazone, antitumor activity, cardiotoxicity.

1 Introduction

Doxorubicin (DOX) is a cytotoxic anthracycline widely used in chemotherapy due to its efficacy in fighting many cancers, such as carcinomas, sarcomas, and hematologic malignancies. However, its use can result in cumulative and dose-dependent cardiotoxicity as one of the most serious adverse effects, ranging from structural and functional changes in cardiomyocytes to severe cardiomyopathy and congestive heart failure (Carvalho *et al.*, 2009; Zhao e Zhang, 2017). DOX-loaded nanocarriers aim to overcome the challenges associated with cancer therapy, providing a reduction in toxicity and an improvement in the drug's safety profile (Cagel *et al.*, 2017; Shafei *et al.*, 2017). Moreover, nanocarriers can present superior therapeutic efficacy than free drugs due to the enhanced permeability and retention (EPR) effect, which allows the passive targeting and accumulation of nanostructures in the interstitial tissue of malignant tumors since they can pass through the leaky blood vessels (Fang, Nakamura e Maeda, 2011; Kalyane *et al.*, 2019).

Among the promising nanoplatforms for drug delivery in cancer therapy, nanostructured lipid carriers (NLC) have attracted expanding attention. They are composed of a blend of solid and liquid lipids that results in an unstructured system, which imparts many advantages over other lipid-based carriers, including enhanced physical stability, improved drug loading capacity, and flexible modulation of drug release (Khosa, Reddi e Saha, 2018; Haider *et al.*, 2020).

In our previous report, we developed an NLC formulation for co-delivery of DOX, docosahexaenoic acid (DHA), and α-tocopherol succinate (TS) to cancer cells (Lages *et al.*, 2020). DHA is an omega-3 polyunsaturated fatty acid, and TS is a vitamin E derivative. Several studies have shown that these compounds can act as anticancer adjuvants, enhancing the antitumor activity of DOX and reducing its adverse effects (Prasad *et al.*, 2003; Siddiqui *et al.*, 2011; Serini *et al.*, 2017). Interestingly, both DHA and TS were used as functional excipients in that formulation: DHA is an oil that can form the lipid matrix of NLC and TS is an anionic counterion that can increase DOX encapsulation efficiency through hydrophobic ion-pairing (Oliveira *et al.*, 2016a).

In the present work, we conducted for the first time pharmacokinetic studies comparing DOX-TS ion-pair-loaded NLC and free DOX after intravenous administration in mice. The data obtained prompted us to synthesize DOX-TS covalent conjugates to be loaded into the NLC system. This strategy turned out to be interesting to increase the lipophilicity of DOX and enhance its retention in the lipid matrix of NLC.

Covalent conjugation of DOX and TS has been performed via amide or hydrazone bonds. Duhem *et al.* prepared an amide prodrug of DOX and TS that self-assembled into nanoparticles in the presence of TPGS (Duhem *et al.*, 2014). Treatment with the formulation resulted in comparable efficacy to free DOX in CT-26 tumor-bearing mice, but with reduced toxicity. Recently, Xiong *et al.* also synthesized DOX-TS prodrugs through amide and hydrazone bonds and encapsulated them in TPGS micelles for drug co-delivery (Xiong *et al.*, 2019). The amide-loaded micelles had low efficacy in inhibiting tumor growth in MCF-7 tumor-bearing mice, unlike the hydrazone-loaded formulation, which showed an antitumor activity comparable to free DOX. Furthermore, both conjugates-loaded formulations were able to reduce the toxic effects of DOX.

Based on the physiological differences between normal and tumor tissues, one attractive approach to improve the efficacy of chemotherapy is the development of nanocarriers with pH-triggered drug release. Typically, tumor tissues have lower extracellular pH values (pH ≈ 6.8) than normal tissues and the bloodstream, and moreover, endosomes and lysosomes inside cells exhibit much lower pH values (< 5.4) (Zeng *et al.*, 2017). Thus, the use of acid unstable chemical bonds, such as amide, hydrazone, and imine, has attracted widespread interest (Sonawane, Kalhapure e Govender, 2017; Li *et al.*, 2021). DOX-loaded pH-sensitive nanocarriers have been shown to improve specific targeting to tumor tissues, enhance cell internalization, allow controlled drug release, and minimize potential damage to normal cells (Sonawane, Kalhapure e Govender, 2017; Zeng *et al.*, 2017; Cheng *et al.*, 2019; Xiong *et al.*, 2019; Li *et al.*, 2021).

Herein, we report the synthesis of DOX-TS conjugates by either an amide (DOX-ami-TS) or a hydrazone (DOX-hyd-TS) bond. We performed *in vitro* studies to investigate

their cytotoxicity in 4T1 breast cancer cells. We encapsulated the most active derivative in a DHA-based nanocarrier, characterized its physicochemical properties, investigated its pharmacokinetics and potential cardiotoxic effects *in vivo*. We also evaluated the antitumor efficacy and preliminary toxicity in a murine model of breast cancer.

2 Materials and methods

2.1 Materials

We obtained DOX·HCl from ACIC Chemicals (Ontario, Canada). We purchased α-tocopherol succinate (TS), ethylenediaminetetraacetic acid sodium (EDTA), 1-hydroxybenzotriazole (HOBt), 1-ethyl-3-(3-dimethylaminopropyl)carbodiimide hydrochloride (EDC), N-hydroxysulfosuccinimide (NHS), and N,N-dimethylformamide (DMF) from Sigma-Aldrich (St. Louis, USA). We obtained triethanolamine (TEA), triethylamine, glycerol, and hydrazine hydrate solution from Merck (Darmstadt, Germany). Compritol® 888 ATO (a mixture of mono-, di-, and triglycerides of behenic acid) was kindly provided by Gattefossé (Saint-Priest, France), and super-refined Polysorbate 80TM (Tween 80) and docosahexaenoic acid as triglyceride (OmeRx™ DHA 500TG) by Croda Inc. (Edison, USA). We purchased RPMI 1640 medium, fetal bovine serum, and trypsin-EDTA (0.25%) from Gibco-Invitrogen (Grand Island, USA). All other chemicals and reagents used in this study were of analytical grade.

2.2 Animals

In vivo experiments were conducted under the approval of the local Ethics Committee on Animal Use following the National Institutes of Health guide for the care and use of Laboratory Animals (Protocols #264/2018, #252/2020, #255/2020, and APAFiS#20238-2019041116256696 v2). Healthy Swiss mice (male, 5-6 weeks old, 25-30 g) were used to assess the pharmacokinetics and short-term cardiotoxicity. To establish a murine model of breast cancer, we used BALB/c mice (female, 8-weeks old, 18-22 g) in the antitumor efficacy study. We kept the animals in an environment with a light cycle and controlled ventilation and allowed free access to food and water in all experiments.

2.3 Synthesis of DOX derivatives

DOX-TS conjugates were synthesized as previously described, with some modifications (Duhem *et al.*, 2014; Xiong *et al.*, 2019). The synthesis routes are illustrated in Fig. 1. To prepare the amide derivative, we dissolved DOX·HCl (500 mg, 0.86 mmol) in 10 mL of warm DMF (55 ºC) before the addition of triethylamine (200 µL, 1.43 mmol), HOBt (135 mg, 1.00 mmol), and TS (382 mg, 0.72 mmol). Then, EDC (192 mg, 1.00 mmol) dissolved in dichloromethane (30 mL) was added dropwise to the reaction mixture under stirring, and the solution was heated at 55 °C for 24 h. We transferred the reaction mixture to a separatory funnel, added diethyl ether (40 mL), and washed the mixture three times with 100 mL of brine. The organic phase was dried with Na_2SO_4, filtered, and evaporated using a vacuum rotary evaporator. DOX-ami-TS was collected as a red powder and dried in a vacuum (yield 662 mg, 87%, melting point range 102–105 °C).

To synthesize the hydrazone derivative, we dissolved TS (500 mg, 0.94 mmol), EDC (217 mg, 1.13 mmol), and NHS (130 mg, 1.13 mmol) in 2 mL of DMF, and stirred the solution overnight at room temperature. After that, hydrazine hydrate (100 µL, 2.04 mmol) was added to the reaction mixture, and the solution was further stirred for 20 min. We transferred the reaction mixture to a separatory funnel, added ethyl acetate (30 mL), and washed the mixture three times with 30 mL of 0.1 M HCl solution. The organic phase was dried with Na_2SO_4, filtered, and evaporated using a vacuum rotary evaporator. We immediately dissolved the hydrazide obtained (500 mg, 0.92 mmol) in 20 mL of methanol before adding DOX·HCl (178 mg, 0.31 mmol) and trifluoroacetic acid (25 µL, 0.33 mmol). After stirring overnight at room temperature, the solution was concentrated to approximately 5 mL using a vacuum rotary evaporator. Then, we added diethyl ether (35 mL) to precipitate the product, which was collected by centrifugation (16,800 × g, 15 min, 4 °C) and washed three times with water to remove the unreacted DOX. DOX-hyd-TS was collected as a red powder and dried in a vacuum (yield 238 mg, 72%, melting point range 157–160 °C).

Fig. 1. Synthesis routes of DOX-ami-TS (A) and DOX-hyd-TS (B).

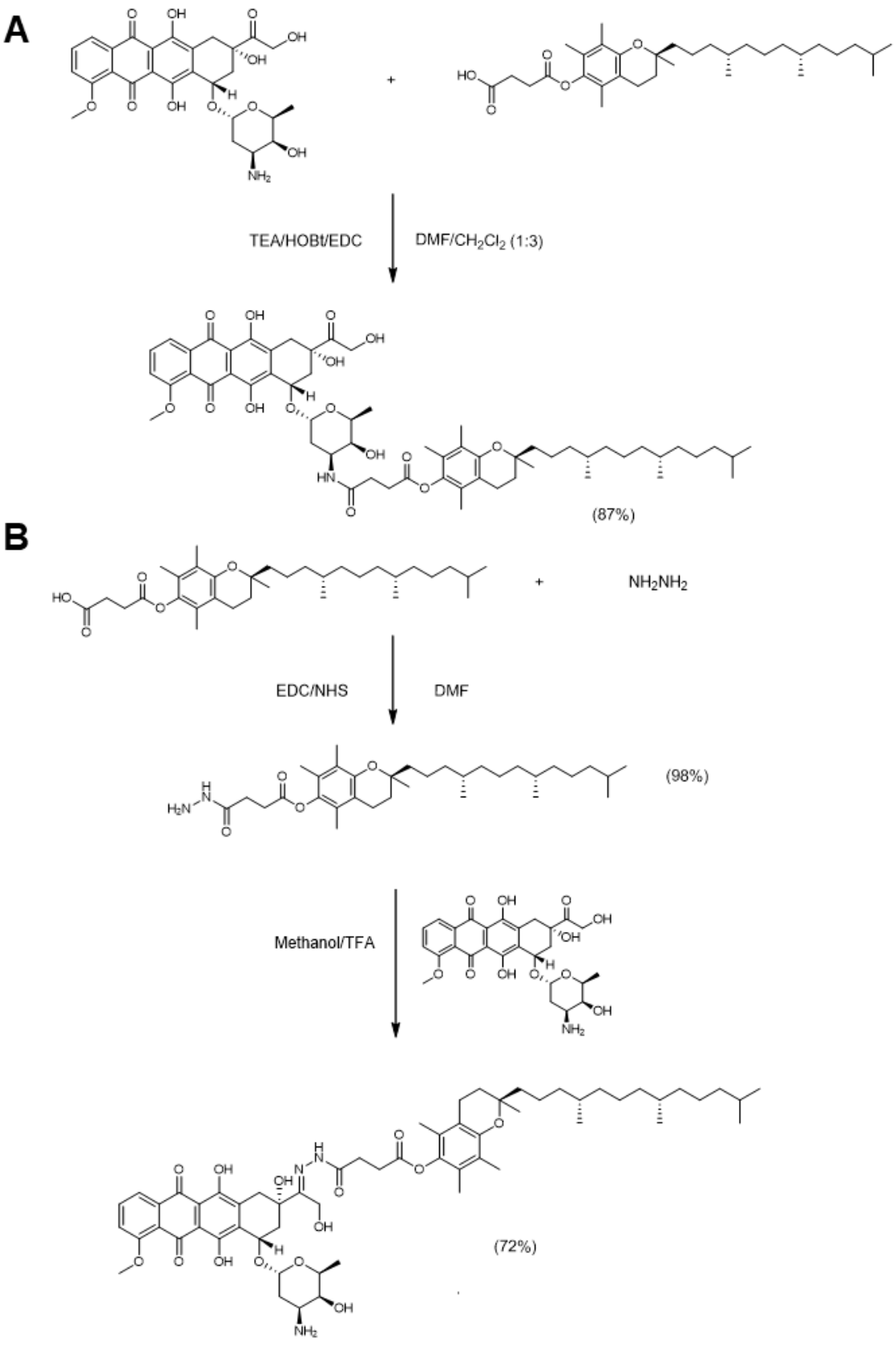

The chemical identities of the conjugates were confirmed by the ^{1}H NMR spectra recorded on a Bruker AVANCE DRX400 instrument (Bruker, MA, USA) using tetramethylsilane as an internal standard. The ^{1}H NMR spectra are represented in Fig. 2 and are in accordance with previous published data (Duhem *et al.*, 2014; Xiong *et al.*, 2019). ^{1}H NMR of DOX-ami-TS (400 MHz, $CDCl_3$): *δ* 8.01 (s, 1H), 7.97 (d, *J* = 5.4 Hz, 1H), 7.75 (t, *J* = 5.4 Hz, 1H), 7.35 (d, *J* = 5.4 Hz, 1H), 6.23 (bs, 1H), 5.47 (bs, 1H), 5.22 (bs, 1H), 4.77–4.76 (m, 2H), 4.18–4.12 (m, 2H), 4.04 (s, 3H), 3.65 (bs, 1H), 2.97–2.94 (m, 3H), 2.88–2.85 (m, 2H), 2.57–2.49 (m, 5H), 2.35–2.32 (m, 1H), 2.13 (dd, *J* = 9.7, 2.6 Hz, 1H), 2.03 (s, 3H), 1.93 (s, 3H), 1.89 (s, 3H), 1.84–1.81 (m, 2H), 1.55–1.48 (m, 4H), 1.39–1.33 (m, 4H), 1.28–1.25 (m, 6H), 1.19 (s, 3H), 1.15–1.10 (m, 3H), 1.09–1.03 (m, 5H), 0.88–0.82 (m, 15H). ^{1}H NMR of DOX-hyd-TS (400 MHz, DMSO-d6): *δ* 10.49 (s, 1H), 7.82–7.76 (m, 2H), 7.53 (d, *J* = 5.2 Hz, 1H), 5.85 (bs, 1H), 5.48 (bs, 2H), 5.30 (bs, 1H), 4.94 (bs, 1H), 4.48–4.38 (m, 2H), 4.09–4.06 (m, 1H), 3.91 (s, 3H), 3.68–3.58 (m, 1H), 3.60–3.20 (m, overlapped with the residual HOD signal of the solvent), 2.47–2.40 (m, 3H), 1.91–1.86 (m, 5H), 1.75–1.65 (m, 8H), 1.49–1.42 (m, 3H), 1.26–1.11 (m, 15H), 1.10–0.96 (m, 7H), 0.83–0.77 (m, 12H).

Fig. 2. Stacked ^{1}H NMR spectra of DOX, TS, DOX-ami-TS, and DOX-hyd-TS. DOX and DOX-hyd-TS were solubilized in DMSO-d6. TS and DOX-ami-TS were solubilized in $CDCl_3$.

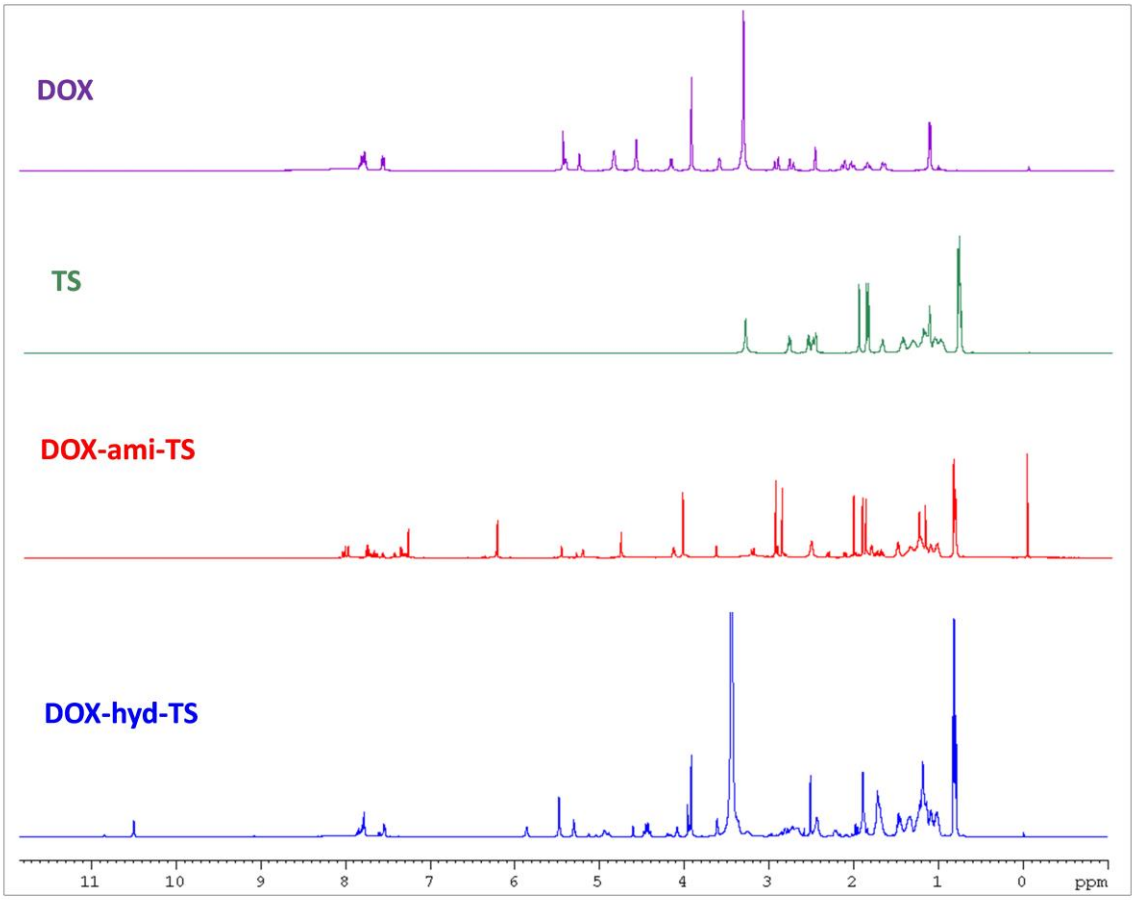

2.4 Cell culture and cytotoxicity assay

Murine 4T1 breast cancer cells were purchased from ATCC® (CRL-2539, American Type Culture Collection, USA). We grew and maintained cells in RPMI medium supplemented with FBS (10% v/v), penicillin (100 IU/mL), and streptomycin (100 µg/mL) in a 5% CO_2 atmosphere at 37 °C.

The in vitro cytotoxic effects of DOX and DOX-TS conjugates (DOX-ami-TS and DOX-hyd-TS) were assessed using the sulforhodamine B (SRB) assay as published elsewhere (Fernandes *et al.*, 2018b). Briefly, 4T1 cells were seeded in 96-well plates (5×10^3 cells/well) 24 h before treatment. Then, we exposed the cells to a range of concentrations of DOX, DOX-ami-TS, and DOX-hyd-TS (DOX concentration range

0.08–10 μM; drug solutions were prepared by dissolving DOX in purified water and the conjugates in DMSO). After 48 h of incubation, 10% trichloroacetic acid (TCA) was added to each well to fix cells for one hour. Then, plates were washed with water to remove TCA and stained with SRB for 30 min, followed by a 1% acetic acid wash to remove unbound SRB. Then, we added 10 mM Tris-Base solution (pH 10.5) to solubilize the protein-bound dye, and the optical density was read at 510 nm using a microplate spectrophotometer Spectra Max Plus 384 (Molecular Devices, Sunnyvale, CA, USA). All experiments were performed in triplicate and IC_{50} values were calculated with GraphPad Prism® 6 software.

2.5 Preparation of NLC

DOX-TS ion-pair/NLC, in which DOX was encapsulated using the hydrophobic ion-pairing approach, was prepared and characterized as previously described (Lages *et al.*, 2020). In this work, after evaluating the cytotoxicity of the conjugates, we selected DOX-hyd-TS for further studies and encapsulated it in the NLC (DOX-hyd-TS/NLC). DHA was used in a triglyceride form (OmeRx™ DHA 500TG) to compose the lipid matrix of the nanocarrier. The oily phase consisted of Compritol: 110 mg, DHA: 40 mg, Tween 80: 100 mg, TS: 40 mg, TEA: 6 mg, Glycerol: 220 mg, and DOX-hyd-TS: 20 mg; and the aqueous phase by EDTA: 4 mg and ultrapure water: 10 mL. We added glycerol to enhance the solubility of the hydrazone conjugate in the oil phase and prepared the formulation using the emulsification-ultrasound method (Fig. 3) as previously reported (Lages *et al.*, 2020). Blank-NLC was prepared similarly but in the absence of DOX-hyd-TS.

Fig. 3. Schematic illustration of DOX-hyd-TS/NLC preparation using the emulsification-ultrasound method. Briefly, the heated oily and aqueous phases were mixed under constant agitation with an Ultra Turrax T-25 homogenizer. The formed emulsion was immediately submitted to a high-intensity probe sonication and cooled down to room temperature with manual agitation to produce the NLC.

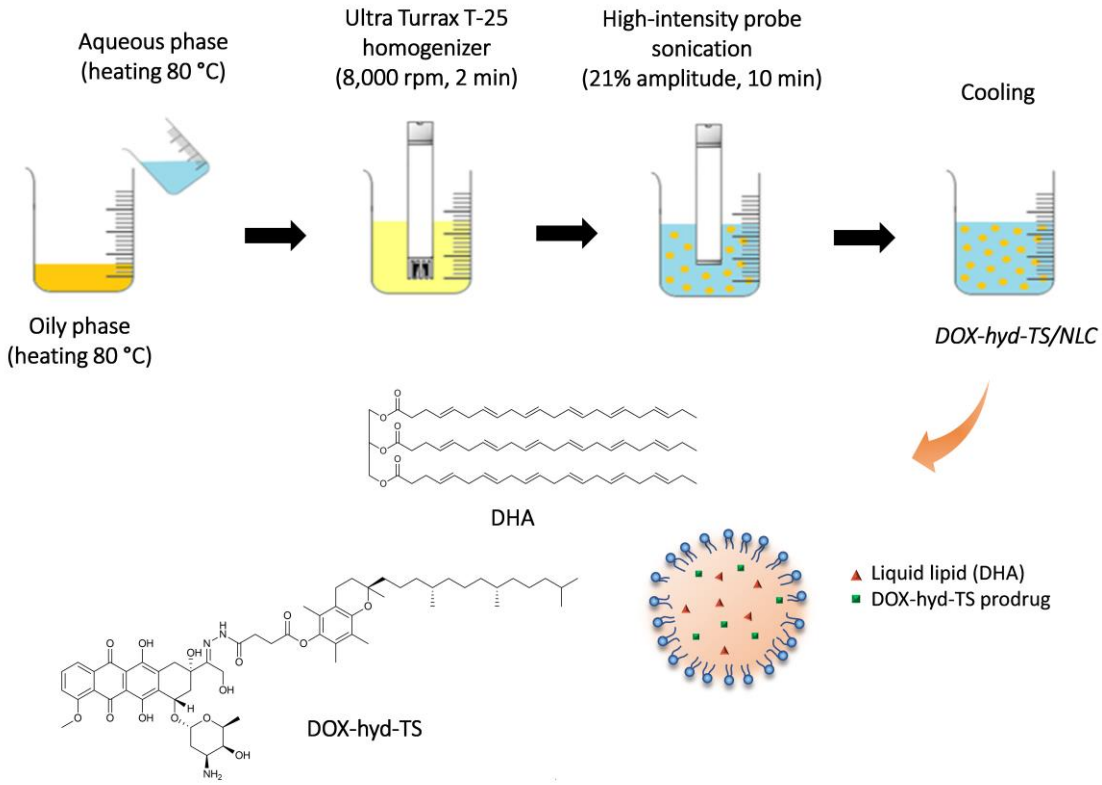

2.6 Characterization of NLC

2.6.1 Size distribution and shape

The mean particle size and zeta potential (ZP) were measured by dynamic light scattering (DLS) and DLS coupled with electrophoretic mobility, respectively, using Zetasizer Nano-ZS90 (Malvern Instruments, UK) with a fixed angle (90°) laser beam at 25 °C. We diluted the formulations 100 times in ultrapure water before the analyses. All experiments were performed in triplicate and data were reported as average size, polydispersity index (PDI), and ZP. Particle size distribution was also assessed by nanoparticle tracking analysis (NTA), carried out with a NanoSight

NS300 (Malvern Instruments, UK). Data collection and analysis were performed using NTA 3.1 software. NLC was diluted 1×10^5 times in ultrapure water and introduced into the sample chamber with a disposable syringe. The analyses were made at room temperature for 60 s with automatic detection. All measurements were performed in triplicate. The morphology of nanocarriers was examined by cryogenic transmission electron microscopy (cryo-TEM). We prepared the samples by plunge freezing technique by spreading 3 µL of NLC into a thin film across a Formvar-copper grid and rapidly submerging it in liquid ethane. The vitrified samples were stored in liquid nitrogen during the analysis and observed using a transmission electron microscope (Tecnai G2-12, 120 kV, FEI, Hillsboro, USA).

2.6.2 Drug content and encapsulation efficiency (EE)

NLC was purified by filtration in a 0.45 µm polyvinylidene fluoride membrane to evaluate the encapsulation efficiency (Castro *et al.*, 2009). In this way, the entrapped drug passes freely through the membrane while the non-encapsulated remains precipitated in the filter. Briefly, samples of total NLC (before filtration) and purified NLC (after filtration) were dissolved first in THF and then in the mobile phase before injection in HPLC. We also determined the amount of drug soluble in the aqueous phase of the formulation using ultracentrifugal devices (Amicon® Ultra-4 100 kDa, Millipore, USA) (Mussi *et al.*, 2013), but the values were negligible since DOX-hyd-TS is highly hydrophobic. HPLC analyses were performed using an ACE C8 column (250 x 4.6 mm, 5 µm) and a mixture of 10 mM phosphate buffer pH 3: methanol (35:65) as the mobile phase with a flow rate of 1.0 mL/min. The injection volume was 20 µL and fluorescence detection was performed at ex/em wavelengths of 470/555 nm. %EE was calculated using the following equation: $\%EE = C_{AF}/C_T \times 100$; where: C_T = total concentration in NLC and C_{AF} = concentration after filtration of the NLC.

2.6.3 *In vitro* drug release

In vitro release studies were performed using the dialysis method under three different pH conditions (7.4, 6.8, and 5.0) (Xiong *et al.*, 2019; Lages *et al.*, 2020). Dialysis tubes with a cutoff size of 14 kDa (cellulose ester membrane; Sigma–Aldrich, St Louis, USA) were filled with 2 mL of NLC formulation, sealed, and incubated with

50 mL of release medium containing 1% Tween 80 (PBS pH 7.4 and 6.8; isotonic acetate buffer pH 5.0). The samples were kept under magnetic stirring at 250 rpm and 37 °C. We withdrew aliquots of 0.5 mL at several time points and determined drug concentrations by HPLC as described above. The release medium was completed with the same volume after each sample collection. The values were plotted as the cumulative percentage of DOX released.

2.6.4 Preliminary evaluation of stability

The formulations (n = 3 batches) were kept in amber borosilicate glass bottles within a nitrogen atmosphere and stored at 4 °C. At 15 and 30 days after preparation, aliquots of the samples were analyzed for particle size, PDI, ZP, and EE. The mean values for each parameter were compared with those obtained at the time of preparation (day 0).

2.7 Pharmacokinetics

We randomly divided Swiss mice into three groups (n = 4 mice per group): free DOX, DOX-hyd-TS/NLC, and DOX-TS ion-pair/NLC. Non-encapsulated DOX-hyd-TS was not used in the *in vivo* experiments since this conjugate is highly hydrophobic, and solubilizers such as Chemophor or DMSO have been associated with toxicity issues (Strickley, 2004). Briefly, the animals received a single dose equivalent to 5 mg/kg of DOX via the tail vein. At 5 min, 0.5 h, 1 h, 2 h, 4 h, and 24 h post-injection, the animals were anesthetized with a mixture of ketamine (80 mg/kg) and xylazine (15 mg/kg), and blood was collected by puncture of the brachial plexus in tubes containing an anticoagulant (0.1% w/v EDTA). After centrifugation at 1,400 × g for 10 min, an aliquot of 125 µL of the supernatant plasma was collected and fortified with 25 µL of a daunorubicin solution (internal standard, 400 µg/mL in acetonitrile). Then, the samples were mixed with 150 µL of 0.1% perchloric acid in acetonitrile to precipitate the proteins. After centrifugation at 9,400 × g for 15 min, the supernatants were collected and injected in HPLC to determine DOX concentrations. Standard calibration curves were prepared using plasma from untreated mice. The pharmacokinetic parameters were calculated by the PKSolver software using non-compartmental analyses and the linear trapezoidal method (Zhang *et al.*, 2010).

2.8 Short-term cardiotoxic effects

We randomly divided Swiss mice into three groups (n = 10 mice per group): blank-NLC, DOX-hyd-TS/NLC, and free DOX. The animals were injected through the tail vein with repeated doses equivalent to 5 mg/kg/day of DOX. The injections were performed every two days, in a total of five administrations, reaching a cumulative dose of 25 mg/kg. We assessed cardiac function and electrophysiology before treatment (baseline) and two days after the last administration by electrocardiogram (ECG) and echocardiogram analyses. ECG was continuously recorded during 10 min under anesthesia (1-2% isoflurane inhalation) using two limb leads and monitored with a Power Lab system (LabChart v7, AD Instruments, Australia). Beat rate and PR, QRS, and QT intervals were measured from the ECG signal. We performed high-resolution echocardiography on a Vevo 3100 system (Fujifilm VisualSonics, Canada) equipped with an MX550D 40 MHz ultrasound probe. Data were acquired under anesthesia (1-2% isoflurane inhalation) and monitoring of body temperature, ECG, and respiration (Sicard *et al.*, 2019). Morphological and functional cardiac parameters were characterized in the M-mode from a short-axis view. We also recorded the mitral inflow by pulsed-wave Doppler in an apical four-chamber view (Branquinho *et al.*, 2017). Offline image analyses were performed using dedicated Visual Sonics Vevo 3100 3.1.0 software.

2.9 Evaluation of antitumor activity

Cultured 4T1 cells (1.0×10^6 cells in 100 µL PBS) were collected and injected subcutaneously into the right thigh of BALB/c mice to establish the tumor-bearing mouse model. When tumor volume reached approximately 150 mm^3, we randomly divided the animals into four groups (n = 6 mice per group): blank-NLC, DOX-hyd-TS/NLC, free DOX, and Lip-DOX (pegylated liposomal DOX). Lip-DOX is similar to commercial Doxil® in size, lipid composition, and the amount of encapsulated drug and was prepared as described elsewhere (Boratto *et al.*, 2020). The animals were injected through the tail vein with repeated doses equivalent to 5 mg/kg/day of DOX. The injections were performed every two days, in a total of five administrations, reaching a cumulative dose of 25 mg/kg. The antitumor efficacy was determined by

measuring the tumor volume with a fine caliper (Mitutoyo, MIP/E-103) every two days, from the first day of treatment until two days after the last administration (Lages *et al.*, 2020).

2.10 Toxicity evaluation

During the assessment of antitumor efficacy, we evaluated behavioral/clinical modifications, body weight, and mice mortality. On the last day of the study, blood was collected from anesthetized mice by puncturing the brachial plexus. We performed hematologic and biochemical analyses as described elsewhere (Boratto *et al.*, 2020). After blood collection, the animals were euthanized and the heart, lungs, spleen, liver, kidneys, and tumor were removed for histopathological examination (Lages *et al.*, 2020).

2.11 Data analysis

Statistical analyses were performed using GraphPad Prism software (version 6.00, La Jolla, California, USA). We tested the difference between the experimental groups by Student's t-test or one-way ANOVA followed by Tukey's test. Survival curves were analyzed by the Log-rank (Mantel-Cox) test. For all analyses, a 95% confidence interval was adopted, and differences were considered significant when the p-value was less than 0.05 ($p < 0.05$).

3 Results

3.1 Cytotoxicity assay

We investigated the cytotoxicity of DOX derivatives in 4T1 breast cancer cells after 48 h of incubation. DMSO used to solubilize the compounds did not affect cell viability and showed similar results to non-treated cells (data not shown). As shown in Fig. 4A, DOX-ami-TS exhibited low cytotoxicity, with cell viability above 60% even at the highest concentration. Consequently, we were not able to calculate the IC_{50} value for the amide derivative. On the other hand, DOX-hyd-TS effectively inhibited the proliferation of tumor cells (IC_{50} value: 0.32 ± 0.10 μM). This conjugate exhibited

cytotoxicity comparable to DOX (IC_{50} value: 0.15 ± 0.02 μM) and higher than DOX-ami-TS. Therefore, we selected DOX-hyd-TS for further studies due to its more significant cytotoxic effect against tumor cells.

Fig. 4. (A) *In vitro* cytotoxicity of DOX, DOX-ami-TS, and DOX-hyd-TS in 4T1 breast cancer cells (data represented as mean ± SD, n = 3, * and # Represents a significant difference compared to DOX and DOX-hyd-TS, respectively ($p < 0.05$)). (B) Plot of particle size distribution x intensity for DOX-hyd-TS/NLC measured by nanoparticle tracking analysis. (C) Cryo-TEM image of DOX-hyd-TS/NLC. White arrows indicate nanostructures. (D) *In vitro* release studies of DOX-hyd-TS/NLC performed in different pH conditions (pH 5.0, 6.8, and 7.4), at 37 °C, by the dialysis method (data represented as mean ± SD, n = 3, * Represents significant differences between the groups ($p < 0.05$)). (E) Semi-logarithmic plasma concentration-time curves after intravenous administration of DOX solution, DOX-TS ion-pair/NLC, or DOX-hyd-TS/NLC in Swiss mice at a dose of 5 mg/kg (data represented as mean ± SEM, n = 4, * Represents significant differences between the groups ($p < 0.05$)).

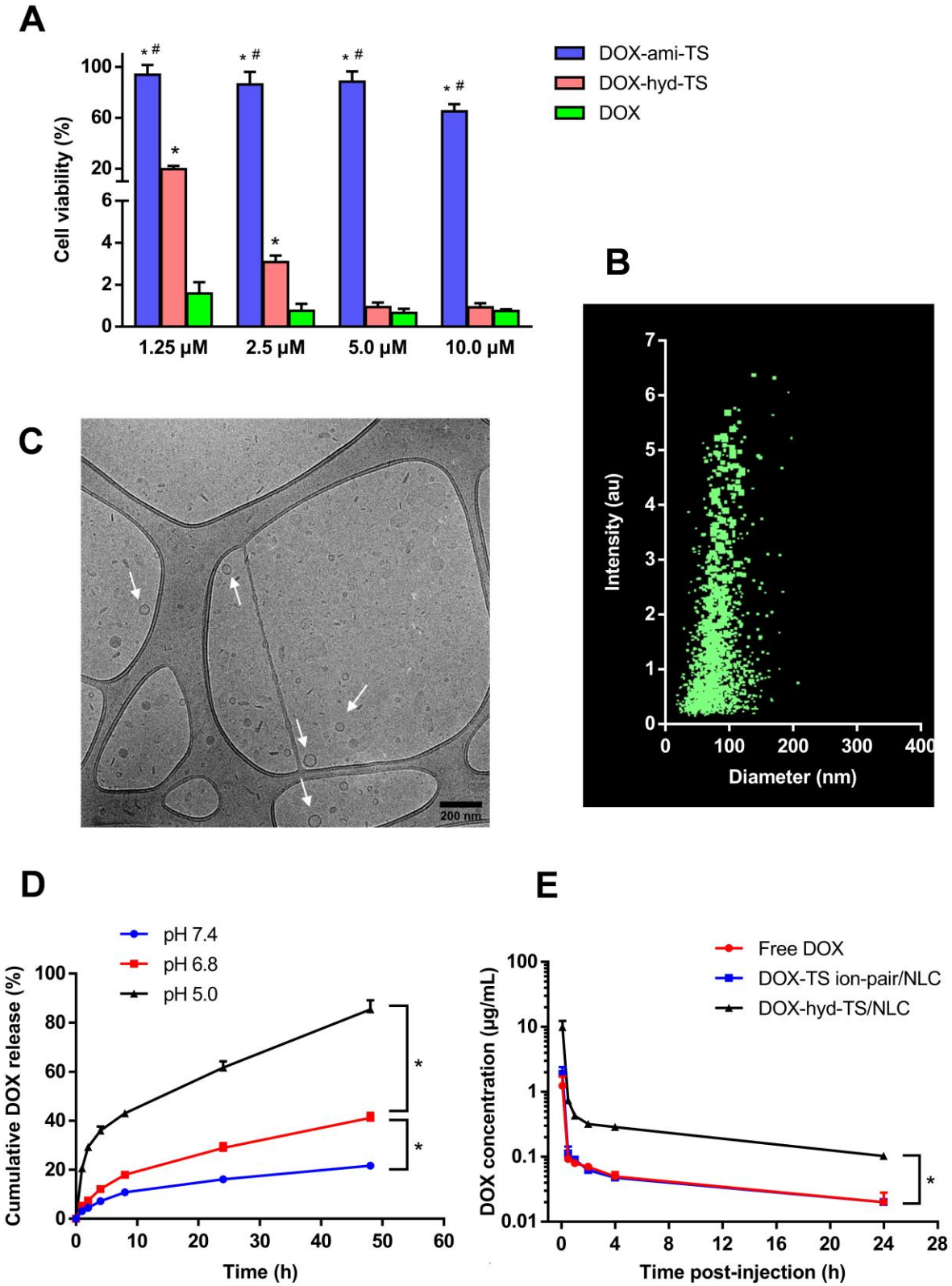
A
Cell viability (%)
100
60
20
6
4
2
0
1.25 μM
2.5 μM
5.0 μM
10.0 μM
DOX-ami-TS
DOX-hyd-TS
DOX
B
Intensity (au)
Diameter (nm)
C
200 nm
D
pH 7.4
pH 6.8
pH 5.0
Cumulative DOX release (%)
Time (h)
E
Free DOX
DOX-TS ion-pair/NLC
DOX-hyd-TS/NLC
DOX concentration (μg/mL)
Time post-injection (h)

3.2 NLC characterization

We prepared NLC formulations with and without DOX-hyd-TS by the hot melting homogenization method. Table 1 presents the physicochemical data. Both blank-NLC and DOX-hyd-TS/NLC showed an average size close to 90 nm with narrow size distribution (PDI < 0.30), suggesting monodisperse systems. The zeta potential was highly negative, probably due to the free TS used in the NLC composition, which is ionized on the particle surface. The addition of DOX-hyd-TS did not increase the particle size, indicating that the lipid matrix could properly incorporate the hydrophobic derivative. The encapsulation rate near 100% confirmed the effective entrapment of the conjugate in the nanocarrier. These characterization data were similar to those reported for DOX-TS ion-pair/NLC (Lages *et al.*, 2020). We also evaluated nanoparticle size distribution by NTA (Table S1). The average diameter measured by NTA was similar to that determined by DLS. In addition, the size distribution profile (approximately 90% < 140 nm, 50% < 90 nm, 10% < 70 nm) confirmed the narrow distribution (Fig. 4B) as observed before. Morphological analyses of the NLC were performed by cryo-TEM and a representative image for DOX-hyd-TS/NLC is shown in Fig. 4C. The particles generally showed reasonably uniform diameters, with spherical morphology, smooth surface, and visible boundary. These results confirmed a single population of particles as previously demonstrated by DLS and NTA. In the short-term stability test, no significant variation in the parameters was observed, indicating no loss of formulation stability (Fig. S1). These results suggest no aggregation or fusion phenomena that could alter the average diameter and unwanted release of the encapsulated DOX.

Table 1. Physicochemical characterization of blank-NLC and DOX-hyd-TS/NLC.

Parameters	blank-NLC	DOX-hyd-TS/NLC
Mean size (nm)	84 ± 2	91 ± 2
PDI	0.22 ± 0.01	0.25 ± 0.02
Zeta potential (mV)	- 43 ± 2	- 39 ± 2
EE (%)	–	99 ± 1

Note: Results expressed as mean ± SD (n = 3).

Abbreviations: PDI: polydispersity index; EE: encapsulation efficiency.

Table S1. NTA measurements of blank-NLC and DOX-hyd-TS/NLC.

Formulation	Mean size (nm)	Size distribution (nm)		
		D10	D50	D90
blank-NLC	87 ± 1	68 ± 1	91 ± 1	135 ± 6
DOX-hyd-TS/NLC	89 ± 2	72 ± 2	90 ± 1	141 ± 5

Note: Results expressed as mean ± SD (n = 3).

Fig. S1. Preliminary evaluation of the stability of DOX-hyd-TS/NLC at 15 and 30 days after preparation. Samples were stored in amber borosilicate glass bottles at 4 °C and analyzed for mean particle size (white bars) and PDI (black squares) (A), zeta potential (B), and encapsulation efficiency (C). Results expressed as mean ± SD (n = 3). There was no significant difference in the mean particle size, PDI, ZP, and EE during the study ($p > 0.05$).

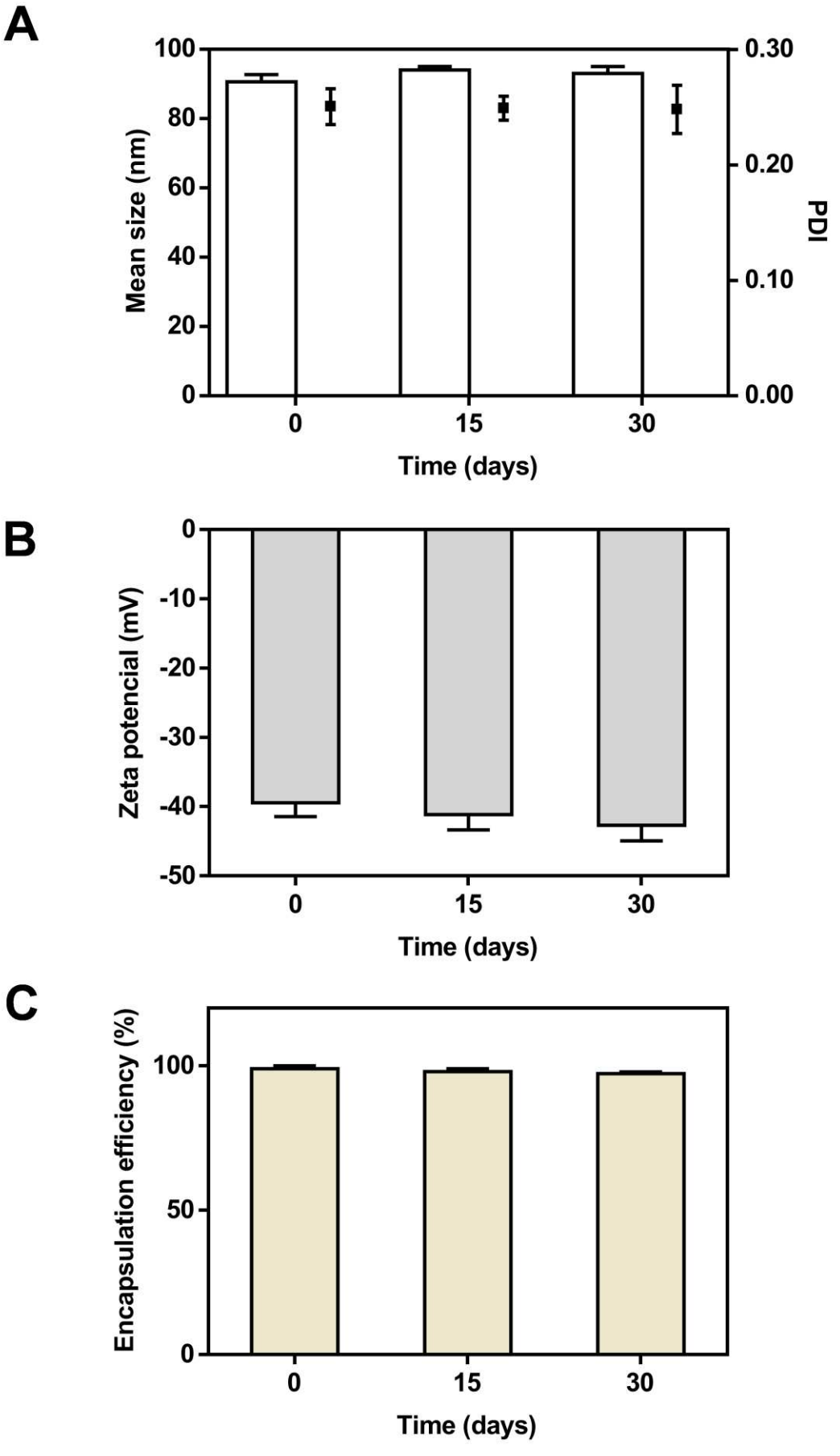
A
Mean size (nm)
PDI
100
80
60
40
20
0
0.30
0.20
0.10
0.00
0
15
30
Time (days)
B
Zeta potencial (mV)
0
-10
-20
-30
-40
-50
0
15
30
Time (days)
C
Encapsulation efficiency (%)
100
50
0
0
15
30
Time (days)

We investigated the *in vitro* drug release at 37 °C under different pH conditions (7.4, 6.8, and 5.0). These conditions correspond to the normal physiological pH, the tumor microenvironment, and the endosomal compartments of tumor cells, respectively (Xiong *et al.*, 2019; Lages *et al.*, 2020). As shown in Fig. 4D, around 16% of DOX was released from DOX-hyd-TS/NLC after 24 h at pH 7.4, reaching only 22% in 48 h. We observed a more pronounced drug release at pH 6.8, with 41% of DOX released within 48 h. In turn, at pH 5.0, a release of 62% of DOX occurred within 24 h and approximately 85% up to 48 h. Therefore, DOX was released from the NLC in a controlled and significantly pH-dependent manner ($p < 0.05$).

3.3 Pharmacokinetics

Pharmacokinetic studies were performed in mice after a single intravenous administration of free DOX, DOX-hyd-TS/NLC, and DOX-TS ion-pair/NLC. Fig. 4E and Table 2 show, respectively, the plasma concentration-time profiles and the major pharmacokinetic parameters. We found comparable *in vivo* behavior for free DOX and DOX-TS ion-pair/NLC, with virtually identical pharmacokinetic parameters. These data suggest that DOX encapsulated by the ion-pairing approach was quickly released from the NLC after administration to the animals, exhibiting behavior similar to the free drug. On the other hand, a significant improvement in pharmacokinetics was achieved when DOX was encapsulated as a hydrophobic conjugate with TS. Higher plasma concentrations were observed for DOX-hyd-TS/NLC throughout the study. Noteworthy, we found an 8-fold increase in plasma concentration at 5 min compared to free DOX and DOX-TS ion-pair/NLC. Furthermore, the plasma kinetics of DOX-hyd-TS/NLC showed significantly higher AUC and C_{max}, lower clearance rate, and lower volume of distribution compared to the other groups. Therefore, we conducted further *in vivo* studies using DOX-hyd-TS/NLC, as the pharmacokinetics of DOX-TS ion-pair/NLC was comparable to that of the free drug.

Table 2. Pharmacokinetic parameters of DOX solution and NLC formulations. Each treatment was intravenously administered in mice at a dose of 5 mg/kg of DOX.

Parameters	Groups		
	Free DOX	DOX-TS ion-pair/NLC	DOX-hyd-TS/NLC
C_{max} (µg/mL)	1.23 ± 0.25	1.88 ± 0.26	9.90 ± 1.23[a]
$t_{1/2}$ (h)	12.7 ± 1.6	11.9 ± 0.6	13.9 ± 1.4
AUC_{0-t} (µg/mL*h)	1.32 ± 0.12	1.51 ± 0.12	8.49 ± 0.52[a]
AUC_{0-inf} (µg/mL*h)	1.69 ± 0.19	1.79 ± 0.12	10.59 ± 0.32[a]
MRT_{0-inf} (h)	13.2 ± 2.2	10.1 ± 0.8	12.7 ± 1.9
Cl (L/h)	0.092 ± 0.009	0.085 ± 0.005	0.014 ± 0.001[a]
V_z (L)	1.64 ± 0.15	1.46 ± 0.13	0.29 ± 0.03[a]

Note: Results expressed as mean ± SEM (n = 4). [a] Represents a significant difference compared to free DOX and DOX-TS ion-pair/NLC ($p < 0.05$).

Abbreviations: C_{max}: maximum concentration in plasma; $t_{1/2}$: elimination half-life; AUC: area under the concentration-time curve; MRT: mean residence time; Cl: clearance; V_z: apparent volume of distribution during the terminal phase.

3.4 Evaluation of cardiotoxic effects

We recorded ECG signals before and after the animals received the fifth treatment dose of blank-NLC, DOX-hyd-TS/NLC, and free DOX. No significant changes in heart rate, PR, and QRS intervals were found compared to the baseline for all treatment groups (Fig. 5). In turn, significant prolongation in the QT interval at the end of treatment was observed in animals receiving free DOX, which did not occur for the blank-NLC and DOX-hyd-TS/NLC groups. Fig. 6 shows echocardiographic analyses. The left ventricular ejection fraction, fractional shortening, and cardiac output of mice treated with nanoformulations did not show any changes compared to the baseline. In contrast, animals repeatedly administered free DOX displayed impaired left ventricular systolic function two days after the end of treatment, reflected in reduced ejection fraction, fractional shortening, and cardiac output. No deaths occurred precisely during this study, but 70% of the animals treated with free DOX died a few

days later, hampering the investigation of late cardiotoxicity. On the other hand, the survival of all animals was verified in the other groups, even some time later. We also determined the E/A ratio by pulsed-wave Doppler as an index of left ventricular diastolic function. Similar values at the study's beginning and end were found for all groups, indicating that the treatments did not compromise diastolic function.

Fig. 5. (A-D) ECG parameters measured in Swiss mice before and after repeated administration of DOX solution, blank-NLC, and DOX-hyd-TS/NLC. (E) Representative ECG signals recorded at the end of the experiment showing QT prolongation for the free DOX group (red arrows). Each treatment was intravenously administered five times, every two days, at 5 mg/kg (data represented as individual values and mean ± SEM, n = 10). * Represents significant differences between the groups ($p < 0.05$).

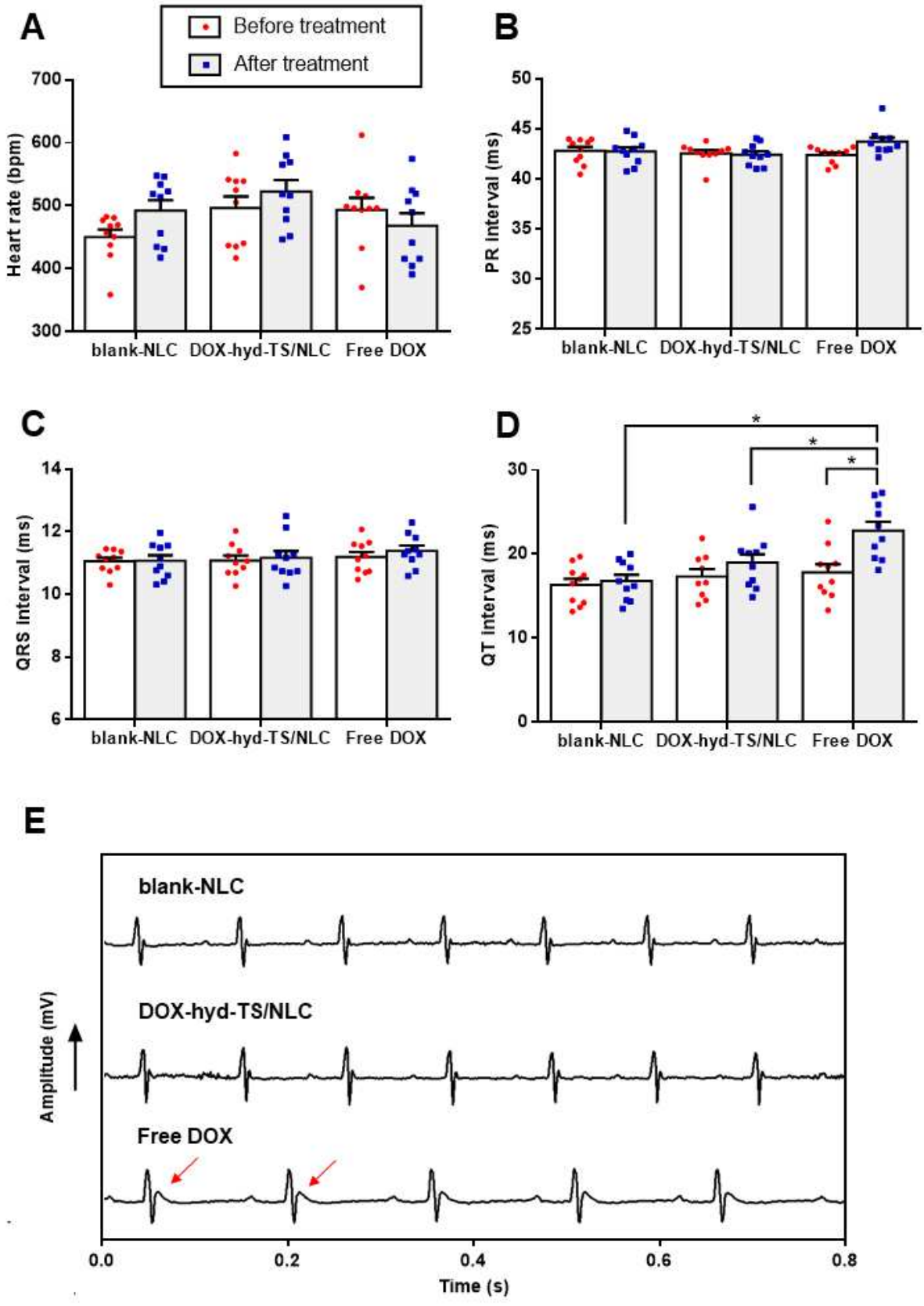
A
Before treatment
After treatment
Heart rate (bpm)
700
600
500
400
300
blank-NLC
DOX-hyd-TS/NLC
Free DOX
B
PR Interval (ms)
50
45
40
35
30
25
blank-NLC
DOX-hyd-TS/NLC
Free DOX
C
QRS Interval (ms)
14
12
10
8
6
blank-NLC
DOX-hyd-TS/NLC
Free DOX
D
QT interval (ms)
30
20
10
0
*
*
*
blank-NLC
DOX-hyd-TS/NLC
Free DOX
E
blank-NLC
DOX-hyd-TS/NLC
Free DOX
Amplitude (mV)
0.0
0.2
0.4
0.6
0.8
Time (s)

Fig. 6. Echocardiographic parameters measured in Swiss mice before and after repeated administration of DOX solution, blank-NLC, and DOX-hyd-TS/NLC. (A) Representative M-mode echocardiography parasternal short-axis view recorded at the end of the experiment, (B) Left ventricular ejection fraction, (C) Fractional shortening, (D) Cardiac output, and (E) E/A ratio. Each treatment was intravenously administered five times, every two days, at a 5 mg/kg (data represented as individual values and mean ± SEM, n = 10). * Represents significant differences between the groups ($p < 0.05$).

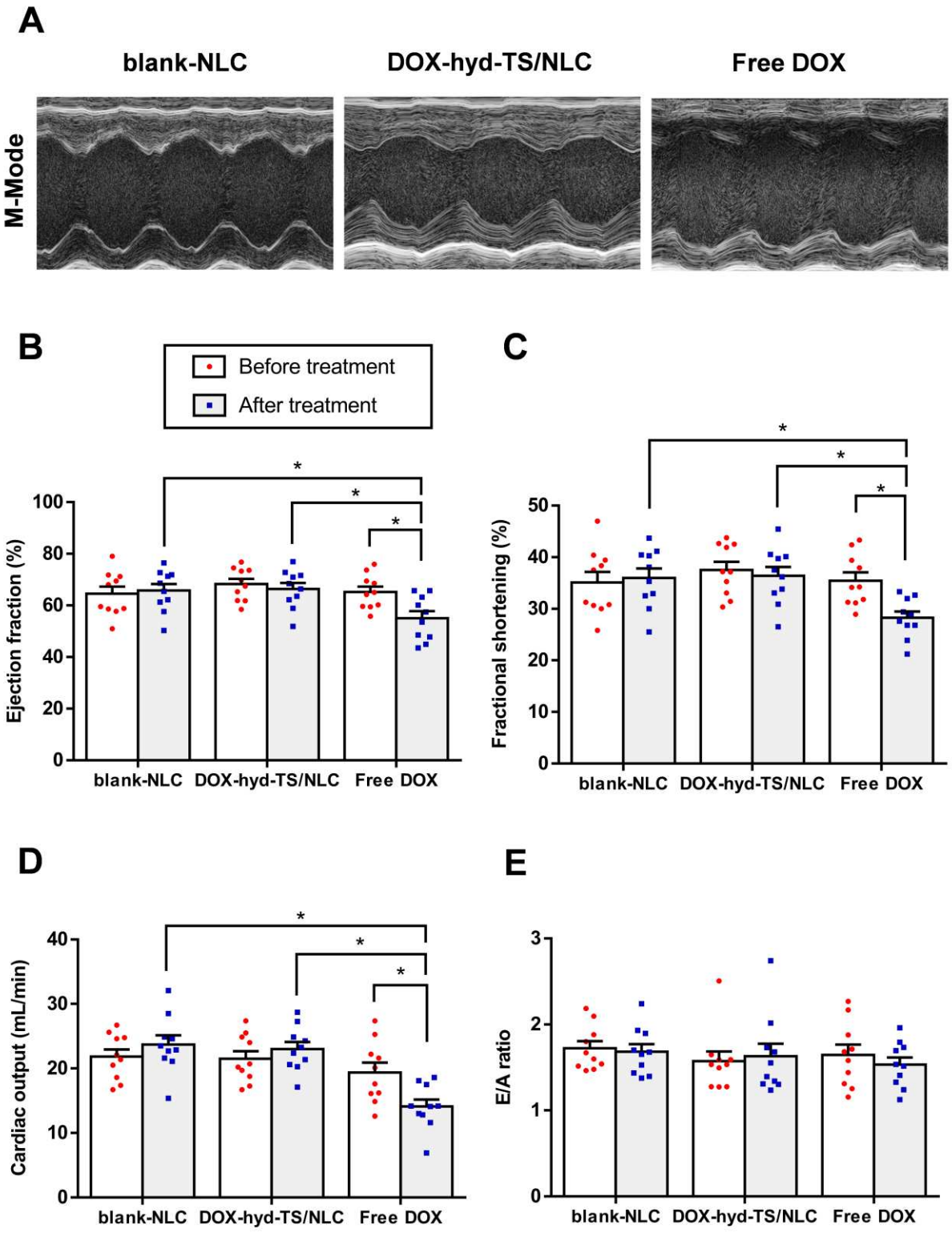
A
blank-NLC
DOX-hyd-TS/NLC
Free DOX
M-Mode
B
Before treatment
After treatment
Ejection fraction (%)
blank-NLC
DOX-hyd-TS/NLC
Free DOX
C
Fractional shortening (%)
D
Cardiac output (mL/min)
E
E/A ratio

3.5 *In vivo* antitumor efficacy

The antitumor activity was investigated by measuring tumor volume every other day in 4T1 tumor-bearing mice treated with blank-NLC, DOX-hyd-TS/NLC, free DOX, and Lip-DOX. As shown in Fig. 7A, rapid tumor growth was observed in the animals from the control group, given the aggressiveness and high rate of cell proliferation of the 4T1 cell line. In contrast, we observed slower tumor growth in the other groups that received formulations containing DOX. Treatment with DOX-hyd-TS/NLC was the most effective in controlling tumor progression since the animals that received this formulation had the smallest tumor volumes at the end of the study. Indeed, a higher tumor inhibition ratio was achieved after treatment with DOX-hyd-TS/NLC (61%) compared to free DOX (44%) and Lip-DOX (56%).

Fig. 7. (A) In vivo therapeutic efficacy of DOX solution, blank-NLC, DOX-hyd-TS/NLC, and Lip-DOX in 4T1 tumor-bearing BALB/c mice. (B) Percentage of body weight variation during the experiment. (C) Representative images of mice treated with free DOX and DOX-hyd-TS/NLC showing clinical signs of toxicity for the free DOX group. (D) Kaplan-Meier survival curves in the different groups. Blank-NLC, DOX-hyd-TS/NLC, and Lip-DOX curves were plotted together because no deaths were observed in these groups. Each treatment was intravenously administered five times, every two days, at 5 mg/kg (data represented as mean ± SEM, n = 6). * Represents significant differences between the groups ($p < 0.05$).

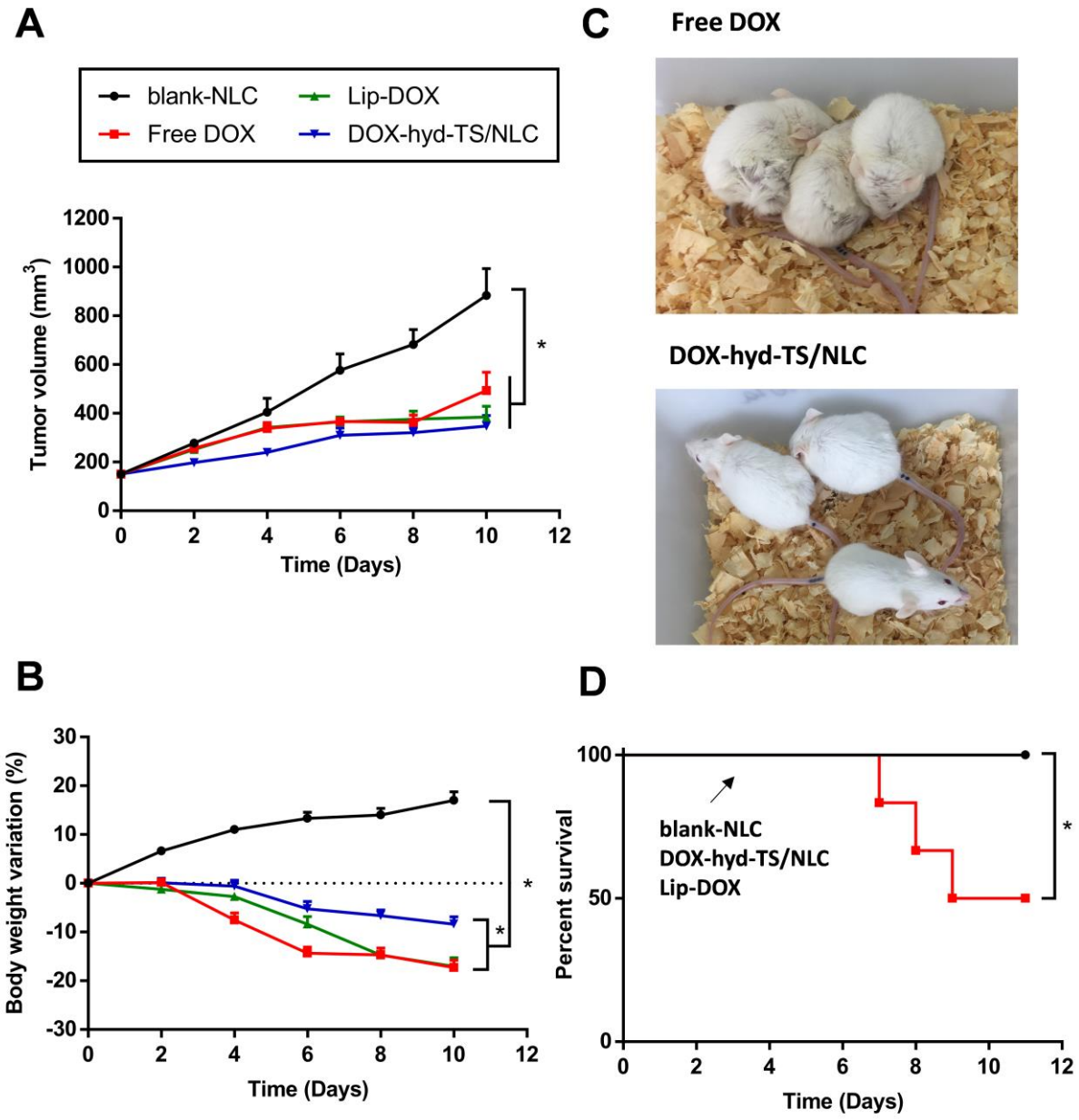

Fig. S2 shows histological sections of tumor tissue evaluated after treatment. Mice that received blank-NLC showed tumors with ulceration, a central area of necrosis, and vast regions of viable cells with mitotic figures, indicating a high rate of cell proliferation. In contrast, all other groups had smaller tumors and larger necrosis areas due to DOX-induced cell death compared to the control group.

Fig. S2. Photomicrographs of the tumor tissue of 4T1 tumor-bearing BALB/c mice treated with blank-NLC (A), DOX solution (B), Lip-DOX (C), and DOX-hyd-TS/NLC (D). Hematoxylin-eosin staining, original magnification x 2. Black asterisks indicate necrotic areas in the tumors.

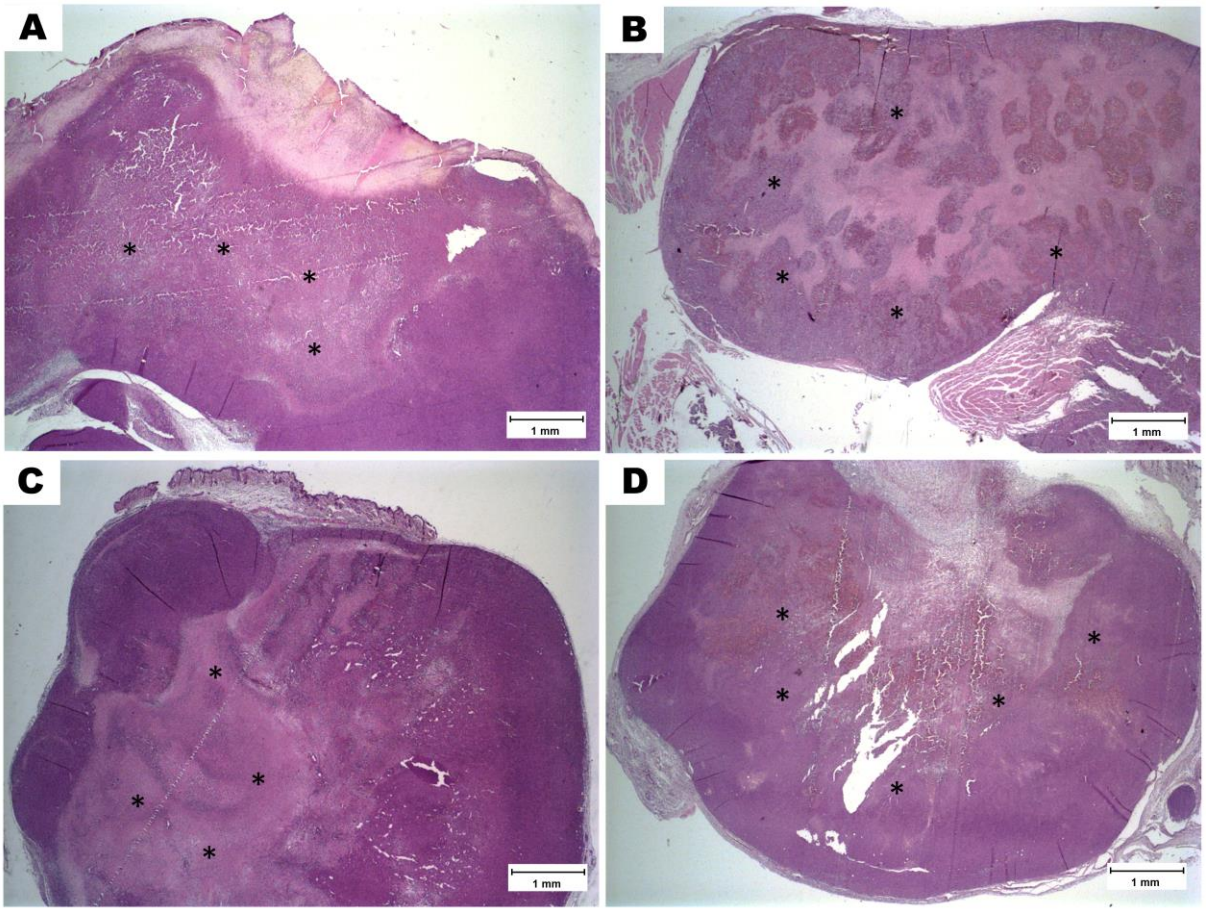

3.6 Preliminary toxicity evaluation

We monitored mice's body weight every two days throughout the study and the results are shown in Fig. 7B. Weight gain was observed only in the animals treated with blank-NLC, evidencing the safety of blank-formulation. Weight loss was significantly lower in the animals treated with DOX-hyd-TS/NLC than free DOX and Lip-DOX. As shown in Fig. 7C, pronounced clinical signs of toxicity, such as prostration and intense piloerection, were observed in animals from the free DOX group, while no or few alterations were found in mice treated with nanoformulations (data shown for DOX-hyd-TS/NLC). In fact, only in the free DOX group did the death of mice occur from the seventh day after the beginning of the study, corresponding to the fourth injected dose (Fig. 7D).

3.7 Hematologic analyses

Hematologic analyses were performed at the end of treatment and results are summarized in Table 3. We found alterations in some parameters compared to the reference values (Everds, 2007) in all groups due to the 4T1 breast cancer, which induces a severe leukemoid reaction and an anemic phenotype in mice with low red blood cell count, platelets, hematocrit, and hemoglobin levels (duPre' e Hunter, 2007). The animals that received blank-NLC showed a significant increase in the number of white blood cells due to the rapid tumor growth, while this was not observed in the other groups. Treatment with all formulations containing DOX led to a reduction in platelet count, indicating a certain level of DOX-induced bone marrow toxicity. However, this reduction was significantly lower for mice treated with DOX-hyd-TS/NLC than those who received free DOX. Red blood cells count, hemoglobin, hematocrit, and RDW were similar in all treatment groups.

Table 3. Hematologic parameters of 4T1 tumor-bearing BALB/c mice after different treatments. Each treatment was intravenously administered five times, every two days, at a dose of 5 mg/kg of DOX.

Parameters	Reference values (Everds, 2007)	Groups			
		blank-NLC	Free DOX	Lip-DOX	DOX-hyd-TS/NLC
White blood cells (10^9/L)	2 – 10	56.2 ± 6.9	3.7 ± 0.8[a]	5.3 ± 1.0[a]	5.9 ± 1.4[a]
Red blood cells (10^{12}/L)	7 – 11	5.9 ± 0.4	4.3 ± 0.3	5.1 ± 0.2	4.7 ± 0.2
Hemoglobin (g/L)	13 – 18	9.9 ± 1.1	7.8 ± 0.6	9.8 ± 0.5	8.7 ± 0.4
Hematocrit (%)	40 – 50	28.0 ± 2.4	19.8 ± 1.4	23.8 ± 0.9	21.7 ± 0.8
RDW (%)	11 – 15	14.6 ± 0.2	13.3 ± 0.1	13.9 ± 0.1	13.9 ± 0.1
Platelets (10^9/L)	1000 – 2000	387 ± 39	199 ± 16[a]	244 ± 28[a]	264 ± 23[a,b]

Note: Results expressed as mean ± SEM (n = 6). [a] Represents a significant difference compared to blank-NLC. [b] Represents a significant difference compared to free DOX ($p < 0.05$).
Abbreviations: RDW: red cell distribution width.

3.8 Biochemical analyses

Biochemical analyses were also performed in order to investigate renal, hepatic, and cardiac toxicity. Both urea and creatinine were similar in all groups, indicating no renal toxicity. As an indicator of DOX-induced hepatic injury, mice treated with free DOX showed a significant increase in ALT and AST levels compared to those treated with blank-NLC. Were also found increased AST levels in animals that received Lip-DOX. In contrast, mice treated with DOX-hyd-TS/NLC showed ALT and AST levels similar to the control group. Concerning cardiac toxicity, treatment with free DOX resulted in significantly higher levels of CK-MB, while animals that received Lip-DOX and DOX-hyd-TS/NLC showed values similar to those in the control group.

Table 4. Biochemical parameters of 4T1 tumor-bearing BALB/c mice after different treatments. Each treatment was intravenously administered five times, every two days, at a dose of 5 mg/kg of DOX.

Parameters	Groups			
	blank-NLC	Free DOX	Lip-DOX	DOX-hyd-TS/NLC
Creatinine (mg/dL)	0.38 ± 0.03	0.28 ± 0.03	0.25 ± 0.02	0.28 ± 0.01
Urea (mg/dL)	62.4 ± 6.4	109.7 ± 12.8	75.7 ± 11.7	64.5 ± 4.1
ALT (U/L)	29.0 ± 2.2	141.4 ± 31.1[a]	75.8 ± 8.0	52.8 ± 3.7[b]
AST (U/L)	114.6 ± 12.2	298.6 ± 40.6[a]	252.6 ± 32.4[a]	154.6 ± 13.6[b,c]
CK-MB (U/L)	40.1 ± 4.7	194.1 ± 49.2[a]	72.9 ± 17.7[b]	49.3 ± 3.2[b]

Note: Results expressed as mean ± SEM (n = 6). [a] Represents a significant difference compared to blank-NLC. [b] Represents a significant difference compared to free DOX. [c] Represents a significant difference compared to Lip-DOX ($p < 0.05$).

Abbreviations: ALT: alanine aminotransferase; AST: aspartate aminotransferase; CK-MB: creatine kinase-myocardial band.

3.9 Histopathological examination

After treatment, histopathologic analyses were carried out on mice's kidneys, spleen, lungs, liver, and heart. In agreement with the biochemical results, all groups showed preserved renal tissues with their typical architecture. We observed an enlarged spleen in animals that received blank-NLC, consistent with the leukemoid reaction and splenomegaly caused by the 4T1 tumor. In contrast, mice from the other groups showed normal-sized spleens, indicating that the treatments could overcome splenomegaly. We found pulmonary metastases in all groups due to the 4T1 breast tumor (Fig. S3), which is highly tumorigenic, invasive, and spontaneously metastasizing to distant organs (duPre' e Hunter, 2007). However, while most mice treated with blank-NLC had extensive and numerous metastatic foci in the lungs, in the other groups, only a few animals presented small and localized metastases, indicating that DOX therapy reduced the potential for tumor invasiveness.

We also evidenced multiple metastatic foci in the liver of mice receiving blank-NLC (Fig. 8A). In contrast, animals in the other groups did not show metastatic foci, and only mild hydropic degeneration and rare inflammatory cell infiltration were found, especially for those treated with Lip-DOX and DOX-hyd-TS/NLC, possibly due to the high uptake of these particles by the liver (Blanco, Shen e Ferrari, 2015). Regarding the histologic evaluation of the heart, mice treated with blank-NLC revealed cardiac tissue with typical architecture and cardiac fibers of the usual thickness (Fig. 9). In contrast, we detected large areas of cardiomyocyte vacuolization and hyaline degeneration in animals treated with free DOX. Mice that received Lip-DOX and DOX-hyd-TS/NLC showed fewer vacuoles and mild hyalinization, indicating better protection against the cardiotoxic effects of DOX.

Fig. S3. Photomicrographs of the lung tissue of 4T1 tumor-bearing BALB/c mice treated with blank-NLC (A), DOX solution (B), Lip-DOX (C), and DOX-hyd-TS/NLC (D). Hematoxylin-eosin staining, original magnification x 40. Red arrows indicate metastasis in the lung.

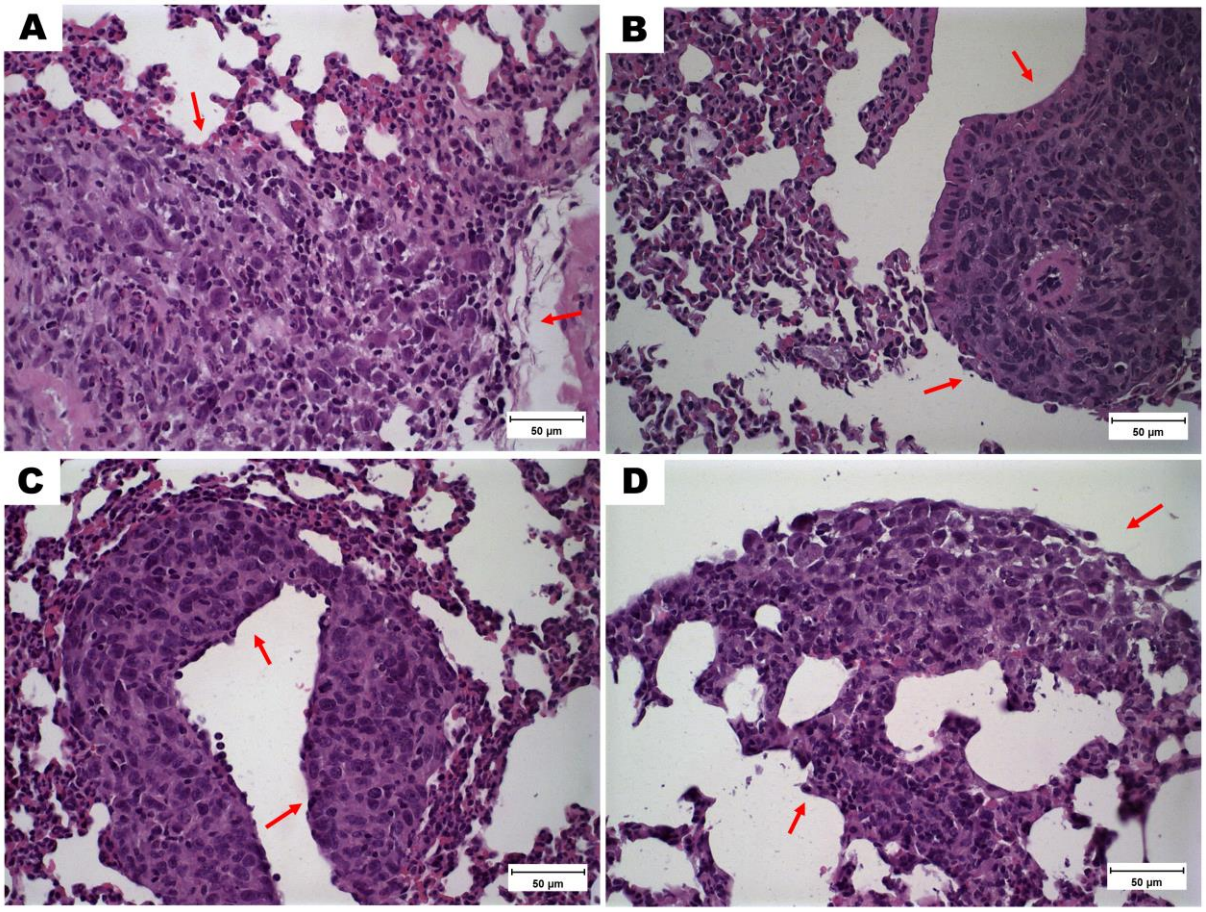

Fig. 8. Histological sections of the liver of 4T1 tumor-bearing BALB/c mice treated with blank-NLC (A), DOX solution (B), Lip-DOX (C), and DOX-hyd-TS/NLC (D). Hematoxylin-eosin staining. Original magnification x 20. Red arrows indicate metastasis (inset: metastatic focus – amplification 40 x) and black arrows represent inflammatory cells infiltration in the liver.

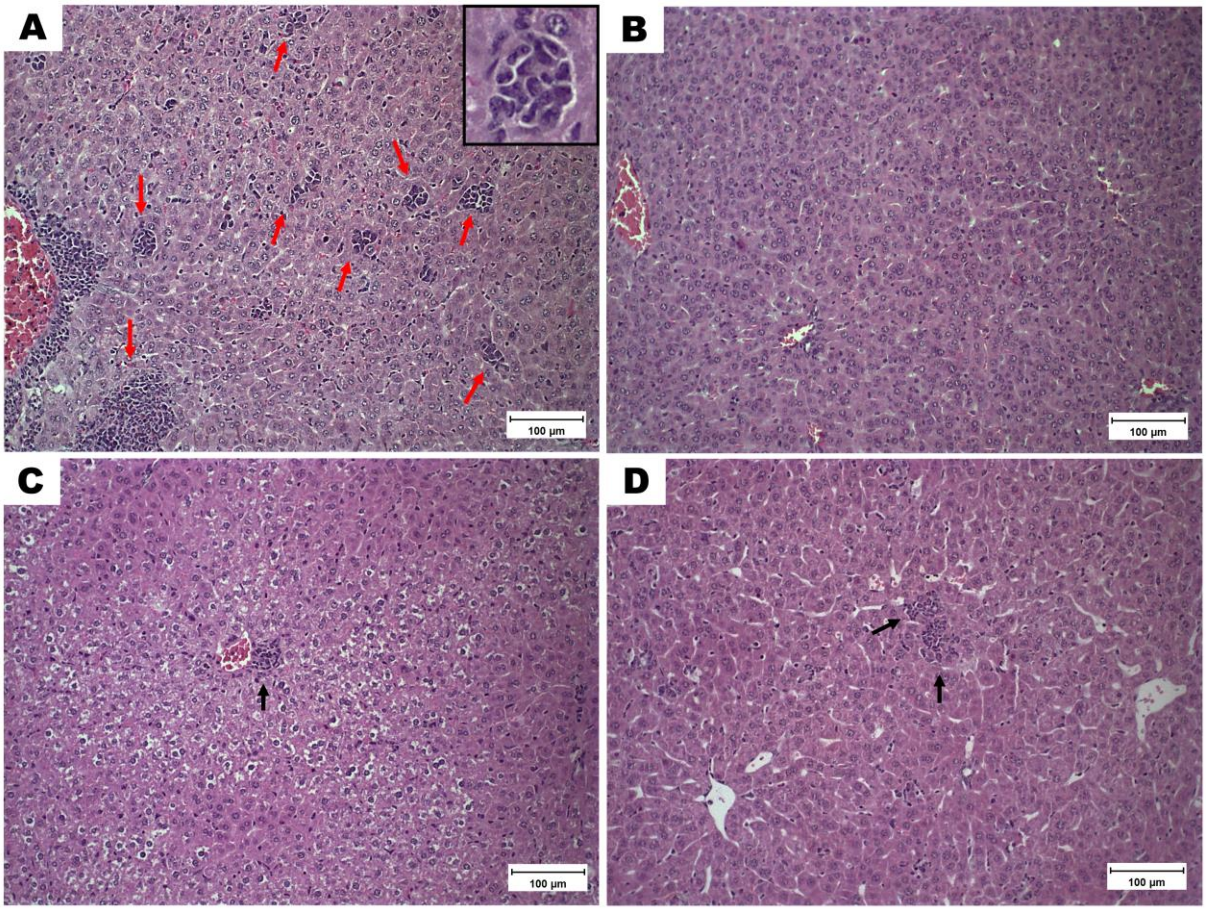

Fig. 9. Histological sections of the heart of 4T1 tumor-bearing BALB/c mice treated with blank-NLC (A), DOX solution (B), Lip-DOX (C), and DOX-hyd-TS/NLC (D). Hematoxylin-eosin staining. Original magnification x 40. Yellow arrows indicate vacuolization in the heart (inset: vacuoles – amplification 60 x).

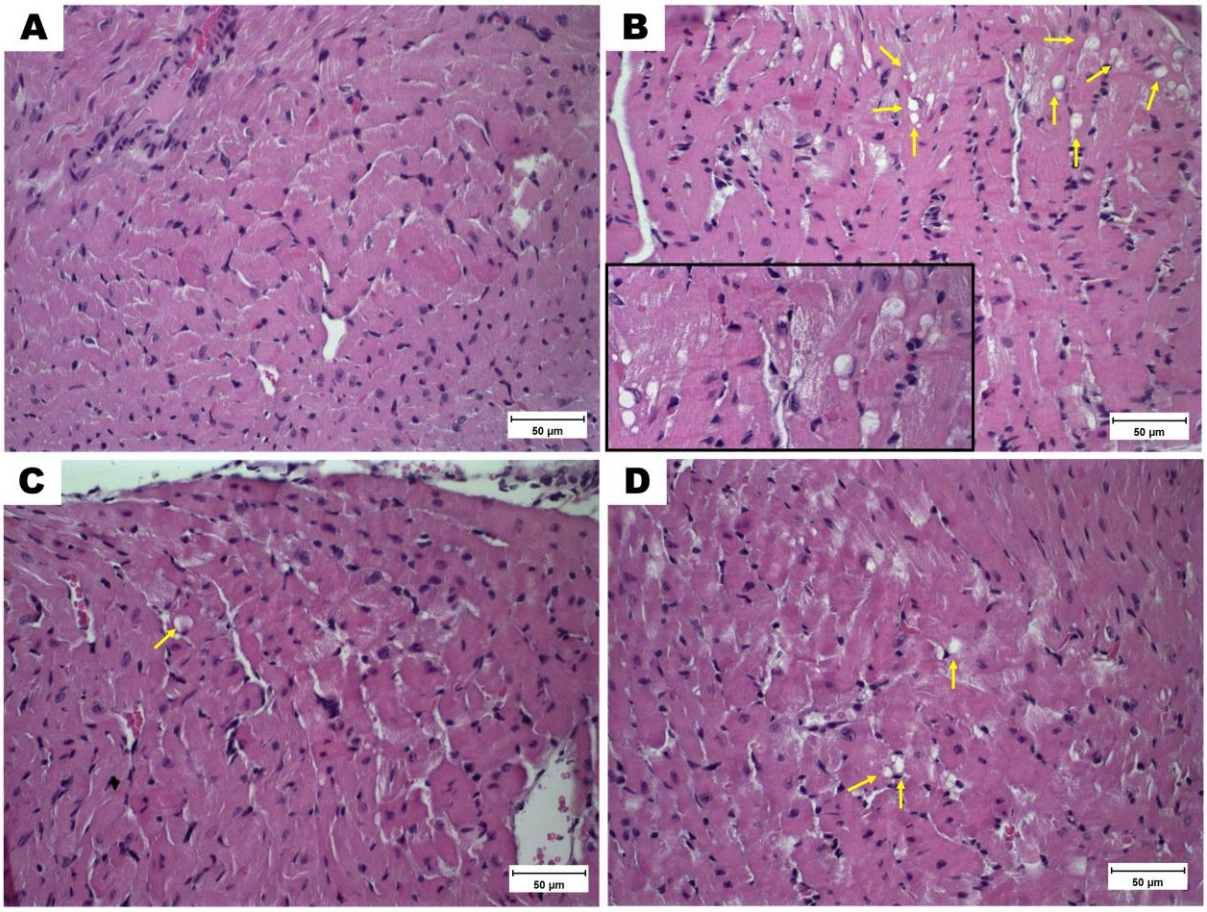

4 Discussion

Hydrophobic ion-pairing has emerged as a method to modulate the solubility of hydrophilic charged molecules and improve their incorporation into several delivery nanocarriers, such as lipid nanoparticles, nanoemulsions, and polymeric micelles (Mussi *et al.*, 2013; Oliveira *et al.*, 2016a; Ristroph e Prud'homme, 2019). Recently, our group used this approach to develop an NLC system encapsulating DOX with the anticancer adjuvants DHA and TS (Lages *et al.*, 2020). We achieved high DOX encapsulation efficiency due to ion-pairing with TS. Our data confirmed the therapeutic potential of this new formulation, given its high antitumor activity *in vivo* and lower toxicity than those observed for free DOX due to the synergistic effect of the drugs. However, pharmacokinetic studies had not been performed, and this has

been one of the critical challenges associated with the ion-pairing approach (Li *et al.*, 2016; Gamboa *et al.*, 2020).

In the present work, we extended our studies by evaluating the pharmacokinetics after intravenous administration in mice. The data obtained indicated pharmacokinetics virtually equal to free DOX, suggesting a rapid destabilization of the ion-pair and the consequent release of DOX from the NLC after administration to the animals. Li *et al.* reported a similar behavior for polymeric nanoparticles encapsulating DOX and hyaluronic acid via electrostatic interactions, which showed a significant burst effect in the plasma after intravenous injection (Li *et al.*, 2016). Considering that one of the nanomedicine principles is to improve the pharmacokinetics of encapsulated drugs, the results obtained with DOX-TS ion-pair/NLC were not satisfactory, making us give up on this approach.

To overcome this drawback, we proposed the synthesis of DOX-TS hydrophobic conjugates to improve the retention of DOX in the lipid nanocarrier. TS is a succinic acid ester of vitamin E and one of the most effective anticancer compounds in the vitamin E family. It can enhance the efficacy of conventional anticancer drugs and protect normal cells from chemotherapy-induced toxicity by multiple pathways (Neuzil, 2003; Prasad *et al.*, 2003; Liang e Qiu, 2021). Several anticancer prodrugs were obtained in recent years by conjugating TS with cytotoxic drugs, such as paclitaxel, camptothecin, and DOX (Duhem *et al.*, 2014; Lu *et al.*, 2015; Zhang *et al.*, 2018; Xiong *et al.*, 2019).

In this study, we synthesized amide and hydrazone prodrugs of DOX and TS according to the procedures previously described, with some modifications (Duhem *et al.*, 2014; Xiong *et al.*, 2019). The conjugates were obtained without laborious purification methods and with good yields, above 70% for both. The amide derivative showed low cytotoxic effects to kill 4T1 breast cancer cells, which was later confirmed in preliminary studies using 4T1 tumor-bearing mice (data not shown). This behavior can probably be explained by the intracellular stability of the conjugate, which did not release a substantial amount of DOX. Previous studies have shown that some amide bonds can be very chemically stable, even in biological environments (Chhikara *et al.*, 2011; Chhikara, Mandal e Parang, 2012). On the

other hand, the hydrazone conjugate effectively decreased cell viability, presenting an antitumor activity comparable to DOX in some tested concentrations. However, this conjugate had a higher IC_{50} value, resulting from an incomplete or delayed *in vitro* conversion of the conjugate to release DOX and TS.

To investigate the *in vivo* therapeutic potential of DOX-hyd-TS, we encapsulated it in a DHA-based nanocarrier. DHA is an omega-3 fatty acid that can enhance the cytotoxic activity of anticancer drugs, primarily by increasing the sensitivity of cancer cells and producing oxidative damage species (Siddiqui *et al.*, 2011; Song e Kim, 2016). In addition, cardioprotective effects have been attributed to it, which can be extremely useful when used in combination therapy with DOX (Adkins e Kelley, 2010; Serini *et al.*, 2017; Lages *et al.*, 2021). Both blank-NLC and DOX-hyd-TS/NLC showed mean diameters close to 90 nm and uniform size distribution determined by DLS and NTA, which may favor the passive targeting of these nanoparticles to the tumor tissue through the EPR effect (Fang, Nakamura e Maeda, 2011; Kalyane *et al.*, 2019). Furthermore, nanoparticles smaller than 5 nm are rapidly removed from the circulation via renal clearance, while particles larger than 200 nm are more likely to be removed by the mononuclear phagocyte system (Blanco, Shen e Ferrari, 2015).

The hydrophobic conjugate showed a high affinity for the lipid matrix of the NLC with an encapsulation rate near 100%. *In vitro* release studies revealed a slow DOX release from DOX-hyd-TS/NLC at pH 7.4, while fast release occurred at acidic conditions due to the pH-sensitive hydrazone bond. This indicates that the conjugate remains stable at physiological pH, while DOX can be rapidly released under low pH conditions of tumor cells, especially in the internal compartments of endosomes. Similar findings were reported by Xiong et al. for a hydrazone prodrug of DOX and TS encapsulated in TPGS micelles (Xiong *et al.*, 2019). This selective release profile makes the use of hydrazone linkages one of the most attractive and well-studied approaches to the delivery of anticancer drugs, including paclitaxel, docetaxel, and DOX (Manchun, Dass e Sriamornsak, 2012; Sonawane, Kalhapure e Govender, 2017).

Pharmacokinetic studies performed in mice after a single intravenous injection revealed an improved behavior for DOX-hyd-TS/NLC, confirming that the chemical

conjugation with TS increased DOX retention in the NLC. Previous studies have shown that the synthesis of DOX derivatives and encapsulation in lipid nanocarriers can prolong blood circulation, enhance tumor accumulation, and reduce off-target toxicity. Ni *et al.* produced an NLC formulation loading vincristine and a hydrolyzable prodrug of DOX and gemcitabine that showed better pharmacokinetics than DOX and greater antitumor efficacy in a lymph cancer mouse model (Ni *et al.*, 2017). Câmara *et al.* also described an acid-sensitive hydrophobic DOX prodrug encapsulated in a nanoemulsion system as an approach to improve pharmacokinetics and reduce systemic toxicity of DOX (Santos Câmara *et al.*, 2017).

Besides the better pharmacokinetics, cardiotoxicity studies showed that DOX-hyd-TS/NLC avoided the acute effects evoked by DOX. Repeated treatment with free DOX, reaching a cumulative dose of 25 mg/kg, resulted in prolonged QT interval and impaired left ventricular systolic function, with reduced ejection fraction, fractional shortening, and cardiac output. Several studies have reported similar short-term changes in cardiac function and electrical integrity of the heart after administration of free DOX (Pecoraro *et al.*, 2017; Silva *et al.*, 2019; Zhang *et al.*, 2019). On the other hand, treatment with DOX-hyd-TS/NLC for approximately two weeks did not alter the ECG signal or echocardiographic parameters. The role of nanomedicine in reducing chemotherapy-induced cardiotoxicity is widely known (Cagel *et al.*, 2017; Borges *et al.*, 2021). Nanocarriers can modulate both pharmacokinetic and pharmacodynamic profiles of drugs, thereby decreasing their delivery and toxicity to non-target organs. Moreover, they accumulate to a lesser extent in the heart than free drugs since they cannot cross the tight junctions of myocardial vessels, which minimizes their cardiotoxic effects (Cagel *et al.*, 2017; Fojtu *et al.*, 2017).

In vivo studies in 4T1 tumor-bearing mice showed that DOX-hyd-TS/NLC was more effective than free DOX in controlling tumor growth. Treatment with this formulation led to a tumor inhibition rate of 61%, against 44% for free DOX and 56% for Lip-DOX, a liposomal system similar to commercial Doxil®. Fernandes *et al.* reported similar findings for a DOX-loaded NLC system that also had superior antitumor efficacy than liposomes and the free drug in an animal model of breast cancer (Fernandes *et al.*, 2016). The excellent therapeutic performance of DOX-hyd-TS/NLC can be attributed to its improved pharmacokinetics and the pH-sensitive release of DOX, in addition to

the adjuvant effects of DHA and TS. DHA induces cancer cell apoptosis, cell cycle arrest, and oxidative DNA damage through multiple mechanisms, including membrane incorporation, lipid peroxidation, and action on nuclear receptors (Song e Kim, 2016; Newell *et al.*, 2017). TS also has anticancer properties due to the induction of apoptosis, inhibition of cell proliferation, and disruption of DNA synthesis (Neuzil, 2003; Prasad *et al.*, 2003). Moreover, several *in vitro* and animal studies have shown that the combination of DHA or TS with DOX can enhance anticancer efficacy and reduce therapy-associated side effects (Prasad *et al.*, 2003; Siddiqui *et al.*, 2011; Serini *et al.*, 2017; Xiong *et al.*, 2019)

Treatment with free DOX resulted in clinical signs of toxicity and a high mortality rate during the investigation of acute cardiotoxicity and antitumor efficacy. Hematologic, biochemical, and histopathologic analyses confirmed the damage caused by DOX to the bone marrow, liver, and heart. DOX is a myelosuppressive drug and can directly induce platelet cytotoxicity through ROS generation, reducing glutathione levels, and depleting thiol proteins (Kim *et al.*, 2009). The liver is a common site for DOX-induced cell death and tissue damage. The metabolism of high DOX concentrations results in the production of many ROS, which causes DNA damage, lipid peroxidation, and reduced levels of vitamin E (Boratto *et al.*, 2020; Prasanna, Renu e Valsala Gopalakrishnan, 2020). In turn, cardiotoxicity is its most severe and debilitating toxic effect. Acute DOX cardiotoxicity is characterized by cardiomyocyte degeneration, QT interval prolongation, and increased plasma cardiac markers, such as CK-MB, released in the early response to cardiac injury (Pecoraro *et al.*, 2017; Silva *et al.*, 2019).

On the other hand, the administration of DOX-hyd-TS/NLC and Lip-DOX could prevent or reduce most of these toxic effects. In previous studies carried out by our group, both NLC and liposomes radiolabeled with technetium-99m showed an altered biodistribution profile compared to DOX solution, with increased accumulation in the tumor site and reduced uptake by non-target organs, which justifies the lower toxicity of these systems concerning the free drug (Fernandes *et al.*, 2018b; Silva *et al.*, 2019). Interestingly, DOX-hyd-TS/NLC showed a better toxicity profile than the liposomal formulation, reflected in lower weight loss and unchanged liver enzymes at the end of treatment. These results reinforce an essential role for the combination of

DHA and TS in reducing the toxic effects of DOX, in line with our previous report (Lages *et al.*, 2020), and confirm that the co-encapsulation of these compounds in nanocarriers is an exciting approach for cancer therapy.

5 Conclusion

Hydrophobic DOX derivatives were synthesized in good yields by covalent conjugation to TS via an amide or hydrazone bond. *In vitro* cell analyses indicated that DOX-ami-TS had low cytotoxicity against 4T1 tumor cells, while DOX-hyd-TS effectively reduced cell viability. The hydrazone conjugate was successfully incorporated into a DHA-based NLC, which showed reduced particle size, homogeneous size distribution, and high encapsulation efficiency. *In vitro* release studies revealed a controlled DOX release from the NLC, with increased drug release in the acidic environment due to the pH-sensitive hydrazone linkage. DOX-hyd-TS/NLC showed better pharmacokinetics than free DOX and DOX-TS ion-pair/NLC after intravenous injection in mice. It was also able to avoid the short-term cardiotoxic effects evoked by repeated DOX administration. In the 4T1 tumor-bearing mice model, this formulation presented significant efficacy in inhibiting tumor growth, reducing mice mortality, and decreasing DOX-induced toxicity to the heart and liver. Therefore, DOX-hyd-TS/NLC can be considered a promising formulation for breast cancer treatment.

4 DISCUSSÃO GERAL

No Capítulo 1 deste trabalho, uma formulação NLC encapsulando DOX e os adjuvantes anticâncer DHA e TS foi preparada e caracterizada. O DHA foi utilizado na forma de triglicerídeos como constituinte da matriz lipídica, em uma abordagem já descrita por nosso grupo de pesquisa e que vem sendo empregada para a obtenção de NLC, nanocápsulas e nanoemulsões (Mussi *et al.*, 2014; Fernandes *et al.*, 2018a; de Castro Leão *et al.*, 2021; Lanna *et al.*, 2021). Por sua vez, o TS foi utilizado como um contra íon aniônico para melhorar a eficiência de encapsulação da DOX por meio da formação de um par iônico hidrofóbico. Oliveira *et al*. (2016a) reportaram anteriormente que a adição de 0,4% de TS na composição de uma formulação SLN, aumentou de 30% para 96% a encapsulação da DOX no sistema.

O uso do método convencional de emulsificação-ultrassom para a incorporação da DOX no NLC resultou na degradação do fármaco (cerca de 18%) durante o processo de fabricação. Sabe-se que a DOX é extremamente susceptível à hidrólise alcalina mesmo em temperatura ambiente (Karadaş Bakirhan *et al.*, 2019; Kaushik e Bansal, 2015). Assim, o uso da trietanolamina para formação do par iônico *in situ*, somado à exposição ao calor e a aplicação de sonda ultrassônica de alta intensidade, pode ter contribuído para a degradação do fármaco. Estudos prévios de Mussi e Oliveira não relataram esse mesmo comportamento, o que pode estar relacionado com o grau de seletividade das técnicas empregadas para o doseamento da DOX (HPLC versus espectrofotometria UV-Vis) e variações no insumo farmacêutico ativo utilizado (diferentes fabricantes e rotas de síntese, por exemplo). Além disso, a formulação desenvolvida neste trabalho difere das anteriores quanto ao tipo de nanossistema (SLN versus NLC) e/ou composição empregada (massa de DOX adicionada, presença ou não de um antioxidante, etc), o que também poderia justificar o perfil de degradação diferente.

Por sua vez, o procedimento de incubação da DOX com um NLC previamente preparado foi capaz de prevenir a degradação do fármaco. Assim, o método de incubação foi selecionado para os estudos posteriores já que não foram encontradas diferenças entre as duas formulações quanto ao perfil de liberação da DOX *in vitro* e na estrutura cristalina da matriz lipídica, o que foi demonstrado por SAXS.

Estudos de liberação *in vitro* foram realizados pelo método de diálise e indicaram liberação controlada da DOX a partir do NLC em comparação com o fármaco livre (solução), em concordância com trabalhos anteriores (Mussi *et al.*, 2014; Fernandes *et al.*, 2018b; Borges *et al.*, 2019). Uma liberação mais rápida da DOX em pH 6,8 do que em pH 7,4 foi observada e atribuída ao par iônico DOX-TS. A redução do pH propicia a protonação do grupo carboxila do TS (pKa 5,64), diminuindo a interação do par iônico e reduzindo a retenção da DOX na matriz lipídica. Além disso, a redução do pH diminui o coeficiente de distribuição (log D) da DOX, favorecendo sua partição na fase aquosa. Apesar da liberação controlada observada *in vitro*, estudos de farmacocinética realizados posteriormente mostraram concentrações plasmáticas de DOX em função do tempo similares para o nanocarreador e a DOX livre, sugerindo uma rápida liberação da DOX a partir do NLC. Isso pode ser atribuído à desestabilização do par iônico após administração intravenosa em camundongos. Vale ressaltar que os estudos de farmacocinética foram conduzidos com o NLC em que a DOX foi incorporada por incubação. Porém, ensaios preliminares também foram realizados com a formulação obtida pelo método convencional de emulsificação-ultrassom (dados não mostrados), a fim de garantir que o método de incorporação da DOX não estivesse influenciando no perfil farmacocinético. Os dados obtidos nos estudos de farmacocinética nos revelaram também que o protocolo de liberação *in vitro* precisa ser aprimorado, a fim de aumentar o poder preditivo do ensaio.

Estudos anteriores demonstraram que a estratégia de formação de pares iônicos hidrofóbicos é capaz de melhorar a farmacocinética da DOX (Zara *et al.*, 1999; Zhang *et al.*, 2011), o que não foi observado no presente trabalho. Uma possível justificativa é o fato da formação do par iônico DOX-TS ter ocorrido *in situ*, durante o preparo do NLC. Na literatura, a grande maioria dos complexos são sintetizados previamente, o que permite sua caracterização físico-química por técnicas como DSC, difração de raios-X e RMN, e posteriormente incorporados no nanocarreador (Ristroph e Prud'homme, 2019). Já com a utilização do preparo *in situ*, não é possível garantir inequivocamente a formação do par iônico e nem o rendimento dessa reação, podendo restar moléculas de DOX sem interação com o contra íon lipofílico.

Apesar da limitação no perfil farmacocinético, a formulação NLC usando a estratégia de par iônico mostrou grande potencial terapêutico *in vivo*, possivelmente pelo efeito sinérgico da DOX, DHA e TS. A administração dessa formulação resultou em baixo crescimento do tumor 4T1 em camundongos, além de toxicidade sistêmica consideravelmente menor em comparação à DOX livre. Esses achados estão em concordância com relatos prévios do nosso grupo para nanocarreadores que também encapsularam a DOX pela formação de pares iônicos (Fernandes *et al.*, 2018a,b; Borges *et al.*, 2019). É possível que nos minutos iniciais após a injeção intravenosa a DOX tenha se mantido encapsulada e tenha ocorrido uma entrega significativa do fármaco na região do tumor. No estudo de farmacocinética, o primeiro tempo de coleta correspondeu a 5 minutos após a administração, o que representa um período relativamente longo em camundongos, já que o tempo de uma circulação completa nesses animais é de cerca de 5 a 10 segundos (Hall *et al.*, 2012; Liu *et al.*, 2021). Além disso, Fernandes *et al*. (2018a,b) demonstraram que sistemas NLC radiomarcados com tecnécio-99m apresentaram perfil de biodistribuição alterado em relação à DOX livre, com aumento do acúmulo na região tumoral e redução da captação por órgãos não-alvo. Assim, mesmo que a DOX tenha sido liberada rapidamente após administração endovenosa, é provável que os nanocarreadores contendo DHA e TS (constituintes hidrofóbicos) tenham se acumulado preferencialmente no tumor, levando a um efeito sinérgico na ação antitumoral e redução da toxicidade.

A fim de aumentar a retenção da DOX na matriz lipídica do NLC e aprimorar a farmacocinética, no Capítulo 2 foi proposta a síntese de conjugados covalentes DOX-TS. Essa estratégia foi selecionada a partir dos resultados interessantes obtidos por Duhem *et al*. (2014) e Xiong *et al*. (2019), que sintetizaram pró-fármacos hidrofóbicos DOX-TS por meio de ligações amida e hidrazona. No presente trabalho, a síntese dos conjugados foi realizada de acordo com os procedimentos descritos anteriormente, com algumas modificações, e permitiu a obtenção dos compostos em bons rendimentos e sem métodos laboriosos de purificação.

O derivado amida mostrou baixa citotoxicidade frente células de câncer de mama 4T1 tanto *in vitro* quanto *in vivo* (ensaios preliminares), o que também foi relatado

por Xiong *et al*. (2019) em células tumorais MCF-7. Entretanto, esses dados estão em discordância com os estudos de Duhem *et al*. (2014), que reportaram citotoxicidade relativamente baixa frente células MCF-7, mas eficácia antitumoral promissora em um modelo animal, com atividade superior à DOX livre. Já o derivado hidrazona apresentou alta capacidade em inibir a proliferação de células 4T1 *in vitro* e em camundongos portadores de tumor. Achados semelhantes já haviam sido reportados para esse conjugado em linhagem celular MCF-7 (Xiong *et al.*, 2019).

A encapsulação do derivado hidrazona no sistema NLC mostrou-se uma estratégia eficiente para melhorar significativamente a farmacocinética da DOX, aumentando as concentrações plasmáticas, diminuindo a taxa de depuração e reduzindo o volume de distribuição em comparação à DOX livre e à formulação encapsulando DOX na forma de par iônico. A investigação da farmacocinética não foi realizada nos trabalhos prévios com os conjugados covalentes DOX-TS (Duhem *et al.*, 2014; Xiong *et al.*, 2019). Entretanto, diversos autores já relataram que a síntese de pró-fármacos da DOX e encapsulação em nanocarreadores é uma abordagem útil para aprimorar o perfil cinético (Liang e Qiu, 2021; Ni *et al.*, 2017; Santos Câmara, Dos *et al.*, 2017).

O monitoramento da função cardíaca por eletrocardiograma e ecocardiograma revelou que a administração da formulação também foi capaz de evitar os efeitos cardiotóxicos agudos provocados pela injeção repetida da DOX, como prolongamento do intervalo QT e prejuízo da função sistólica ventricular esquerda. Em um modelo de camundongos com tumor 4T1, o tratamento com o nanocarreador resultou em alta eficácia antitumoral e toxicidade sistêmica consideravelmente menor em comparação ao fármaco livre, o que foi demonstrado por análises hematológicas, bioquímicas e histológicas. Esses resultados estão em consonância com o que foi descrito por Xiong *et al*. (2019) em um modelo de camundongos com tumor MCF-7.

5 CONCLUSÕES GERAIS

Neste trabalho, foi preparado pela primeira vez um sistema NLC encapsulando DOX e os adjuvantes anticâncer DHA e TS. A encapsulação da DOX após a preparação do NLC, utilizando-se o método de incubação, pôde prevenir a degradação do fármaco durante o processo de fabricação. Foi demonstrado que o par iônico DOX-TS possui menor solubilidade aquosa e cristalinidade reduzida em comparação à DOX, o que contribui para a alta encapsulação da DOX na matriz lipídica. Estudos *in vitro* em células tumorais 4T1 revelaram que a associação da DOX, DHA e TS possui efeitos sinérgicos na ação antitumoral. Além disso, mostrou-se que a encapsulação da DOX no NLC aumentou sua captação celular em comparação com o fármaco livre. O estudo de eficácia em camundongos confirmou o potencial terapêutico da formulação, que inibiu consideravelmente o crescimento do tumor 4T1 e reduziu a toxicidade induzida pela DOX. Apesar disso, a estratégia de formação do par iônico não foi capaz de melhorar a farmacocinética em comparação à DOX livre após administração intravenosa em camundongos. A fim de aumentar a retenção da DOX no NLC, derivados hidrofóbicos unindo-se covalentemente a DOX ao TS foram propostos e sintetizados com bons rendimentos. O derivado hidrazona apresentou grande citotoxicidade frente as células 4T1 e foi encapsulado com sucesso no sistema NLC, o que se mostrou uma estratégia eficiente para melhorar a farmacocinética. A administração repetida do nanocarreador não resultou em efeitos cardiotóxicos de curto prazo causados pela DOX. A formulação também apresentou grande eficácia *in vivo* ao inibir o crescimento do tumor 4T1 e diminuir a toxicidade sistêmica da DOX. Portanto, a formulação NLC contendo DHA e o conjugado hidrazona DOX-TS pode ser considerada uma alternativa promissora para o tratamento do câncer.

6 PERSPECTIVAS

- Investigar os possíveis efeitos cardiotóxicos crônicos da formulação contendo o derivado hidrazona em modelo experimental murino;
- Investigar a eficácia antitumoral da formulação contendo o derivado hidrazona em células de câncer de mama humano;
- Investigar se a formação prévia do par iônico DOX-TS e sua posterior encapsulação no sistema NLC poderia ser uma estratégia mais viável para aprimorar a farmacocinética da DOX.

REFERÊNCIAS

Abel, E. L. e DiGiovanni, J. (2011) “Multistage carcinogenesis”, *Current Cancer Research*, 6, p. 27–51. doi: 10.1007/978-1-61737-995-6_2.

Adkins, Y. e Kelley, D. S. (2010) “Mechanisms underlying the cardioprotective effects of omega-3 polyunsaturated fatty acids”, *Journal of Nutritional Biochemistry*, p. 781–792. doi: 10.1016/j.jnutbio.2009.12.004.

Angulo-Molina, A. *et al.* (2014) “The role of alpha tocopheryl succinate (α-TOS) as a potential anticancer agent”, *Nutrition and Cancer*, 66(2), p. 167–176. doi: 10.1080/01635581.2014.863367.

Barenholz, Y. (2012) “Doxil® - The first FDA-approved nano-drug: Lessons learned”, *Journal of Controlled Release*, p. 117–134. doi: 10.1016/j.jconrel.2012.03.020.

Battaglia, L. *et al.* (2014) “Solid lipid nanoparticles for potential doxorubicin delivery in glioblastoma treatment: Preliminary in vitro studies”, *Journal of Pharmaceutical Sciences*, 103(7), p. 2157–2165. doi: 10.1002/jps.24002.

Beloqui, A. *et al.* (2016) “Nanostructured lipid carriers: Promising drug delivery systems for future clinics”, *Nanomedicine: Nanotechnology, Biology, and Medicine*, p. 143–161. doi: 10.1016/j.nano.2015.09.004.

Berquin, I. M., Edwards, I. J. e Chen, Y. Q. (2008) “Multi-targeted therapy of cancer by omega-3 fatty acids”, *Cancer Letters*, p. 363–377. doi: 10.1016/j.canlet.2008.03.044.

Berthiaume, J. M. *et al.* (2005) “Dietary vitamin E decreases doxorubicin-induced oxidative stress without preventing mitochondrial dysfunction”, *Cardiovascular Toxicology*, 5(3), p. 257–267. doi: 10.1385/CT:5:3:257.

Bertram, J. S. (2000) “The molecular biology of cancer”, *Molecular Aspects of Medicine*, p. 167–223. doi: 10.1016/S0098-2997(00)00007-8.

Bidram, E. *et al.* (2019) “A concise review on cancer treatment methods and delivery systems”, *Journal of Drug Delivery Science and Technology*, p. 101350. doi: 10.1016/j.jddst.2019.101350.

Blanco, E., Shen, H. e Ferrari, M. (2015) “Principles of nanoparticle design for overcoming biological barriers to drug delivery”, *Nature Biotechnology*, p. 941–951. doi: 10.1038/nbt.3330.

Bobo, D. *et al.* (2016) “Nanoparticle-Based Medicines: A Review of FDA-Approved Materials and Clinical Trials to Date”, *Pharmaceutical Research*, p. 2373–2387. doi: 10.1007/s11095-016-1958-5.

Boix-Montesinos, P. *et al.* (2021) “The past, present, and future of breast cancer models for nanomedicine development”, *Advanced Drug Delivery Reviews*, p. 306–

330. doi: 10.1016/j.addr.2021.03.018.

Boratto, F. A. *et al.* (2020) “Alpha-tocopheryl succinate improves encapsulation, pH-sensitivity, antitumor activity and reduces toxicity of doxorubicin-loaded liposomes”, *European Journal of Pharmaceutical Sciences*, p. 105205. doi: 10.1016/j.ejps.2019.105205.

Borges, G. S. M. *et al.* (2019) “Sclareol is a potent enhancer of doxorubicin: Evaluation of the free combination and co-loaded nanostructured lipid carriers against breast cancer”, *Life Sciences*, p. 116678. doi: 10.1016/j.lfs.2019.116678.

Borges, G. S. M. *et al.* (2021) “Nanomedicine in Oncocardiology: Contribution and Perspectives of Preclinical Studies”, *Frontiers in Cardiovascular Medicine,* 8, p. 690533. doi: 10.3389/fcvm.2021.690533.

Bradley, M. O. *et al.* (2001) “Tumor targeting by covalent conjugation of a natural fatty acid to paclitaxel”, *Clinical Cancer Research*, 7(10), p. 3329–3338.

Branquinho, R. T. *et al.* (2017) “Biodegradable Polymeric Nanocapsules Prevent Cardiotoxicity of Anti-Trypanosomal Lychnopholide”, *Scientific Reports*, 7, p. 44998. doi: 10.1038/srep44998.

Cagel, M. *et al.* (2017) “Doxorubicin: nanotechnological overviews from bench to bedside”, *Drug Discovery Today*, p. 270–281. doi: 10.1016/j.drudis.2016.11.005.

Calder, P. C. (2016) “Docosahexaenoic acid”, *Annals of Nutrition and Metabolism*, 69(1), p. 8–21. doi: 10.1159/000448262.

Cardinale, D., Iacopo, F. e Cipolla, C. M. (2020) “Cardiotoxicity of Anthracyclines”, *Frontiers in Cardiovascular Medicine*, 7, p. 26. doi: 10.3389/fcvm.2020.00026.

Carvalho, C. *et al.* (2009) “Doxorubicin: The Good, the Bad and the Ugly Effect”, *Current Medicinal Chemistry*, 16(25), p. 3267–3285. doi: 10.2174/092986709788803312.

Castro, G. A. *et al.* (2009) “Formation of ion pairing as an alternative to improve encapsulation and stability and to reduce skin irritation of retinoic acid loaded in solid lipid nanoparticles”, *International Journal of Pharmaceutics*, 381(1), p. 77–83. doi: 10.1016/j.ijpharm.2009.07.025.

Castro Leão, M. *et al.* (2021) “Docosahexaenoic acid nanoencapsulated with anti-PECAM-1 as co-therapy for atherosclerosis regression”, *European Journal of Pharmaceutics and Biopharmaceutics,* 159, p. 99–107. doi: 10.1016/j.ejpb.2020.12.016.

Chen, J., Garssen, J. e Redegeld, F. (2021) “The efficacy of bortezomib in human multiple myeloma cells is enhanced by combination with omega-3 fatty acids DHA and EPA: Timing is essential”, *Clinical Nutrition*, 40(4), p. 1942–1953. doi: 10.1016/j.clnu.2020.09.009.

Cheng, W. *et al.* (2019) “Versatile Polydopamine Platforms: Synthesis and Promising Applications for Surface Modification and Advanced Nanomedicine,” *ACS Nano*, 13(8), pp. 8537–8565. doi:10.1021/acsnano.9b04436.

Chhikara, B. S. *et al.* (2011) “Fatty acyl amide derivatives of doxorubicin: Synthesis and in vitro anticancer activities”, *European Journal of Medicinal Chemistry*, 46(6), p. 2037–2042. doi: 10.1016/j.ejmech.2011.02.056.

Chhikara, B. S., Mandal, D. e Parang, K. (2012) “Synthesis, anticancer activities, and cellular uptake studies of lipophilic derivatives of doxorubicin succinate”, *Journal of Medicinal Chemistry*, 55(4), p. 1500–1510. doi: 10.1021/jm201653u.

Chou, T. C. (2006) “Theoretical basis, experimental design, and computerized simulation of synergism and antagonism in drug combination studies”, *Pharmacological Reviews*, p. 621–681. doi: 10.1124/pr.58.3.10.

D’Eliseo, D. e Velotti, F. (2016) “Omega-3 Fatty Acids and Cancer Cell Cytotoxicity: Implications for Multi-Targeted Cancer Therapy”, *Journal of Clinical Medicine*, 5(2), p. 15. doi: 10.3390/jcm5020015.

Das, S., Nesaretnam, K. e Das, D. K. (2007) “Tocotrienols in Cardioprotection”, *Vitamins and Hormones*, p. 419–433. doi: 10.1016/S0083-6729(07)76016-8.

Di, X. *et al.* (2009) “Apoptosis, autophagy, accelerated senescence and reactive oxygen in the response of human breast tumor cells to Adriamycin”, *Biochemical Pharmacology*, 77(7), p. 1139–1150. doi: 10.1016/j.bcp.2008.12.016.

Duhem, N. *et al.* (2014) “Self-assembling doxorubicin-tocopherol succinate prodrug as a new drug delivery system: Synthesis, characterization, and in vitro and in vivo anticancer activity”, *Bioconjugate Chemistry*, 25, p. 72–81. doi: 10.1021/bc400326y.

duPre’, S. A. e Hunter, K. W. (2007) “Murine mammary carcinoma 4T1 induces a leukemoid reaction with splenomegaly: Association with tumor-derived growth factors”, *Experimental and Molecular Pathology*, 82(1), p. 12–24. doi: 10.1016/j.yexmp.2006.06.007.

Everds, N. E. (2007) “Hematology of the Laboratory Mouse”, in *The Mouse in Biomedical Research*. Elsevier Inc., p. 133–170. doi: 10.1016/B978-012369454-6/50059-5.

Fabian, C. J., Kimler, B. F. e Hursting, S. D. (2015) “Omega-3 fatty acids for breast cancer prevention and survivorship”, *Breast Cancer Research*. BioMed Central Ltd., p. 62. doi: 10.1186/s13058-015-0571-6.

Falzone, L., Salomone, S. e Libra, M. (2018) “Evolution of cancer pharmacological treatments at the turn of the third millennium”, *Frontiers in Pharmacology*, p. 1300. doi: 10.3389/fphar.2018.01300.

Fane, M. e Weeraratna, A. T. (2020) “How the ageing microenvironment influences tumour progression”, *Nature Reviews Cancer*, p. 89–106. doi: 10.1038/s41568-019-

0222-9.

Fang, J., Nakamura, H. e Maeda, H. (2011) “The EPR effect: Unique features of tumor blood vessels for drug delivery, factors involved, and limitations and augmentation of the effect”, *Advanced Drug Delivery Reviews*, p. 136–151. doi: 10.1016/j.addr.2010.04.009.

Fernandes, R. S. *et al.* (2016) “Doxorubicin-loaded nanocarriers: A comparative study of liposome and nanostructured lipid carrier as alternatives for cancer therapy”, *Biomedicine and Pharmacotherapy*, 84, p. 252–257. doi: 10.1016/j.biopha.2016.09.032.

Fernandes, R. S. *et al.* (2018a) “Nanostructured Lipid Carrier Co-loaded with Doxorubicin and Docosahexaenoic Acid as a Theranostic Agent: Evaluation of Biodistribution and Antitumor Activity in Experimental Model”, *Molecular Imaging and Biology,* 20(3), p. 437–447. doi: 10.1007/s11307-017-1133-3.

Fernandes, R. S. *et al.* (2018b) “α- Tocopherol succinate loaded nano-structed lipid carriers improves antitumor activity of doxorubicin in breast cancer models in vivo”, *Biomedicine and Pharmacotherapy,* 103, p. 1348–1354. doi: 10.1016/j.biopha.2018.04.139.

Fojtu, M. *et al.* (2017) “Reduction of Doxorubicin-Induced Cardiotoxicity Using Nanocarriers: A Review”, *Current Drug Metabolism*, 18(3), p. 237–263. doi: 10.2174/1389200218666170105165444.

Gamboa, A. *et al.* (2020) “Delivery of ionizable hydrophilic drugs based on pharmaceutical formulation of ion pairs and ionic liquids”, *European Journal of Pharmaceutics and Biopharmaceutics*, 156, p. 203–218. doi: 10.1016/j.ejpb.2020.09.007.

Gordillo-Galeano, A. e Mora-Huertas, C. E. (2018) “Solid lipid nanoparticles and nanostructured lipid carriers: A review emphasizing on particle structure and drug release”, *European Journal of Pharmaceutics and Biopharmaceutics,* p. 285–308. doi: 10.1016/j.ejpb.2018.10.017.

Haider, M. *et al.* (2020) “Nanostructured lipid carriers for delivery of chemotherapeutics: A review”, *Pharmaceutics*, p. 288. doi: 10.3390/pharmaceutics12030288.

Hall, C. *et al.* (2012) “Interspecies scaling in pharmacokinetics: A novel whole-body physiologically based modeling framework to discover drug biodistribution mechanisms in vivo”, *Journal of Pharmaceutical Sciences,* 101(3), p. 1221–1241. doi: 10.1002/jps.22811.

Ho-Lun, W. *et al.* (2006) “A mechanistic study of enhanced doxorubicin uptake and retention in multidrug resistant breast cancer cells using a polymer-lipid hybrid nanoparticle system”, *Journal of Pharmacology and Experimental Therapeutics*, 317(3), p. 1372–1381. doi: 10.1124/jpet.106.101154.

Hsu, H. C., Chen, C. Y. e Chen, M. F. (2014) “N-3 polyunsaturated fatty acids decrease levels of doxorubicin-induced reactive oxygen species in cardiomyocytes -- involvement of uncoupling protein UCP2”, *Journal of biomedical science*, 21, p. 101. doi: 10.1186/s12929-014-0101-3.

Huang, R. Y. *et al.* (2019) “Isobologram analysis: A comprehensive review of methodology and current research”, *Frontiers in Pharmacology*. doi: 10.3389/fphar.2019.01222.

Jiao, Y. *et al.* (2018) “Sorafenib and docosahexaenoic acid act in synergy to suppress cancer cell viability: a role of heme oxygenase 1”, *BMC Cancer,* 18(1). doi: 10.1186/s12885-018-4946-9.

Kalyanaraman, B. (2020) “Teaching the basics of the mechanism of doxorubicin-induced cardiotoxicity: Have we been barking up the wrong tree?”, *Redox Biology*, p. 101394. doi: 10.1016/j.redox.2019.101394.

Kalyane, D. *et al.* (2019) “Employment of enhanced permeability and retention effect (EPR): Nanoparticle-based precision tools for targeting of therapeutic and diagnostic agent in cancer”, *Materials Science and Engineering C*, p. 1252–1276. doi: 10.1016/j.msec.2019.01.066.

Kanwal, U. *et al.* (2018) “Advances in nano-delivery systems for doxorubicin: an updated insight”, *Journal of Drug Targeting,* p. 296–310. doi: 10.1080/1061186X.2017.1380655.

Karadaş Bakirhan, N. *et al.* (2019) “Degradation studies and thermodynamic parameters in aqueous solution of chemotherapeutic agents: Daunorubicin, doxorubicin and vincristine”, *Journal of Research in Pharmacy,* 23(5), p. 822–831. doi: 10.35333/jrp.2019.30.

Kaushik, D. e Bansal, G. (2015) “Four new degradation products of doxorubicin: An application of forced degradation study and hyphenated chromatographic techniques”, *Journal of Pharmaceutical Analysis,* 5(5), p. 285–295. doi: 10.1016/j.jpha.2015.05.003.

Kawase, M. *et al.* (2002) “Increase of ceramide in adriamycin-induced HL-60 cell apoptosis: Detection by a novel anti-ceramide antibody”, *Biochimica et Biophysica Acta - Molecular and Cell Biology of Lipids*, 1584(2–3), p. 104–114. doi: 10.1016/S1388-1981(02)00301-3.

Khosa, A., Reddi, S. e Saha, R. N. (2018) “Nanostructured lipid carriers for site-specific drug delivery”, *Biomedicine and Pharmacotherapy*, p. 598–613. doi: 10.1016/j.biopha.2018.04.055.

Kim, E. J. *et al.* (2009) “Doxorubicin-induced platelet cytotoxicity: A new contributory factor for doxorubicin-mediated thrombocytopenia”, *Journal of Thrombosis and Haemostasis*, 7(7), p. 1172–1183. doi: 10.1111/j.1538-7836.2009.03477.x.

Lages, E. B. *et al.* (2020) “Co-delivery of doxorubicin, docosahexaenoic acid, and α-

tocopherol succinate by nanostructured lipid carriers has a synergistic effect to enhance antitumor activity and reduce toxicity", *Biomedicine and Pharmacotherapy*, 132, p. 110876. doi: 10.1016/j.biopha.2020.110876.

Lages, E.B. *et al.* (2021) "Nanomedicine to deliver docosahexaenoic acid: Potential applications to improve health," *Nanomedicine*, pp. 1549–1552. doi:10.2217/nnm-2021-0128.

Lanna, E. G. *et al.* (2021) "Lipid-based nanocarriers co-loaded with artemether and triglycerides of docosahexaenoic acid: Effects on human breast cancer cells", *Biomedicine and Pharmacotherapy*, 134, p. 111114. doi: 10.1016/j.biopha.2020.111114.

Lee, K. Y. *et al.* (2015) "Vitamin E containing polymer micelles for reducing normal cell cytotoxicity and enhancing chemotherapy efficacy", *Acta Biomaterialia*, 24, p. 286–296. doi: 10.1016/j.actbio.2015.06.014.

Li, W. *et al.* (2016) "Hyaluronic acid ion-pairing nanoparticles for targeted tumor therapy", *Journal of Controlled Release*, 225, p. 170–182. doi: 10.1016/j.jconrel.2016.01.049.

Li, Z. *et al.* (2021) "Applications of Surface Modification Technologies in Nanomedicine for Deep Tumor Penetration," *Advanced Science*, p. 2002589. doi:10.1002/advs.202002589.

Liang, L., Peng, Y. e Qiu, L. (2021) "Mitochondria-targeted vitamin E succinate delivery for reversal of multidrug resistance", *Journal of Controlled Release,* 337, p. 117–131. doi: 10.1016/j.jconrel.2021.07.023.

Liang, L. e Qiu, L. (2021) "Vitamin E succinate with multiple functions: A versatile agent in nanomedicine-based cancer therapy and its delivery strategies", *International Journal of Pharmaceutics*, p. 120457. doi: 10.1016/j.ijpharm.2021.120457.

Liu, S. *et al.* (2021) "Long circulating tracer tailored for magnetic particle imaging", *Nanotheranostics,* 5(3), p. 348–361. doi: 10.7150/ntno.58548.

Liu, X. *et al.* (2020) "Safety Considerations of Cancer Nanomedicine—A Key Step toward Translation", *Small,* p. 2000673. doi: 10.1002/smll.202000673.

Lu, J. *et al.* (2015) "The self-assembling camptothecin-tocopherol prodrug: An effective approach for formulating camptothecin", *Biomaterials*, 62, p. 176–187. doi: 10.1016/j.biomaterials.2015.05.046.

Ma, W. *et al.* (2020) "Molecular Mechanisms of Cardiomyocyte Death in Drug-Induced Cardiotoxicity", *Frontiers in Cell and Developmental Biology*, p. 434. doi: 10.3389/fcell.2020.00434.

Ma, Y. J. *et al.* (2015) "The consumption of omega-3 polyunsaturated fatty acids improves clinical outcomes and prognosis in pancreatic cancer patients: A systematic

evaluation", *Nutrition and Cancer,* 67(1), p. 112–118. doi: 10.1080/01635581.2015.976315.

Mahéo, K. *et al.* (2005) "Differential sensitization of cancer cells to doxorubicin by DHA: A role for lipoperoxidation", *Free Radical Biology and Medicine*, 39(6), p. 742–751. doi: 10.1016/j.freeradbiomed.2005.04.023.

Manchun, S., Dass, C. R. e Sriamornsak, P. (2012) "Targeted therapy for cancer using pH-responsive nanocarrier systems", *Life Sciences*, p. 381–387. doi: 10.1016/j.lfs.2012.01.008.

McGowan, J. V. *et al.* (2017) "Anthracycline Chemotherapy and Cardiotoxicity", *Cardiovascular Drugs and Therapy*, 31(1), p. 63–75. doi: 10.1007/s10557-016-6711-0.

Merendino, N. *et al.* (2013) "Dietary ω-3 polyunsaturated fatty acid DHA: A potential adjuvant in the treatment of cancer", *BioMed Research International*, p. 310186. doi: 10.1155/2013/310186.

Mohan, P. e Rapoport, N. (2010) "Doxorubicin as a molecular nanotheranostic agent: Effect of doxorubicin encapsulation in micelles or nanoemulsions on the ultrasound-mediated intracellular delivery and nuclear trafficking", *Molecular Pharmaceutics*, 7(6), p. 1959–1973. doi: 10.1021/mp100269f.

Mohanty, R. K., Thennarasu, S. e Mandal, A. B. (2014) "Resveratrol stabilized gold nanoparticles enable surface loading of doxorubicin and anticancer activity", *Colloids and Surfaces B: Biointerfaces,* 114, p. 138–143. doi: 10.1016/j.colsurfb.2013.09.057.

Müller, R. H., Radtke, M. e Wissing, S. A. (2002) "Solid lipid nanoparticles (SLN) and nanostructured lipid carriers (NLC) in cosmetic and dermatological preparations", in *Advanced Drug Delivery Reviews*, p. S131–S155. doi: 10.1016/S0169-409X(02)00118-7.

Mussi, S. V. *et al.* (2013) "New approach to improve encapsulation and antitumor activity of doxorubicin loaded in solid lipid nanoparticles", *European Journal of Pharmaceutical Sciences*, 48(1–2), p. 282–290. doi: 10.1016/j.ejps.2012.10.025.

Mussi, S. V. *et al.* (2014) "Novel nanostructured lipid carrier co-loaded with doxorubicin and docosahexaenoic acid demonstrates enhanced in vitro activity and overcomes drug resistance in MCF-7/Adr cells", *Pharmaceutical Research*, 31(8), p. 1882–1892. doi: 10.1007/s11095-013-1290-2.

Nabavi, S. F. *et al.* (2015) "Omega-3 polyunsaturated fatty acids and cancer: lessons learned from clinical trials", *Cancer and Metastasis Reviews*, 34(3), p. 359–380. doi: 10.1007/s10555-015-9572-2.

Neuzil, J. (2003) "Vitamin E succinate and cancer treatment: A vitamin E prototype for selective antitumour activity", *British Journal of Cancer*, p. 1822–1826. doi: 10.1038/sj.bjc.6601360.

Neuzil, J. *et al.* (2007) “α-Tocopheryl succinate inhibits angiogenesis by disrupting paracrine FGF2 signalling”, *FEBS Letters*, 581(24), p. 4611–4615. doi: 10.1016/j.febslet.2007.08.051.

Newell, M. *et al.* (2017) “A critical review on the effect of docosahexaenoic acid (Dha) on cancer cell cycle progression”, *International Journal of Molecular Sciences*, p. 1784. doi: 10.3390/ijms18081784.

Newell, M. *et al.* (2019) “Comparing docosahexaenoic acid (DHA) concomitant with neoadjuvant chemotherapy versus neoadjuvant chemotherapy alone in the treatment of breast cancer (DHA WIN): Protocol of a double-blind, phase II, randomised controlled trial”, *BMJ Open,* 9(9). doi: 10.1136/bmjopen-2019-030502.

Newell, M. *et al.* (2021) “N-3 long-chain polyunsaturated fatty acids, eicosapentaenoic and docosahexaenoic acid, and the role of supplementation during cancer treatment: A scoping review of current clinical evidence”, *Cancers*, p. 1206. doi: 10.3390/cancers13061206.

Ni, S. *et al.* (2017) “Lymph cancer chemotherapy: Delivery of doxorubicin-gemcitabine prodrug and vincristine by nanostructured lipid carriers”, *International Journal of Nanomedicine*, 12, p. 1565–1576. doi: 10.2147/IJN.S120685.

Nitiss, J. L. (2009) “Targeting DNA topoisomerase II in cancer chemotherapy”, *Nature Reviews Cancer*, p. 338–350. doi: 10.1038/nrc2607.

Oliveira, M. S. *et al.* (2016a) “α-Tocopherol succinate improves encapsulation and anticancer activity of doxorubicin loaded in solid lipid nanoparticles”, *Colloids and Surfaces B: Biointerfaces,* 140, p. 246–253. doi: 10.1016/j.colsurfb.2015.12.019.

Oliveira, M. S. *et al.* (2016b) “Solid lipid nanoparticles co-loaded with doxorubicin and α-tocopherol succinate are effective against drug-resistant cancer cells in monolayer and 3-D spheroid cancer cell models”, *International Journal of Pharmaceutics,* 512(1), p. 292–300. doi: 10.1016/j.ijpharm.2016.08.049.

Oliveira, M. S. *et al.* (2017) “Hydrophobic ion pairing as a strategy to improve drug encapsulation into lipid nanocarriers for the cancer treatment”, *Expert Opinion on Drug Delivery*, p. 983–995. doi: 10.1080/17425247.2017.1266329.

Silva, J. *et al.* (2019) “Folate-coated, long-circulating and pH-sensitive liposomes enhance doxorubicin antitumor effect in a breast cancer animal model”, *Biomedicine and Pharmacotherapy*, 118, p. 109323. doi: 10.1016/j.biopha.2019.109323.

Park, J. *et al.* (2019) “Alliance with EPR effect: Combined strategies to improve the EPR effect in the tumor microenvironment”, *Theranostics,* 9(26), p. 8073–8090. doi: 10.7150/thno.37198.

Payne, M. *et al.* (2006) “DHA-paclitaxel (Taxoprexin) as first-line treatment in patients with stage IIIB or IV non-small cell lung cancer: Report of a phase II open-label multicenter trial”, *Journal of Thoracic Oncology*, 1(9), p. 984–990. doi: 10.1097/01243894-200611000-00011.

Pecoraro, M. *et al.* (2017) “Cardiotoxic effects of short-term doxorubicin administration: Involvement of connexin 43 in calcium impairment”, *International Journal of Molecular Sciences*, 18(10), p. 2121. doi: 10.3390/ijms18102121.

Peer, D. *et al.* (2007) “Nanocarriers as an emerging platform for cancer therapy”, *Nature Nanotechnology*, p. 751–760. doi: 10.1038/nnano.2007.387.

Peres Diaz, L. S. *et al.* (2020) “Short-term doxorubicin cardiotoxic effects: involvement of cardiac Thyrotropin Releasing Hormone system”, *Life Sciences*, 261, p. 118346. doi: 10.1016/j.lfs.2020.118346.

Prasad, K. N. *et al.* (2003) “α-tocopheryl succinate, the most effective form of vitamin e for adjuvant cancer treatment: A review”, *Journal of the American College of Nutrition*, 22(2), p. 108–117. doi: 10.1080/07315724.2003.10719283.

Prasanna, P. L., Renu, K. e Valsala Gopalakrishnan, A. (2020) “New molecular and biochemical insights of doxorubicin-induced hepatotoxicity”, *Life Sciences*, p. 117599. doi: 10.1016/j.lfs.2020.117599.

Riediger, N. D. *et al.* (2009) “A Systemic Review of the Roles of n-3 Fatty Acids in Health and Disease”, *Journal of the American Dietetic Association*, 109(4), p. 668–679. doi: 10.1016/j.jada.2008.12.022.

Ristroph, K. D. e Prud’homme, R. K. (2019) “Hydrophobic ion pairing: Encapsulating small molecules, peptides, and proteins into nanocarriers”, *Nanoscale Advances*. doi: 10.1039/c9na00308h.

Rizwanullah, M. *et al.* (2021) “Advancement in design of nanostructured lipid carriers for cancer targeting and theranostic application”, *Biochimica et Biophysica Acta - General Subjects,* p. 129936. doi: 10.1016/j.bbagen.2021.129936.

Salvi, V. R. e Pawar, P. (2019) “Nanostructured lipid carriers (NLC) system: A novel drug targeting carrier”, *Journal of Drug Delivery Science and Technology,* p. 255–267. doi: 10.1016/j.jddst.2019.02.017.

Santos Câmara, A. L. *et al.* (2017) “Acid-sensitive lipidated doxorubicin prodrug entrapped in nanoemulsion impairs lung tumor metastasis in a breast cancer model”, *Nanomedicine*, 12(15), p. 1751–1765. doi: 10.2217/nnm-2017-0091.

Santos, D. S. dos e Goldenberg, R. C. dos S. (2018) “Doxorubicin-Induced Cardiotoxicity: From Mechanisms to Development of Efficient Therapy”, in *Cardiotoxicity*, p. 79588. doi: 10.5772/intechopen.79588.

Schirrmacher, V. (2019) “From chemotherapy to biological therapy: A review of novel concepts to reduce the side effects of systemic cancer treatment (Review)”, *International Journal of Oncology*, 54(2), p. 407–419. doi: 10.3892/ijo.2018.4661.

Selvamuthukumar, S. e Velmurugan, R. (2012) “Nanostructured Lipid Carriers: A potential drug carrier for cancer chemotherapy”, *Lipids in Health and Disease,* p. 159.

doi: 10.1186/1476-511X-11-159.

Serini, S. *et al.* (2016) “How plausible is the use of dietary n-3 PUFA in the adjuvant therapy of cancer?”, *Nutrition Research Reviews,* p. 102–125. doi: 10.1017/S0954422416000044.

Serini, S. *et al.* (2017) “Protective effects of ω-3 PUFA in anthracycline-induced cardiotoxicity: A critical review”, *International Journal of Molecular Sciences*, p. 2689. doi: 10.3390/ijms18122689.

Serpe, L. *et al.* (2004) “Cytotoxicity of anticancer drugs incorporated in solid lipid nanoparticles on HT-29 colorectal cancer cell line”, *European Journal of Pharmaceutics and Biopharmaceutics*, 58(3), p. 673–680. doi: 10.1016/j.ejpb.2004.03.026.

Shafei, A. *et al.* (2017) “A review on the efficacy and toxicity of different doxorubicin nanoparticles for targeted therapy in metastatic breast cancer”, *Biomedicine and Pharmacotherapy*, p. 1209–1218. doi: 10.1016/j.biopha.2017.09.059.

Shi, J. *et al.* (2017) “Cancer nanomedicine: Progress, challenges and opportunities”, *Nature Reviews Cancer,* p. 20–37. doi: 10.1038/nrc.2016.108.

Shirai, K. e Iso, H. (2014) *Social determinants of health in non-communicable diseases: Case studies from Japan*, *Springer Series on Epidemiology and Public Health*.

Sicard, P. *et al.* (2019) “Right coronary artery ligation in mice: a novel method to investigate right ventricular dysfunction and biventricular interaction”, *American Journal of Physiology - Heart and Circulatory Physiology*, 316(3), p. 684–692. doi: 10.1152/ajpheart.00573.2018.

Siddiqui, R. A. *et al.* (2011) “Docosahexaenoic acid: A natural powerful adjuvant that improves efficacy for anticancer treatment with no adverse effects”, *BioFactors*, p. 399–412. doi: 10.1002/biof.181.

Sonawane, S. J., Kalhapure, R. S. e Govender, T. (2017) “Hydrazone linkages in pH responsive drug delivery systems”, *European Journal of Pharmaceutical Sciences*, p. 45–65. doi: 10.1016/j.ejps.2016.12.011.

Song, E. A. e Kim, H. (2016) “Docosahexaenoic acid induces oxidative DNA damage and apoptosis, and enhances the chemosensitivity of cancer cells”, *International Journal of Molecular Sciences*, p. 1257. doi: 10.3390/ijms17081257.

Strickley, R. G. (2004) “Solubilizing Excipients in Oral and Injectable Formulations”, *Pharmaceutical Research*, p. 201–230. doi: 10.1023/B:PHAM.0000016235.32639.23.

Subramaniam, B., Siddik, Z. H. e Nagoor, N. H. (2020) “Optimization of nanostructured lipid carriers: understanding the types, designs, and parameters in the process of formulations”, *Journal of Nanoparticle Research,* p. 141. doi:

10.1007/s11051-020-04848-0.

Sung, H. *et al.* (2021) “Global Cancer Statistics 2020: GLOBOCAN Estimates of Incidence and Mortality Worldwide for 36 Cancers in 185 Countries”, *CA: A Cancer Journal for Clinicians*, 71(3), p. 209–249. doi: 10.3322/caac.21660.

Tacar, O., Sriamornsak, P. e Dass, C. R. (2013) “Doxorubicin: An update on anticancer molecular action, toxicity and novel drug delivery systems”, *Journal of Pharmacy and Pharmacology*, p. 157–170. doi: 10.1111/j.2042-7158.2012.01567.x.

Talkar, S. S., Kharkar, P. B. e Patravale, V. B. (2020) “Docetaxel Loaded Pomegranate Seed Oil Based Nanostructured Lipid Carriers: A Potential Alternative to Current Formulation”, *AAPS PharmSciTech,* 21(8), p. 295. doi: 10.1208/s12249-020-01839-1.

Thorn, C. F. *et al.* (2011) “Doxorubicin pathways: Pharmacodynamics and adverse effects”, *Pharmacogenetics and Genomics*, 21(7), p. 440–446. doi: 10.1097/FPC.0b013e32833ffb56.

Toh, M. R. e Chiu, G. N. C. (2013) “Liposomes as sterile preparations and limitations of sterilisation techniques in liposomal manufacturing”, *Asian Journal of Pharmaceutical Sciences,* p. 88–95. doi: 10.1016/j.ajps.2013.07.011.

Vieira, R. *et al.* (2020) “Sucupira oil-loaded nanostructured lipid carriers (NLC): Lipid screening, factorial design, release profile, and cytotoxicity”, *Molecules,* 25(3), p. 685. doi: 10.3390/molecules25030685.

Weber, S., Zimmer, A. e Pardeike, J. (2014) “Solid Lipid Nanoparticles (SLN) and Nanostructured Lipid Carriers (NLC) for pulmonary application: A review of the state of the art”, *European Journal of Pharmaceutics and Biopharmaceutics*, p. 7–22. doi: 10.1016/j.ejpb.2013.08.013.

Wehbe, M. *et al.* (2017) “A simple passive equilibration method for loading carboplatin into pre-formed liposomes incubated with ethanol as a temperature dependent permeability enhancer”, *Journal of Controlled Release,* 252, p. 50–61. doi: 10.1016/j.jconrel.2017.03.010.

Wei, C. W. *et al.* (2019) “Anticancer effects of methotrexate in combination with α-tocopherol and α-tocopherol succinate on triple-negative breast cancer”, *Oncology Reports,* 41(3), p. 2060–2066. doi: 10.3892/or.2019.6958.

Wicki, A. *et al.* (2015) “Nanomedicine in cancer therapy: Challenges, opportunities, and clinical applications”, *Journal of Controlled Release*, p. 138–157. doi: 10.1016/j.jconrel.2014.12.030.

Wu, L. P., Wang, D. e Li, Z. (2020) “Grand challenges in nanomedicine”, *Materials Science and Engineering C,* p. 110302. doi: 10.1016/j.msec.2019.110302.

Xiong, S. *et al.* (2019) “A pH-sensitive prodrug strategy to co-deliver DOX and TOS in TPGS nanomicelles for tumor therapy”, *Colloids and Surfaces B: Biointerfaces*, 173,

p. 346–355. doi: 10.1016/j.colsurfb.2018.10.012.

Yang, F. *et al.* (2014) “Doxorubicin, DNA torsion, and chromatin dynamics”, *Biochimica et Biophysica Acta - Reviews on Cancer*, p. 84–89. doi: 10.1016/j.bbcan.2013.12.002.

Zara, G. P. *et al.* (1999) “Pharmacokinetics of doxorubicin incorporated in solid lipid nanospheres (SLN)”, *Pharmacological Research,* 40(3), p. 281–286. doi: 10.1006/phrs.1999.0509.

Zeng, X. *et al.* (2017) “A Drug-Self-Gated Mesoporous Antitumor Nanoplatform Based on pH-Sensitive Dynamic Covalent Bond,” *Advanced Functional Materials*, 27(11), p. 1605985. doi:10.1002/adfm.201605985.

Zhang, L. *et al.* (2019) “Resveratrol solid lipid nanoparticles to trigger credible inhibition of doxorubicin cardiotoxicity”, *International Journal of Nanomedicine*, 14, p. 6061–6071. doi: 10.2147/IJN.S211130.

Zhang, T. *et al.* (2013) “A novel submicron emulsion system loaded with vincristine-oleic acid ion-pair complex with improved anticancer effect: In vitro and in vivo studies”, *International Journal of Nanomedicine*, 8, p. 1185–1196. doi: 10.2147/IJN.S41775.

Zhang, Xuguang *et al.* (2011) “Alpha-tocopheryl succinate enhances doxorubicin-induced apoptosis in human gastric cancer cells via promotion of doxorubicin influx and suppression of doxorubicin efflux”, *Cancer Letters*, 307(2), p. 174–181. doi: 10.1016/j.canlet.2011.04.001.

Zhang, X. *et al.* (2018) “CD44-Targeted Facile Enzymatic Activatable Chitosan Nanoparticles for Efficient Antitumor Therapy and Reversal of Multidrug Resistance”, *Biomacromolecules*, 19(3), p. 883–895. doi: 10.1021/acs.biomac.7b01676.

Zhang, Xuanmiao *et al.* (2011) “Lipid nanoemulsions loaded with doxorubicin-oleic acid ionic complex: Characterization, in vitro and in vivo studies”, *Pharmazie*, 66(7), p. 496–505. doi: 10.1691/ph.2011.0379.

Zhang, Y. *et al.* (2010) “PKSolver: An add-in program for pharmacokinetic and pharmacodynamic data analysis in Microsoft Excel”, *Computer Methods and Programs in Biomedicine*, 99(3), p. 306–314. doi: 10.1016/j.cmpb.2010.01.007.

Zhao, H. *et al.* (2013) “Nanoemulsion loaded with lycobetaine-oleic acid ionic complex: Physicochemical characteristics, in vitro, in vivo evaluation, and antitumor activity”, *International Journal of Nanomedicine*, 8, p. 1959–1973. doi: 10.2147/IJN.S43892.

Zhao, L. e Zhang, B. (2017) “Doxorubicin induces cardiotoxicity through upregulation of death receptors mediated apoptosis in cardiomyocytes”, *Scientific Reports*, 7, p. 44735. doi: 10.1038/srep44735.

Zhao, S. *et al.* (2016) “Doxorubicin hydrochloride-oleic acid conjugate loaded

nanostructured lipid carriers for tumor specific drug release", *Colloids and Surfaces B: Biointerfaces,* 145, p. 95–103. doi: 10.1016/j.colsurfb.2016.04.027.

Zhelev, Z. *et al.* (2016) "Docosahexaenoic acid sensitizes leukemia lymphocytes to barasertib and everolimus by ros-dependent mechanism without affecting the level of ros and viability of normal lymphocytes", *Anticancer Research,* 36(4), p. 1673–1682.

Zheng, R. R. *et al.* (2021) "Self-delivery nanomedicine to overcome drug resistance for synergistic chemotherapy", *Biomaterials Science*, 9(9), p. 3445–3452. doi: 10.1039/d1bm00119a.

Zugazagoitia, J. *et al.* (2016) "Current Challenges in Cancer Treatment", *Clinical Therapeutics*, p. 1551–1566. doi: 10.1016/j.clinthera.2016.03.026.

APÊNDICE A – Produções científicas relacionadas à tese

Biomedicine & Pharmacotherapy 132 (2020) 110876

Contents lists available at ScienceDirect

Biomedicine & Pharmacotherapy

journal homepage: www.elsevier.com/locate/biopha

Original article

Co-delivery of doxorubicin, docosahexaenoic acid, and α-tocopherol succinate by nanostructured lipid carriers has a synergistic effect to enhance antitumor activity and reduce toxicity

Eduardo Burgarelli Lages [a], Renata Salgado Fernandes [a], Juliana de Oliveira Silva [a], Ângelo Malachias de Souza [b], Geovanni Dantas Cassali [c], André Luís Branco de Barros [d], Lucas Antônio Miranda Ferreira [a,*]

[a] Department of Pharmaceutical Products, Faculty of Pharmacy, Universidade Federal de Minas Gerais, Belo Horizonte, MG, Brazil
[b] Department of Physics, Institute of Exact Sciences, Universidade Federal de Minas Gerais, Belo Horizonte, MG, Brazil
[c] Department of General Pathology, Institute of Biological Sciences, Universidade Federal de Minas Gerais, Belo Horizonte, MG, Brazil
[d] Department of Clinical and Toxicological Analyses, Faculty of Pharmacy, Universidade Federal de Minas Gerais, Belo Horizonte, MG, Brazil

ARTICLE INFO

Keywords:
Doxorubicin
Combination therapy
Ion-pairing
Synergism
Antitumor activity
Cardiotoxicity

ABSTRACT

Doxorubicin (DOX) is widely used in cancer treatment, however, its use is often limited due to its side effects. To avoid these shortcomings, the encapsulation of DOX into nanocarriers has been suggested. Herein, we proposed a novel nanostructured lipid carrier (NLC) formulation loading DOX, docosahexaenoic acid (DHA), and α-tocopherol succinate (TS) for cancer treatment. DHA is an omega-3 fatty acid and TS is a vitamin E derivative. It has been proposed that these compounds can enhance the antitumor activity of chemotherapeutics. Thus, we hypothesized that the combination of DOX, DHA, and TS in NLC (NLC-DHA-DOX-TS) could increase antitumor efficacy and also reduce toxicity. NLC-DHA-DOX-TS was prepared using emulsification-ultrasound. DOX was incorporated after preparing the NLC, which prevented its degradation during manufacture. High DOX encapsulation efficiency was obtained due to the ion-pairing with TS. This ion-pairing increases lipophilicity of DOX and reduces its crystallinity, contributing to its encapsulation in the lipid matrix. Controlled DOX release from the NLC was observed *in vitro*, with increased drug release at the acidic environment. *In vitro* cell studies indicated that DOX, DHA, and TS have synergistic effects against 4T1 tumor cells. The *in vivo* study showed that NLC-DHA-DOX-TS exhibited the greatest antitumor efficacy by reducing tumor growth in 4T1 tumor-bearing mice. In addition, this formulation reduced mice mortality, prevented lung metastasis, and decreased DOX-induced toxicity to the heart and liver, which was demonstrated by hematologic, biochemical, and histologic analyses. These results indicate that NLC-DHA-DOX-TS may be a promising carrier for breast cancer treatment.

1. Introduction

Doxorubicin (DOX) is a cytotoxic anthracycline widely used to treat solid tumors and hematologic malignancies, such as acute lymphoblastic leukemia, metastatic breast cancer, and metastatic bone sarcomas [1,2]. Despite the high antitumor activity, DOX causes cumulative and dose-dependent cardiotoxicity, ranging from occult changes in myocardial structure and function to severe cardiomyopathy and congestive heart failure, which restricts its use in clinical practice [3]. In addition, drug resistance is another obstacle that limits the clinical use of DOX, because it often results in therapy failure [2].

DOX-based nanocarriers have been designed to reduce adverse effects and overcome drug resistance since they offer several advantages due to their design, selectivity, and stability in the cancer microenvironment. The entrapment of DOX in nanocarriers can prevent its degradation in circulation, enhance pharmacokinetic profile, and alter biodistribution ultimately reducing its accumulation and toxicity in the heart [4,5]. In addition, nanoparticles can pass through the leaky blood vessels of the tumor and passively accumulate within the target site *via* enhanced permeability and retention (EPR) effect, which can result in superior therapeutic activity [6].

Doxil®, a DOX-loaded liposomal formulation, was the first FDA-

* Corresponding author at: Department of Pharmaceutical Products, Faculty of Pharmacy, Universidade Federal de Minas Gerais, Belo Horizonte, MG, Brazil.
E-mail address: lucas@farmacia.ufmg.br (L.A. Miranda Ferreira).

https://doi.org/10.1016/j.biopha.2020.110876
Received 29 June 2020; Received in revised form 6 October 2020; Accepted 9 October 2020
Available online 28 October 2020

Biomedicine & Pharmacotherapy 144 (2021) 112373

Contents lists available at ScienceDirect

Biomedicine & Pharmacotherapy

journal homepage: www.elsevier.com/locate/biopha

pH-sensitive doxorubicin-tocopherol succinate prodrug encapsulated in docosahexaenoic acid-based nanostructured lipid carriers: An effective strategy to improve pharmacokinetics and reduce toxic effects

Eduardo Burgarelli Lages [a,b], Renata Salgado Fernandes [a], Marina Mol Sena Andrade [a], Nitchawat Paiyabhroma [b], Renata Barbosa de Oliveira [a], Christian Fernandes [a], Geovanni Dantas Cassali [c], Pierre Sicard [b,d], Sylvain Richard [b,d], André Luís Branco de Barros [e], Lucas Antônio Miranda Ferreira [a,*]

[a] Departamento de Produtos Farmacêuticos, Faculdade de Farmácia, Universidade Federal de Minas Gerais, Belo Horizonte, MG, Brazil
[b] PhyMedExp, Université de Montpellier, INSERM, CNRS, Montpellier, France
[c] Departamento de Patologia Geral, Instituto de Ciências Biológicas, Universidade Federal de Minas Gerais, Belo Horizonte, MG, Brazil
[d] IPAM, BioCampus Montpellier, INSERM, CNRS, Université de Montpellier, Montpellier, France
[e] Departamento de Análises Clínicas e Toxicológicas, Faculdade de Farmácia, Universidade Federal de Minas Gerais, Belo Horizonte, MG, Brazil

ARTICLE INFO

Keywords:
Doxorubicin
Nanomedicine
Ion-pairing
Amide
Hydrazone
Antitumor activity
Cardiotoxicity

ABSTRACT

Side effects often limit the use of doxorubicin (DOX) in cancer treatment. We have recently developed a nanostructured lipid carrier (NLC) formulation for synergistic chemotherapy, encapsulating DOX and the anti-cancer adjuvants docosahexaenoic acid (DHA) and α-tocopherol succinate (TS). Hydrophobic ion-pairing with TS allowed a high DOX entrapment in the nanocarrier. In this work, we investigated the pharmacokinetics of this formulation after intravenous administration in mice. The first data obtained led us to propose synthesizing covalent DOX-TS conjugates to increase DOX retention in the NLC. We successfully conjugated DOX to TS via an amide or hydrazone bond. *In vitro* studies in 4T1 tumor cells indicated low cytotoxicity of the amide derivative, while the hydrazone conjugate was effective in killing cancer cells. We encapsulated the hydrazone derivative in a DHA-based nanocarrier (DOX-hyd-TS/NLC), which had reduced particle size and high drug encapsulation efficiency. The pH-sensitive hydrazone bond allowed controlled DOX release from the NLC, with increased drug release at acidic conditions. *In vivo* studies revealed that DOX-hyd-TS/NLC had a better pharmacokinetic profile than free DOX and attenuated the short-term cardiotoxic effects caused by DOX, such as QT prolongation and impaired left ventricular systolic function. Moreover, this formulation showed excellent therapeutic performance by reducing tumor growth in 4T1 tumor-bearing mice and decreasing DOX-induced toxicity to the heart and liver, demonstrated by hematologic, biochemical, and histologic analyses. These results indicate that DOX-hyd-TS/NLC may be a promising nanocarrier for breast cancer treatment.

1. Introduction

Doxorubicin (DOX) is a cytotoxic anthracycline widely used in chemotherapy due to its efficacy in fighting many cancers, such as carcinomas, sarcomas, and hematologic malignancies. However, its use can result in cumulative and dose-dependent cardiotoxicity as one of the most serious adverse effects, ranging from structural and functional changes in cardiomyocytes to severe cardiomyopathy and congestive heart failure [1,2]. DOX-loaded nanocarriers aim to overcome the challenges associated with cancer therapy, providing a reduction in toxicity and an improvement in the drug's safety profile [3,4]. Moreover, nanocarriers can present superior therapeutic efficacy than free drugs due to the enhanced permeability and retention (EPR) effect, which allows the passive targeting and accumulation of nanostructures in the interstitial tissue of malignant tumors since they can pass through the leaky blood vessels [5,6].

Among the promising nanoplatforms for drug delivery in cancer therapy, nanostructured lipid carriers (NLC) have attracted expanding

* Corresponding author.
E-mail address: lucas@farmacia.ufmg.br (L.A.M. Ferreira).

https://doi.org/10.1016/j.biopha.2021.112373
Received 31 August 2021; Received in revised form 16 October 2021; Accepted 25 October 2021
Available online 28 October 2021

frontiers in Cardiovascular Medicine

MINI REVIEW
published: 30 June 2021
doi: 10.3389/fcvm.2021.690533

Nanomedicine in Oncocardiology: Contribution and Perspectives of Preclinical Studies

Gabriel Silva Marques Borges[1,2†], *Eduardo Burgarelli Lages*[1,2†], *Pierre Sicard*[2,3], *Lucas Antônio Miranda Ferreira*[1] *and Sylvain Richard*[2,3*]

[1] Departamento de Produtos Farmacêuticos, Faculdade de Farmácia, Universidade Federal de Minas Gerais, Belo Horizonte, Brazil, [2] PhyMedExp, Université de Montpellier, INSERM, CNRS, Montpellier, France, [3] IPAM, BioCampus, CNRS, INSERM, Université de Montpellier, Montpellier, France

Cancer and cardiovascular diseases are the leading causes of death and morbidity worldwide. Strikingly, cardiovascular disorders are more common and more severe in cancer patients than in the general population, increasing incidence rates. In this context, it is vital to consider the anticancer efficacy of a treatment and the devastating heart complications it could potentially cause. Oncocardiology has emerged as a promising medical and scientific field addressing these aspects from different angles. Interestingly, nanomedicine appears to have great promise in reducing the cardiotoxicity of anticancer drugs, maintaining or even enhancing their efficacy. Several studies have shown the benefits of nanocarriers, although with some flaws when considering the concept of oncocardiology. Herein, we discuss how preclinical studies should be designed as closely as possible to clinical protocols, considering various parameters intrinsic to the animal models used and the experimental protocols. The sex and age of the animals, the size and location of the tumors, the doses of the nanoformulations administered, and the acute vs. the long-term effects of treatments are essential aspects. We also discuss the perspectives offered by non-invasive imaging techniques to simultaneously assess both the anticancer effects of treatment and its potential impact on the heart. The overall objective is to accelerate the development and validation of nanoformulations through high-quality preclinical studies reproducing the clinical conditions.

Keywords: anticancer drugs, cardiotoxicity, nanoformulations, non-invasive imaging, echography, photoacoustic, small animals

OPEN ACCESS

Edited by:
Carlo Gabriele Tocchetti,
University of Naples Federico II, Italy

Reviewed by:
Fabiana Passaro,
University of Naples Federico II, Italy
Gianluca Testa,
University of Molise, Italy

***Correspondence:**
Sylvain Richard
sylvain.richard@inserm.fr

[†] These authors have contributed equally to this work and share first authorship

Specialty section:
This article was submitted to Cardio-Oncology, a section of the journal Frontiers in Cardiovascular Medicine

Received: *07 April 2021*
Accepted: *01 June 2021*
Published: *30 June 2021*

Citation:
Borges GSM, Lages EB, Sicard P, Ferreira LAM and Richard S (2021) Nanomedicine in Oncocardiology: Contribution and Perspectives of Preclinical Studies. Front. Cardiovasc. Med. 8:690533. doi: 10.3389/fcvm.2021.690533

INTRODUCTION

Recent advances in the treatment of cancers have improved patient care and cure rates. Cancer, once fatal, is now emerging as a chronic disease, often at the cost of cardiovascular complications. Moreover, cardiovascular diseases (CVD) are more common and more severe in cancer patients (1–5). In this context, the development of novel treatments with antineoplastic agents still raises concerns about undesirable effects at the acute phase of the treatment and potentially during long-term therapy (6). Therefore, the management of cancer patients has moved from general cardiology to a specialized discipline, oncocardiology, with in-depth cardiovascular monitoring at each stage of cancer therapy (1, 7). Among various areas that can help solve these problems, nanotechnology is being increasingly investigated in preclinical studies to improve anticancer treatments and reduce

Editorial

For reprint orders, please contact: reprints@futuremedicine.com

Nanomedicine

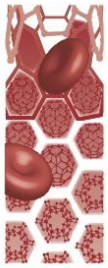

Nanomedicine to deliver docosahexaenoic acid: potential applications to improve health

Eduardo Burgarelli Lages[‡,1], Gabriel Silva Marques Borges[‡,1], Gisele Assis Castro Goulart[1] & Lucas Antônio Miranda Ferreira*[,1]

[1]Departamento de Produtos Farmacêuticos, Faculdade de Farmácia, Universidade Federal de Minas Gerais, Belo Horizonte, Brazil

*Author for correspondence: lucaufmg@gmail.com

‡Authors contributed equally and share first authorship

> "The incorporation of DHA in nanostructures can enhance its physicochemical stability, bioavailability, and delivery to target cells, resulting in increased efficiency."

First draft submitted: 29 March 2021; Accepted for publication: 28 April 2021; Published online: 24 June 2021

Keywords: bioavailability • docosahexaenoic acid • nanocarriers • nanotechnology • nutraceuticals • omega-3

Health benefits of DHA

Some substances can provide health benefits throughout all stages of life. Omega-3 polyunsaturated fatty acids (n-3 PUFA) are in this select group. Several epidemiological studies have suggested that an increased intake of n-3 PUFA is associated with a low incidence of cardiovascular diseases and cancer. Fish, algal, and krill oils are the most popular and well-known sources of n-3 fatty acids, with docosahexaenoic acid (DHA) and eicosapentaenoic acid being their main bioactive components [1,2].

Most of the beneficial health effects of DHA have been attributed to its anti-inflammatory and antioxidant properties. Neurodegenerative and cardiovascular diseases, rheumatoid arthritis, diabetes, autoimmune diseases, and cancer are some of the fields in which the use of DHA has been increasingly investigated [3].

DHA is essential for visual and cognitive development in early childhood, making it a critical nutrient during pregnancy and breastfeeding. It is found in high concentrations in neuronal cell membranes, where it can perform many physiological functions, including regulation of membrane fluidity, release of neurotransmitters, gene expression, and neuronal differentiation and growth [2].

DHA has been recognized as the principal n-3 PUFA with cardiovascular protective effects, showing a broad spectrum of protection [1]. n-3 PUFA can be incorporated into the phospholipid bilayer of cell membranes and alter their physicochemical properties, affecting cell components and signaling pathways. Additionally, they exert both anti-inflammatory and anti-fibrotic effects though the regulation of pro-inflammatory gene expression and production of pro-resolving lipid mediators, such as resolvins, protectins, and maresins. Moreover, the inclusion of n-3 PUFA in cardiomyocytes alters the lipid microenvironment and can modulate the function of ion channels, such as sodium and L-type calcium channels, leading to antiarrhythmic effects [4].

In addition to its cardioprotective effects, DHA can reduce cardiac toxicity evoked by anticancer drugs, such as anthracyclines [5,6]. n-3 PUFA can positively modulate some of the cellular processes and molecular pathways that, oppositely, are harmfully altered by chemotherapeutic drugs. For example, although the mechanism of anthracycline-induced cardiotoxicity is not fully understood, it is known that the inflammatory process plays an important role, with the activation of innate and adaptive immunity and the release of inflammatory cytokines. On the other hand, DHA can generate bioactive mediators with powerful pro-resolution and anti-inflammatory activities, helping to reduce the heart damage induced by chemotherapeutic agents [4].

DHA has also attracted extensive attention due to its adjuvant properties in the treatment of cancer. DHA can decrease cancer cell proliferation and migration, especially through the formation of reactive oxygen species, inducing apoptosis, inhibiting angiogenesis, and reducing cell invasiveness potential [3,7]. Interestingly, these anticancer effects

Future Medicine